COCORA 2016

The Sixth International Conference on Advances in Cognitive Radio

ISBN: 978-1-61208-456-5

February 21 - 25, 2016

Lisbon, Portugal

COCORA 2016 Editors

Mario Freire, University of Beira Interior, Portugal
Claus-Peter Rückemann, Leibniz Universität Hannover / Westfälische Wilhelms-Universität Münster / North-German Supercomputing Alliance (HLRN), Germany

COCORA 2016

Forward

The Sixth International Conference on Advances in Cognitive Radio (COCORA 2016), held between February 21-25, 2016 in Lisbon, Portugal, continued a series of events dealing with various aspects, advanced solutions and challenges in cognitive (and collaborative) radio networks. It covered fundamentals on cognitive and collaborative radio, specific mechanisms and protocols, signal processing and dedicated devices, measurements and applications.

Most of the national and cross-national boards (FCC, European Commission) had/have a series of activities in the technical, economic, and regulatory domains in searching for better spectrum management policies and techniques, due to spectrum scarcity and spectrum underutilization issues. Therefore, dynamic spectrum management via cognition capability can make opportunistic spectrum access possible (either by knowledge management mechanisms or by spectrum sensing functionality). The main challenge for a cognitive radio is to detect the existence of primary users reliably in order to minimize the interference to licensed communications. Optimized collaborative spectrum sensing schemes give better spectrum sensing performance. Effects as hidden node, shadowing, fading lead to uncertainties in a channel; collaboration has been proposed as a solution. However, traffic overhead and other management aspects require enhanced collaboration techniques and mechanisms for a more realistic cognitive radio networking.

The conference had the following tracks:

- Mechanisms and Protocols
- Applications, measurement and management

We take here the opportunity to warmly thank all the members of the COCORA 2016 technical program committee, as well as all the reviewers. The creation of such a high quality conference program would not have been possible without their involvement. We also kindly thank all the authors that dedicated much of their time and effort to contribute to COCORA 2016. We truly believe that, thanks to all these efforts, the final conference program consisted of top quality contributions.

Also, this event could not have been a reality without the support of many individuals, organizations and sponsors. We also gratefully thank the members of the COCORA 2016 organizing committee for their help in handling the logistics and for their work that made this professional meeting a success.

We hope COCORA 2016 was a successful international forum for the exchange of ideas and results between academia and industry and to promote further progress in the area of cognitive (and collaborative) radio networks. We also hope that Lisbon, Portugal provided a pleasant environment during the conference and everyone saved some time to enjoy the beauty of the city.

COCORA 2016 Advisory Committee

Tomohiko Taniguchi, Fujitsu Laboratories Limited, Japan
Adrian Popescu, Blekinge Institute of Technology - Karlskrona, Sweden
Alan A. Varghese, Coherent Logix, USA

COCORA 2016

Committee

COCORA 2016 Advisory Committee

Tomohiko Taniguchi, Fujitsu Laboratories Limited, Japan
Adrian Popescu, Blekinge Institute of Technology - Karlskrona, Sweden
Alan A. Varghese, Coherent Logix, USA

COCORA 2016 Technical Program Committee

Anwer Al-Dulaimi, Brunel University, UK
Annamalai Annamalai, Prairie View A&M University, USA
Cornelia Badoi, Microsoft, Romania
Ilham Benyahia, Université du Québec en Outaouais, Canada
Derya Çavdar, Bogazici University, Istanbul, Turkey
Lingjie Duan, Singapore University of Technology and Design, Singapore
Waleed Ejaz, Ryerson University, Toronto, Canada
Malgorzata Gajewska, Gdansk University of Technology, Poland
Slawomir Gajewski, Gdansk University of Technology, Poland
Matthieu Gautier, Université de Rennes 1, IRISA, INRIA, France
Liljana Gavrilovska, Ss. Cyril and Methodius University -Skopje, Macedonia
Tien-Ke Huang, National Tsing Hua University, Taiwan
Abubakar Sadiq Hussaini, Instituto de Telecomunicações - Aveiro, Portugal | American University of Nigeria, Nigeria
Muhammad Umar Khan, Center for Advanced Studies in Telecommunication (CAST), Pakistan
Insoo Koo, University of Ulsan, South Korea
Jia-Chin Lin, National Central University, Taiwan
Marco Listanti, University of Rome La Sapienza, Italy
Jean-Claude Moissinac, TELECOM ParisTech, France
Homayoun Nikookar, Delft University of Technology, The Netherlands
Sema Oktug, Istanbul Technical University, Turkey
Adrian Popescu, Blekinge Institute of Technology - Karlskrona, Sweden
Arnd-Ragnar Rhiemeier, Cassidian Electronics - Ulm, Germany
Mario Eduardo Rivero Angeles, Computation Research Center (CIC-IPN), Mexico
Daniel Riviello, Politecnico di Torino, Italy
Usman Shahid, NDSU - Fargo, USA
Boyan Soubachov, University of Cape Town, South Africa
Silvian Spiridon, Broadcom - Bunnik, The Netherlands
Marko Suojanen, Finnish Defence Research Agency, Finland

Tomohiko Taniguchi, Fujitsu Laboratories Limited, Japan
Alan A. Varghese, Coherent Logix, USA
Liaoyuan Zeng, University of Electronic Science and Technology of China, China

Copyright Information

For your reference, this is the text governing the copyright release for material published by IARIA.

The copyright release is a transfer of publication rights, which allows IARIA and its partners to drive the dissemination of the published material. This allows IARIA to give articles increased visibility via distribution, inclusion in libraries, and arrangements for submission to indexes.

I, the undersigned, declare that the article is original, and that I represent the authors of this article in the copyright release matters. If this work has been done as work-for-hire, I have obtained all necessary clearances to execute a copyright release. I hereby irrevocably transfer exclusive copyright for this material to IARIA. I give IARIA permission or reproduce the work in any media format such as, but not limited to, print, digital, or electronic. I give IARIA permission to distribute the materials without restriction to any institutions or individuals. I give IARIA permission to submit the work for inclusion in article repositories as IARIA sees fit.

I, the undersigned, declare that to the best of my knowledge, the article is does not contain libelous or otherwise unlawful contents or invading the right of privacy or infringing on a proprietary right.

Following the copyright release, any circulated version of the article must bear the copyright notice and any header and footer information that IARIA applies to the published article.

IARIA grants royalty-free permission to the authors to disseminate the work, under the above provisions, for any academic, commercial, or industrial use. IARIA grants royalty-free permission to any individuals or institutions to make the article available electronically, online, or in print.

IARIA acknowledges that rights to any algorithm, process, procedure, apparatus, or articles of manufacture remain with the authors and their employers.

I, the undersigned, understand that IARIA will not be liable, in contract, tort (including, without limitation, negligence), pre-contract or other representations (other than fraudulent misrepresentations) or otherwise in connection with the publication of my work.

Exception to the above is made for work-for-hire performed while employed by the government. In that case, copyright to the material remains with the said government. The rightful owners (authors and government entity) grant unlimited and unrestricted permission to IARIA, IARIA's contractors, and IARIA's partners to further distribute the work.

Table of Contents

Game based Cognitive Radio Bandwidth Allocation Scheme

Youngjae Park
Computer science and engineering
Sogang University
Seoul, South Korea
yjpark903@sogang.ac.kr

Sungwook Kim
Computer science and engineering
Sogang University
Seoul, South Korea
swkim01@sogang.ac.kr

***Abstract*—Even though wireless Internet service has grown rapidly, the available wireless bandwidth resource is limited. So, efficient network bandwidth resources management has become an important issue. Recently, cognitive radio technology has been getting a lot of attention to improve bandwidth efficiency. In this paper, we propose an adaptive bandwidth management scheme based on the mechanism design and negotiation theory. According to the user`s utility, Quality of Service (QoS) and trust value, the proposed scheme allocates total resources while dynamically controlling the selfish users. In addition, the proposed scheme is able to make a control decision in a distributed manner. This approach can reduce the excessive number of operations and increase the primary user`s profit; it is practical for real world network operations. Simulation results show that the proposed scheme provides much better performance than the existing schemes.**

Keywords— Cognitive Radio; VCG Mechanism; Rubinstein Bargaining; Resource allocation

I. INTRODUCTION

Radio spectrum is the scarcest resource for wireless communications. Therefore, in the next generation wireless network, it may become congested due to diverse types of users and applications. Recently, regulatory bodies like the Federal Communications Commission (FCC) in the United States are recognizing that traditional fixed spectrum allocation can be very inefficient. In order to fully utilize the scarce spectrum resources, Cognitive Radio (CR) technology has becomes a promising approach, which allows unlicensed wireless users (secondary users: SUs) to dynamically access the licensed bands from legacy spectrum holders (primary users: PUs) on a negotiated or an opportunistic basis. Dynamic spectrum access in CR networks can enhance the radio resource utilization. To realize efficient spectrum usage, we must migrate from the current static spectrum access to a dynamic spectrum [1]-[3].

Most existing resource allocation approaches for CR networks assume that SUs are truthful, cooperative and always successful in operation. Therefore, SUs always send truthful information in interference environment, even though they can fail resource allocation. These assumptions are only available in an ideal theoretical situation. However, in the real world, untruthful SUs exist; they can lie in order to get more spectrum resource by using untruthful information. In such cases, the CR network administrator wishes to design a new protocol that extracts the missing information from the SUs. Due to this reason, we need a new game model to force selfish SUs to cooperate.

To effectively manage the limited spectrum resource, extensive research has been carried out. Nowadays, game theory has become a powerful tool to analyze and improve the performance of CR network control protocols. Game theory is the mathematical theory of interactions between self-interested agents. It can describe the possibility to react to the actions of the other decision makers and analyze the situations of conflict and cooperation. In particular, it focuses on decision making in settings where each player's decision can influence the outcomes of other players. In such settings, each player must consider how each other player will act in order to make an optimal choice. In the game theory, a game consists of player, strategies and payoff function [4]-[6].

Recently, researchers have proposed various algorithms to optimally share the spectrum resource using cognitive radio technologies. Auction game models also have been proposed for efficient spectrum sharing in CR networks. Initially, auction game has been studied extensively in the economics literature. Usually, it is implemented with efficient social choice functions; participants have private information about their preferences. An auction is a process of buying and selling goods or services by offering them up for bid, taking bids, and then selling the item to the highest bidder. In game theory, an auction game may refer to any mechanism or set of trading rules for exchange. A well-known auction mechanism is the Vickrey-Clarke-Groves (VCG) mechanism [7]. It is a generalization of the famous Vickery auction where bidders submit written bids without knowing the bid of the other bidders in the auction. The important properties of the VCG mechanism are direct-revelation and strategy proof [8]; each bidder reveals his/her true value no matter what strategies the other bidder chooses. However, the VCG mechanism needs a huge computational overhead. Therefore, the traditional VCG mechanism might be impractical for the system's overall operations.

In 1982, Israeli economist Ariel Rubinstein built up an alternating-offer bargain model based on the Stahl's limited negotiation model; it is known as a Rubinstein bargaining process. This model can provide a possible solution to the problem that two players are bargaining with the division of the benefits [9]. Most of all, the Rubinstein can significantly

 ISBN: 978-1-61208-456-5

reduce the computational complexity and overhead. It is practical and suitable for real implementation.

In this paper, we propose a new spectrum allocation scheme for CR networks. In our game model, SUs are game players, and can make strategic decisions independently while maximizing their payoffs. By using the VCG mechanism, our proposed scheme is designed as a cooperative game model. In addition, to effectively reduce the computational overhead of VCG mechanism, we adopt the Rubinstein bargaining model. This integrated approach can simplify the implementation of VCG mechanism. Therefore, our proposed scheme effective controls selfish SUs to increase the total system utility while reducing the VCG mechanism time complexity.

This paper is organized as follows. Section II explains the related works. In Section III, we present the proposed algorithms in detail. In Section IV, performance evaluation results are presented along with comparisons with other schemes. Finally, concluding remarks are given in Section V.

II. RELATED WORKS

In this section, we introduce two game-theoretic models for the effective resource allocation in CR networks. In Section II-A, we present the desired properties of a VCG mechanism design to effectively control selfish SUs. In Section II-B, we introduce the Rubinstein Bargaining Model, which can help VCG mechanism design to decrease time complexity.

A. VCG mechanism

VCG mechanism is a field of Mechanism Design (MD) to study a solution concept for the class of private information games. Traditional *MD* consists of a specification of possible agent strategies and the mapping of each strategy from a set of strategies to an outcome. Agents are assumed to be autonomous and economically rational; they select a best-response strategy to maximize their expected utility with other agents. The family of *direct-revelation* and *strategy-proof* mechanisms has been derived from the *MD* theory and are referred to as *VCG* mechanism. The *VCG* mechanism has better computational properties than the original *MD* and provides a normative guide for outcomes and payments. When applying the *VCG* mechanism to complex *MD* problems, a feasible outcome can be obtained from the results of computationally tractable heuristic algorithms [10]. Each agent in the *VCG* mechanism is of a specific type. According to its type, an agent selects a specific strategy, which defines the agent's actions. Generally, an agent type is represented by θ, (e.g., each agent i is of type θ_i).

The *VCG* mechanism is a special case among traditional mechanisms, in which the agent-announced type ($\hat{\theta}$) is no longer necessarily truthful; the symbol $\hat{\theta}$ indicates that agents can misreport their true types. Based on agent-announced types, the choice rule ($k^*(\hat{\theta})$) is defined as follows [11]

$$k^*(\hat{\theta}) = \text{argmax}_{k\in\mathcal{K}} \sum_{\text{i}} v_i(k, \hat{\theta}_i) \quad (1)$$

where k is a feasible choice of the set of all possible choices and $v_i(k, \hat{\theta}_i)$ defines the agent i's outcome of a choice k with its type $\hat{\theta}_i$; the *VCG* mechanism implements the choice k^* that maximizes $\sum_i v_i(k, \hat{\theta}_i)$. Therefore, the *VCG* mechanism maximizes the total outcome of the system to the agents. Based on $k^*(\hat{\theta})$, the payment rule ($p_{vcg,i}(\hat{\theta})$) is defined as follows

$$p_{vcg,i}(\hat{\theta}) = v_i(k^*(\hat{\theta}), \hat{\theta}_i) - \{V_N - V_{N-i}\} \quad (2)$$

where V_N is the total reported outcome of k^* and V_{N-i} is the total reported outcome of the choice that would be gotten without agent i, i.e., $V_N = \max_{k\in\mathcal{K}} \sum_{\text{i}} v_i(k, \hat{\theta}_i)$ and $V_{N-i} = \max_{k\in\mathcal{K}} \sum_{j\neq i} v_j(k, \hat{\theta}_j)$.

B. Rubinstein Bargaining Model

In Rubinstein-Stahl bargaining model, players have their own bargaining power (δ). The division proportion of the benefits can be obtained according to the bargaining power, which can be computed at each player individually. The higher the bargaining power, the more a player benefits from the bargaining. Players negotiate with each other by proposing offers alternately. After several rounds of negotiation, they finally reach an agreement as follows

$$(x_1^*, x_2^*) = \begin{cases} \left(\frac{1-\delta_2}{1-\delta_1\delta_2}, \frac{\delta_2(1-\delta_1)}{1-\delta_1\delta_2}\right) \text{ if the } player\_1 \text{ offers first} \\ \left(\frac{\delta_1(1-\delta_2)}{1-\delta_1\delta_2}, \frac{1-\delta_1}{1-\delta_1\delta_2}\right) \text{ if the } player\_2 \text{ offers first} \end{cases} \quad (3)$$
$$s.t., (x_1^*, x_2^*) \in \mathbf{R^2}: x_1^* + x_2^* = 1,$$
$$x_1^* \geq 0, x_2^* \geq 0 \text{ and } 0 \leq \delta_1, \delta_2 \leq 1$$

It is obvious that $\frac{1-\delta_2}{1-\delta_1\delta_2} \geq \frac{\delta_2(1-\delta_1)}{1-\delta_1\delta_2}$ and $\frac{\delta_1(1-\delta_2)}{1-\delta_1\delta_2} \leq \frac{1-\delta_1}{1-\delta_1\delta_2}$. That is to say, there is a first-proposer advantage in the bargaining process. Traditionally, the bargaining power in the *Rubinstein-Stahl's* model is defined as follows

$$\delta = e^{-\xi\times\Delta}, \qquad s.t., \xi > 0 \quad (4)$$

where Δ is the time period of the negotiation round. Given the Δ is fixed (i.e., *unit_time*), δ is monotonic decreasing with the ξ. ξ is an instantaneous discount factor to adaptively adjust the bargaining power.

Especially, Rubinstein bargaining model provides a solution of a class of bargaining games that features alternating offers through an infinite time horizon. For a long time, the solution to this type of bargaining game was a mystery. Therefore, Rubinstein's solution is one of the most influential findings in cooperative game theory [11].

III. PROPOSED SCHEME

In this section, the proposed scheme is explained in detail. The proposed scheme is designed to provide an effective resource allocation for CR network. The main objective of our

 ISBN: 978-1-61208-456-5

scheme is to maximize social welfare by the optimal resource allocation.

A. Bargaining process for distribution of resources

In CR network, SUs use the spectrum bandwidth that should not have interference. Due to this reason, only SUs who are in available interference distance can use spectrum bandwidth. To secure enough interference distance, SUs are grouped as clusters by exchanging SU's distance information, and can guarantee the mutual interference. The SUs are clustered as follows, i) all SUs exchange their distance information and perform the cluster operation only with SUs that are in their mutual interference, ii) in each cluster, leaders are selected by random process, iii) all SUs in each cluster send request message to leader, iv) leaders in each cluster send cluster request message to administrator, v) the administrator calculates each cluster leader's Signal to Interference plus Noise Ratio (SINR), and allocates allocation sequence number by using SINR.

To allocate the total resource, the administrator starts to bargain with each cluster leader, sequentially. In this paper, Rubinstein bargaining approach is used for the fairness allocation. In the Rubinstein bargaining model, the decision of patience factor values is a key issue. For the SU's patience factor on the aggregated SUs' payoff. If the sum of SU's utility increases, the total system payoff also increases. Therefore, δ_g can be defined as follows

$$\delta_g = \frac{1}{\alpha \times v + \beta \times q + \gamma \times tr}, \quad s.t., \ \frac{d\delta_g(v)}{dv} > 0, \delta_g(0) = 1 \text{ and } \delta_g(\infty) = 0 \qquad (5)$$

where α, β, γ are weighted factors for value (v), importance of traffic (q) and trust value (tr). In the proposed scheme, to provide the fairness for each leader, administrator decides patience factor (δ_A) to be the midpoint of all leaders' payoffs like as

$$\delta_A = \frac{2}{\sum_{j=1}^{m}(g_j(v) + g_j(q) + g_j(tr))} \qquad (6)$$

Based on the obtained δ_g and δ_A values, we can develop the Rubinstein bargaining process. The administrator collects each leader's bandwidth request, and defines each cluster's total request (g) as follows,

$$\mathrm{g}_j = \sum_{i=1}^{n} \mathrm{r}_i \qquad (7)$$

where r_i is the agent i's bandwidth request, and g_j is the cluster j's total request. According to the administrator's offer (x) and cluster j's offer (y), the equilibrium point of Rubinstein bargaining model can be obtained. Finally, the Rubinstein bargaining equilibrium point can be expressed as follows:

$$x^* = \frac{1 - \delta_{g_j}}{1 - \delta_A \delta_{g_j}}, \ y^* = 1 - \frac{1 - \delta_{g_j}}{1 - \delta_A \delta_{g_j}} \qquad (8)$$

In this work, VCG mechanism is used to effectively control selfish users and resource allocation, which can increase a social welfare. However, the main disadvantage of VCG mechanism is the higher computation complexity. To reduce the computation complexity, firstly, we group all SUs into each cluster, and the Rubinstein bargaining model is applied to each cluster, iteratively. According to the Rubinstein bargaining process, we can distribute the total bandwidth resource (R) to each cluster. Finally, the VCG mechanism is used in each cluster to effectively control selfish users and resource allocation, which can increase a social welfare. Our distributed approach is more practical and justified for real network operations.

B. Resource allocation based on trust VCG mechanism

In the VCG model, vector of allocation K is defined as follows

$$\boldsymbol{K} = \{\emptyset, \tau^{1<-allo}, \tau^{2<-allo}, \dots, \tau^{i<-allo}\} \qquad (9)$$

Let $\emptyset$ and $<-allo$ be respective non-allocation and resource allocation, respectively. If the SU i gets the resource ($\mathrm{k}=\tau^{i<-allo}, \boldsymbol{K} = \emptyset$), his cost function ($\mathrm{c}_i(\boldsymbol{K})$) is defined as $\mathrm{c}_i(\tau)$. The total system value function ($v_{allo}(\boldsymbol{K})$) can be defined as $v_{allo}(\boldsymbol{K}) = v_{allo}(\tau)$. We define the vector of successful probability $= [p_1(\tau), \dots, p_i(\tau)]$, and the SU i's successful probability ($p_{\mathrm{i}}(\tau)$) can be defined as the ratio of the total successful task operation ($\sum_{l=1}^{L}(\tau_{l_{success}}^{i})$) to the total task ($\sum_{l=1}^{L}(\tau_l^i)$).

$$p_{\mathrm{i}}(\tau) = \frac{\sum_{l=1}^{L}(\tau_{l_{success}}^{i})}{\sum_{l=1}^{L}(\tau_l^i)}, \qquad s.t., (p_{\mathrm{i}}(\tau) \in [0,1] \qquad (10)$$

where τ_l^i represents whether the task allocation is allocated (0) or not (1), and $\tau_{l_{success}}^{i}$ represents whether the task is successfully operated or not. The expected value function ($\bar{v}_{allo}(\boldsymbol{K}, p)$) is defined based on the probability $p_{\mathrm{i}}(\tau)$.

$$\bar{v}_{allo}(\boldsymbol{K}, p) = v_{allo}(\boldsymbol{K}) \times p_i(\tau) \qquad (11)$$

Each SU should send his own information about the probability ($\hat{p}$) and cost function ($\hat{c}$) to the administrator. At the same time, each SU also can send the un-trust information ($\hat{c}, \hat{p}$) to maximize his profit. In the proposed scheme, the resource allocation is adaptively controlled based on the accurate analysis of costs and payoffs. In more detail, the

 ISBN: 978-1-61208-456-5

resource is allocated to the most suitable SU while maximizing the system efficiency.

$$k^*(\hat{c},\hat{p}) = arg\max_{k\in K}\left[\bar{v}(\boldsymbol{K},\hat{p}) - \sum_{i\in I}\hat{c}_i(\boldsymbol{K})\right] \quad (12)$$

Similar to the traditional VCG mechanism, the payoff of each SU is defined as the marginal contribution of the selected SU to the CR system; it is extracted by comparing the second best decision, excluding the selected SU. Without the best SU, the second-best expected payoff for the CR service, which allocates resource can be obtained as follows by considering success and fail cases.

$$\begin{aligned}\bar{u}_i(\hat{c},\hat{p}) = p_i(\tau)\Bigg[&v_{allo}\big(\boldsymbol{K}^*(\hat{c},\hat{p})\big) - c_i\big(\boldsymbol{K}^*(\hat{c},\hat{p})\big)\\ &- \max_{\boldsymbol{K}'\in\boldsymbol{K}_{-i}}\Big(\bar{v}_{allo}(\boldsymbol{K}',\hat{p}) - \sum_{j\in I_{-i}}\hat{c}_j(\boldsymbol{K}')\Big)\Bigg]\\ &+ \big(1-p_i(\tau)\big)\Bigg[-c_i\big(\boldsymbol{K}^*(\hat{c},\hat{p})\big)\\ &- \max_{\boldsymbol{K}'\in\boldsymbol{K}_{-i}}\Big(\bar{v}_{allo}(\boldsymbol{K}',\hat{p}) - \sum_{j\in I_{-i}}\hat{c}_j(\boldsymbol{K}')\Big)\Bigg]\\ = \bar{v}_{op}\big(\boldsymbol{K}^*(\hat{c},\hat{p}),p\big) &- c_i\big(\boldsymbol{K}^*(\hat{c},\hat{p})\big)\\ &- \max_{\boldsymbol{K}'\in\boldsymbol{K}_{-i}}\Big(\bar{v}_{allo}(\boldsymbol{K}',\hat{p}) - \sum_{j\in I_{-i}}\hat{c}_j(\boldsymbol{K}')\Big) \quad (13)\end{aligned}$$

where $\boldsymbol{K}_{-i}$ is a set of allocation without the SU i. With probability $(p_i(\tau))$, the expected utility $(\bar{u}_i(\hat{c},\hat{p}))$ is achieved based on the expected marginal contribution, which is the difference between the best and the second-best expected utility.

IV. Performance Evaluation

In this section, the effectiveness of the proposed scheme is validated through simulation. To emulate a real-world CR environment and for a fair comparison, we carefully select the system parameters as shown in Table 1. Using our simulation model, the performance of the proposed scheme is compared with the two CR resource allocation schemes; the traditional VCG scheme [12] and the single TBMs scheme [13].

TABLE I. System Parameter

Name	Value
Size of network	1000m × 1000m
Number of node	10 ≤ node ≤ 25
Distance of inteference	100m ≤ Distance ≤ 300m
QoS value	Qos ≤ 1
Trust value	Trust ≤ 5
Utility value	10 ≤ utility ≤ 30
Number of iterations	100

Usually, the performance of CR systems depends on the sum of SUs' payoff, total system payoff, the SUs' satisfaction and task succession probability. In this paper, the performance measures are plotted as the number of SUs.

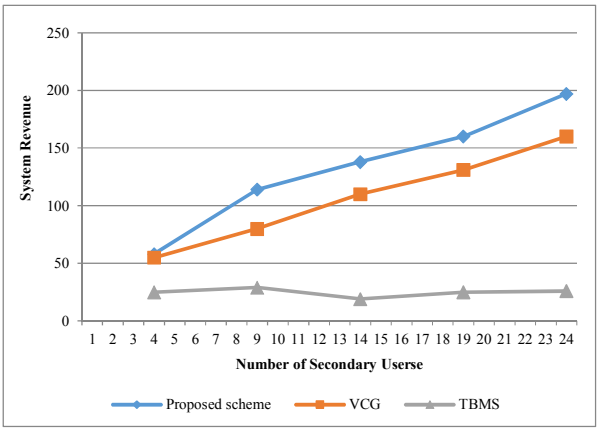

Figure. 1. Total system efficiency due to the number of SUs

In Figure 1, the system revenues of each scheme are compared to each other. System revenue is estimated as the total sum of successful SU task profits. From the service providers' point of view, it is a very important performance factor. From the simulation results, we can see that the system revenue of our proposed scheme is higher than the other existing schemes.

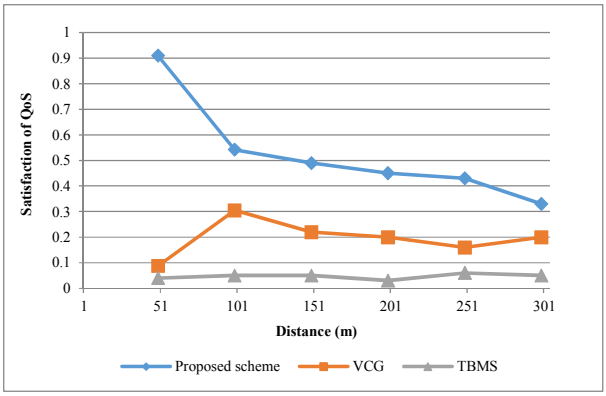

Figure. 2. Satisfaction of QoS with interference

Figure 2 shows the QoS satisfaction of SUs. From the viewpoint of SUs, QoS satisfaction is a critical issue. Usually, QoS evaluation factors are availability (uptime), bandwidth (throughput), latency (delay), error rate, and so on. However, as mentioned earlier, the proposed scheme is designed to

concentrate on the social welfare aspect of bandwidth allocation. Therefore, the total amount of allocated bandwidth for successful task is assumed as a major QoS satisfaction

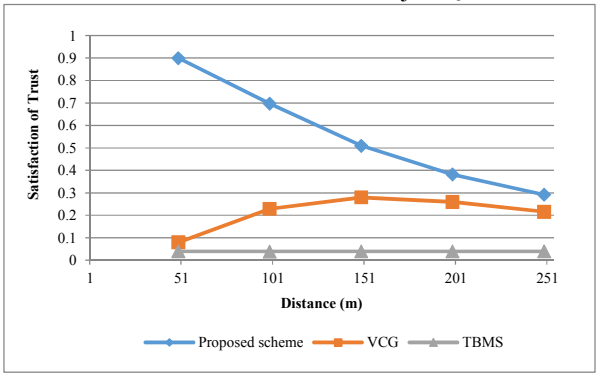

factor. Under various operation times or the number of SUs, the proposed scheme can provide much better QoS satisfaction than other schemes.

Figure. 3. Satisfaction of Trust with distance

Figure 3 shows the performance evaluation about trust satisfaction. When the administrator allocates the spectrum resource, trust satisfaction for all SUs is obtained. These results represent the system's satisfaction. Our proposed scheme considers the trust value, QoS satisfaction and SU's utility. Therefore, the proposed scheme can maintain a better trust satisfaction than other existing schemes.

V. CONCLUSION

Recently, the design of effective CR management algorithms has been one of intense research issues. In this paper, we propose a new adaptive bandwidth management scheme based on the VCG mechanism and Rubinstein bargaining model. Based on the SU's payoff, QoS and trust information, the proposed scheme can dynamically allocate the total bandwidth resources while maximizing PU`s profit. In addition, we make a control decision in a distributed manner. This distributed approach can reduce the excessive computation complexity of original VCG mechanism. It is a highly desirable feature for real-world CR system operations. Simulation results show that the proposed scheme can provides much better system performance than the existing schemes.

ACKNOWLEDGMENT

This research was supported by the MSIP (Ministry of Science, ICT and Future Planning), Korea, under the ITRC (Information Technology Research Center) support program (IITP-2015-H8501-15-1018) supervised by the IITP (Institute for Information & communications Technology Promotion).

REFERENCES

[1] D. Cabric, S. M. Mishra, and R. W. Brodersen, "Implementation issues in spectrum sensing for cognitive radios", IEEE signal Systems and Computers Conference, vol.l, November 2004, pp. 772-776.

[2] S. Haykin, "Cognitive radio: brain-empowered wireless communications", IEEE Journal on Selected Areas in Communications, vol.23, no.2, February 2005, pp. 201-220.

[3] S. Gandhi, C. Buragohain, C. Lili, Z. Haitao, and S. Suri, "A General Framework for Wireless Spectrum Auctions", New Frontiers in Dynamic Spectrum Access Networks 2nd IEEE International Symposium, April 2007, pp. 22-23.

[4] D. C. Parkes, "Computational Mechanism Design", Lecture notes of Tutorials at 10th Conference on Theoretical Aspects of Rationality and Knowledge, December 2008, pp. 4-82.

[5] J. Leino, Applications of Game Theory in Ad Hoc Networks, Master's Thesis, Helisnki University of Technology, 2003.

[6] M. Dirani and T. Chahed, "Framework for resource allocation in heterogeneous wireless networks using game theory", in: EuroNGI Workshop, 2006, pp. 144–154

[7] D. Lucking-Reiley, "Vickrey Auctions in Practice: From Nineteenth Century Philately to Twenty-first Century E-commerce", The journal of Economic Perspectives, July 2000, pp. 183-192.

[8] D. C. Parkes and J. Shneidman, "Distributed Implementations of Vickrey-Clarke-Groves Mechanisms", Proceedings of the Third International Joint Conference on Autonomous Agents and Multiagent Systems, July 2004, pp. 261-268.

[9] B. Xie, W. Zhou, C. Hao, X. Ai, and J. Song, "A Novel Bargaining Based Relay Selection and Power Allocation Scheme for Distributed Cooperative Communication Networks", Vehicular Technology Conference Fall(VTC 2010-Fall), 2010 IEEE 72nd, September 2010, pp. 1-5.

[10] R.K. Dash, D.C. Parkes, and N. R. Jennings, "Computational Mechanism Design: A Call to Arms", IEEE Intelligent Systems, November 2003, pp. 40-47.

[11] Sungwook Kim, Game Theory Applications in Network Design, IGI Global, 2014

[12] Y. Wu, B. Wang, K. J. Ray Liu, and T. Charles Clancy, "A Multi-Winner Cognitive Spectrum Auction Framework with Collusion-Resistant Mechanisms" IEEE Symposium, New Frontiers in Dynamic Spectrum Access Networks Conferences, October 2008, pp. 1-9.

[13] S. D. Ramchurn, et al., "Trust-Based Mechanisms for Robust and Efficient Task Allocation in the Presence of Execution Uncertainty", Journal of Artificial Intelligence Research, vol.35, May 2009, pp. 119-159.

 ISBN: 978-1-61208-456-5

Exploring the Impact of Node Cooperation Level on Routing in Cognitive Radio Networks

Ling Hou, Angus K. Y. Wong
School of Science and Technology
The Open University of Hong Kong (OUHK)
HKSAR, China
e-mail: lhou@ouhk.edu.hk, akywong@ouhk.edu.hk

Alan K. H. Yeung
Department of Electronic Engineering
City University of Hong Kong
HKSAR, China
e-mail: eeayeung@cityu.edu.hk

***Abstract*—In this paper, we analyze the effect of different degrees of node cooperation on the performance of routing protocols for cognitive radio networks. We first present an analytical model of the routing performance in terms of expected end-to-end packet delivery ratio (PDR) for cognitive radio networks with uncooperative node behaviors. We also performed extensive simulations to evaluate the analytical model. The simulation results show that Optimal Primary-Aware Route Quality Protocol (OPERA) could provide better PDR performance under higher degrees of network cooperation and Shortest Path First routing protocol (SPF) works better under lower cooperation degrees. Finally, our results suggest that even a modest level of node cooperation is sufficient to achieve significant performance improvement with respect to the fully non-cooperative network in which all secondary users are selfish.**

Keywords- node selfishness; cognitive radio; routing.

I. INTRODUCTION

The cognitive radio paradigm [1][2] has attracted much attention in the research and industrial community in recent years. Different from conventional spectrum regulation paradigms in which the spectrum is allocated to fixed licensed users (or primary users) for exclusive use, a cognitive radio system permits unlicensed users (or secondary users) to utilize idle spectrum in a dynamic manner. In cognitive radio networks (CRNs), the secondary users (SUs) should sense the spectrum environment, find available spectrum channels and utilize them without interfering the transmission of primary users (PUs) [3].

Communication is opportunistic in CRNs because SUs can transmit in the spectrum channels if PUs are not using them. Meanwhile, connectivity is intermittent due to the unpredictable node mobility. Therefore, to ensure routing services, nodes are requested not only to act as packet forwarders but also to perform spectrum sensing. That means, both energy and computing resources, which are very limited in a typical mobile node, have to be sacrificed for the other nodes' good. Hence, some SUs show lower degree of node cooperation with a selfish motivation to save their own resources [4][5][6]. It will lead to the failure of most existing routing protocols. This is because most existing routing protocols operate under the assumption that all SUs are fully cooperative in the routing operations [6].

Since routing is the most important network functionality in CRNs, in this paper we focus our attention on evaluating the impact of node cooperation level on routing performance in terms of end-to-end packet delivery ratio (PDR). First, we present a theoretical framework for studying the effects of different node cooperation levels for proactive routing protocols. Then, we perform extensive simulations to evaluate the theoretical analysis model. More specifically, we consider three common CRN routing protocols, including Shortest Path First (SPF) [7], Spectrum Aware Mesh Routing Protocol (SAMER) [8], and Optimal Primary-Aware Route Quality Protocol (OPERA) [9]. The main findings of this evaluation are: i) OPERA has the potential to provide the best packet delivery ratio in presence of reduced node cooperation levels; and ii) even a modest level of node cooperation is sufficient to achieve a considerable performance improvement over the fully non-cooperative scenarios.

The rest of this paper is organized as follows. Section II describes the system model. In Section III, we give the analysis framework, and derive the expected Packet Delivery Ratio (PDR) of routing under different degrees of cooperation. In Section IV, we validate the accuracy of our system model by simulation. Finally, we conclude this paper in Section V.

II. SYSTEM MODEL

We consider a CRN with a set of SUs, which is denoted by V. There exist M primary users, which are indexed by 1, 2, … , M. Each PU n holds a licensed frequency channel n and the probability that PU n is active on its channel is denoted by λ_n. And each PU n has a interference range R_n. A SU could utilize channel n, if the SU is not in the interference boundary of PU n or PU n is not active. Then, the CRN could be modeled as a direct graph:

$$G(t) = (V, E), \quad (1)$$

where a vertex $v_i \in V$ denotes a SU, and an edge $e_{ij} \in E$ denotes the presence of at least one communication link e_{ij}^n from SU v_i to SU v_j through the channel n:

$$e_{ij} = 1 \Leftrightarrow \exists n \in \{1,2,\dots,M\}, s.t.\ e_{ij}^n = 1 .$$

 ISBN: 978-1-61208-456-5

Considering the uncooperative behaviors we study in this paper, we cluster the SUs into two groups respectively denoted by V_1 and V_2, where V_1 denote the selfish SUs and V_2 denote the selfless SUs. Let $\gamma = |V_1| / |V|$ denote selfish SU intensity in the CRN where $|V_1|$ means the number of SUs in V_1 and $|V|$ means the total number of nodes in the network.

To model cooperation level of SUs in this paper, we define a cooperation value for each SU by the probability with which it would forward packets from other SUs. Let ρ_i denote the cooperation value of a SU v_i, where $v_i \in V$. In this paper, we assume that SUs in V_2 will always forward packets from other nodes. Therefore, for $v_i \in V_2$, $\rho_i = 1$.

III. PERFORMANCE ANALYSIS

In this section, we characterize the expected Packet Delivery Ratio (PDR) of routing under different degrees of cooperation. For mathematical tractability, we only consider the routing protocols with which routes are determined in proactive manner. Let $D_{i,j}$ denote the event that a packet is generated for a source-destination (v_i, v_j). Denote the route determined for the source-destination (v_i, v_j) by the ordered set $L = \{l_1, l_2, \ldots, l_{|L|}\}$, where $l_k \in L$ denote the index of the k^{th} SU along the route, $l_1 = i$, and $l_{|L|} = j$. For simplicity, we also use l_k to denote the SU v_{l_k}.

In the CRN, whether a packet could be successfully delivered to the destination is dependent on the effect of the PU, SU mobility and/or SU cooperation level. Therefore, we measure the expected end-to-end PDR by explicitly accounting for the effect of the relative movement between two SUs, the relative movement between SU and PU, and the cooperation value of SU.

A. Packet Delivery Ratio over a Link

Let D_{l_k} denote the event that a packet sucessfully arrives at SU l_k. Now we consider the next hop from SU l_k to SU l_{k+1}. Evaluating the expected PDR over the link from SU l_k to SU l_{k+1} is equivalent to computing the conditional probability of the event "the packet is sucessfully received at SU l_{k+1}". Given D_{l_k}, then whether the packet could be successfully transmitted to SU l_{k+1} is totally dependent on the state of the communication link between SU l_k to SU l_{k+1}. If the link is connected and not affected by PU activity, then the packet could be transmitted to SU l_{k+1}. But whether SU l_{k+1} would like to accept the packet and forward it to the next hop is totally dependent on its cooperation value.

We denote the probability that the link between SU l_k and SU l_{k+1} being connected by $\alpha_{k,k+1}$. The calculation of $\alpha_{k,k+1}$ is similar to that in wireless networks, which has been extensively studied by considering the relative movement between two mobile nodes. In this paper, we adopt the approach introduced in [10] to calculate $\alpha_{k,k+1}$. Since the calculation procedure is complex, we do not give an explicit expression of $\alpha_{k,k+1}$. Please refer to [10] to learn more.

Let δ_k^n denote the probability that a SU l_k enters into the interference boundary of PU n. A SU entering into the interference boundary of a PU means that the relative distance between the SU and the PU is less than the interference range of the PU. Similarly to the calculation of $\alpha_{k,k+1}$, we can obtain the probability δ_k^n. The activity of PU n can interfere with the communications between SU l_k and SU l_{k+1} if either SU l_k or SU l_{k+1} enters into the interference boundary of PU n. We use $\delta_{k,k+1}^n$ to denote the probablity that the activity of PU n can interfere with the communications between SU l_k and SU l_{k+1}. Then, the probability $\delta_{k,k+1}^n$ can be calculated by:

$$\delta_{k,k+1}^n = 1 - (1 - \delta_k^n)(1 - \delta_{k+1}^n) \quad (2)$$

Channel n is not available for communication between SU l_k and SU l_{k+1}, if the activity of PU n can interfere with the communications between them and PU is active on channel n. We use spectrum availability $\beta_{k,k+1}^n$ to denote the probability that channel n is available for communication link between SU l_k and SU l_{k+1} to use. Therefore, spectrum availability $\beta_{k,k+1}^n$ could be given as:

$$\beta_{k,k+1}^n = 1 - \delta_{k,k+1}^n \lambda_n \quad (3)$$

where, $\delta_{k,k+1}^n$ is given in (2), and λ_n is the activity probablity of PU n on channel n. And if no channel is avaialble for communication between SU l_k and SU l_{k+1}, then the transmission would be blocked. Let $\beta_{k,k+1}$ denote the block probability due to spectrum unavailability. Then, the block probability $\beta_{k,k+1}$ can be calculated by:

$$\beta_{k,k+1} = \prod_{n=1}^{M} (1 - \beta_{k,k+1}^n) \quad (4)$$

For simplicity, we assume that the relative movement between SU l_k to SU l_{k+1}, the spectrum availability and the cooperative levels of SU l_{k+1} are independent. Therefore, the expected packet delivery ratio over a link from SU l_k to SU l_{k+1} is given by (5), where $\rho_{l_{k+1}}$ is the cooperation value of SU l_{k+1}.

Remark. The expected packet delivery ratio (5) allows us to estimate the packet delivery ratio sent over a link by accounting for three main factors that affect the transmission of this link: (1) the SU movement, via the probability $\alpha_{k,k+1}$; (2) the PU characteristics, via the probability $\beta_{k,k+1}$; (3) the cooperation level of next hop, via cooperation value $\rho_{l_{k+1}}$. Notice that at the last hop, since the receiver of the last hop is the destination, it will always be willing to receive the packet. From (5), we can notice that the smaller is $\rho_{l_{k+1}}$, the smaller is the packet delivery ratio. Thus, the coopeartion value of the SUs should be considered into the route selection.

 ISBN: 978-1-61208-456-5

$$\theta_{k,k+1} = P\left(D_{l_{k+1}} | D_{l_k}\right) = \begin{cases} \alpha_{k,k+1}\left(1-\beta_{k,k+1}\right)\rho_{l_{k+1}}, if\ k < |L|-1 \\ \alpha_{k,k+1}\left(1-\beta_{k,k+1}\right), if\ k = |L|-1 \end{cases} . \quad (5)$$

B. End-to-End Packet Delivery Ratio

Based on the aforementioned work, we now derive the analytical expression of end-to-end packet delivery ratio. Evaluating the end-to-end PDR for the source-destination (v_i, v_j) is equivalent to computing the probability of the event "a packet generated at an SU v_i is successfully delivered to destination v_j". Thus, we have

$$PDR_{i,j} = P\left(D_j | D_{i,j}\right) = \prod_{k=1}^{|L|} P\left(D_{l_{k+1}} | D_{l_k}\right) . \quad (6)$$

Then the expected end-to-end delay over the whole network is calculated as:

$$\overline{PDR} = \sum_{v_i, v_j \in V} P\left(D_{i,j}\right) PDR_{i,j} , \quad (7)$$

where $P(D_{i,j})$ is the probability that a message is generated for the source-destination (v_i, v_j). It could be estimated based on the number of packets generated between v_i and v_j in the past. In this paper, we assume that the source-destination pairs are randomly selected among all SUs. Then, $P(D_{i,j}) = 1/|V|(|V|-1)$.

IV. MODEL VALIDATION

In this section, we evaluate our analysis by comparing the theoretical results obtained based on our model with the simulation results, which are obtained by simulating the packet dissemination under three different routing protocols for CRNs (i.e., SPF, SAMER, and OPERA) with different cooperation levels.

A. Simulaiton Setting

In our simulation, the network topology consists of 50 SUs randomly distributed in a square area of the side of 500 m. All the SUs are mobile and follow the random walk mobility (RWM) model [11], in which each SU's movement consists of a sequence of random length intervals called mobility epochs. During an epoch, a SU moves in a constant direction at a constant speed. The speed and direction of mobile during each epoch is uniformly distributed over (0, 20m/s) and (0, 2π) respectively. The transmission ranges of SUs are set to be 30m.

In the simulated area, there are 10 PUs and each PU possesses a licensed channel. Each channel n is utilized by a PU with a probability $\lambda_n \in [0.05, 0.95]$. And the interference ranges of PUs are all set to be 50m.

We vary the selfish SU intensity γ from 0.0 to 1.0 with step of 0.1. We will also vary the cooperation value ρ_i of selfish SUs with two different values: 0 and 0.5. For each value of γ and ρ_i, we run the simulation for 1000 times.

B. Simulation Results

Simulation results are shown as below. Figure 1 shows the expected end-to-end packet delivery ratio vs. γ for SPF protocol with values of γ from 0.0 to 1.0. Figure 2 shows the results for SAMER protocol and Figure 3 shows the results for OPERA protocol.

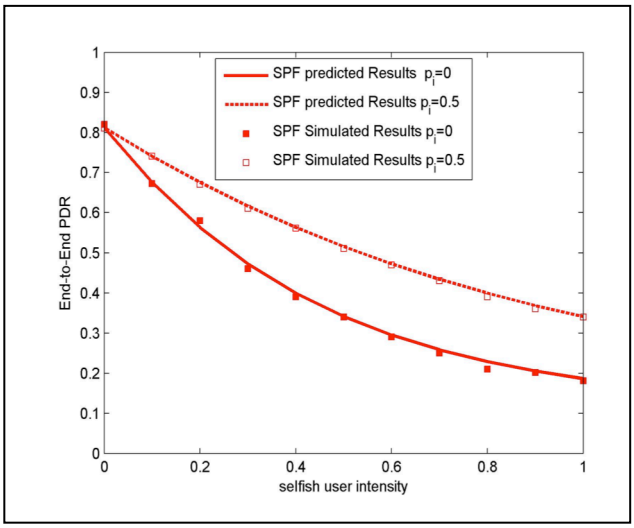

Figure 1. End-to-end PDR with SPF routing v.s. selfish user intensity.

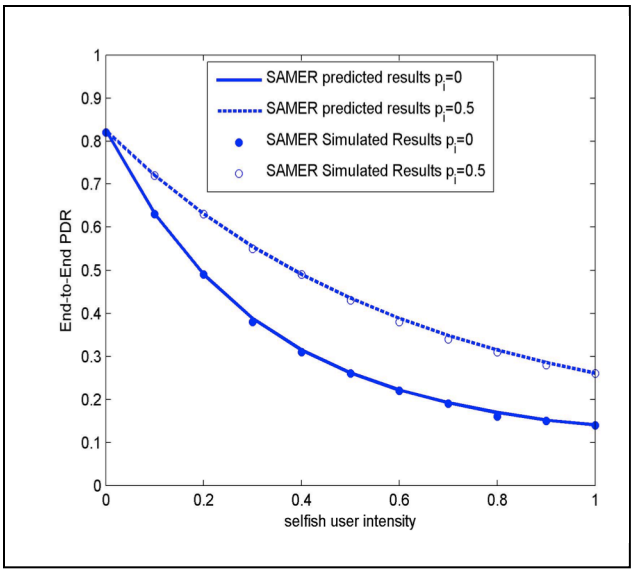

Figure 2. End-to-end PDR with SAMER routing v.s. selfish user intensity.

From the results, we first note that there is a very good agreement between the theoretical and the experimental results for two different cooperation values under SPF, SAMER and OPERA protocols.

 ISBN: 978-1-61208-456-5

Second, we could find that for all three protocols, the expected end-to-end PDR decreases as the number of selfish nodes increases. Thus, to provide efficient routing performance for CRNs, it is necessary to incorporate selfish node detection mechanisms into routing protocol.

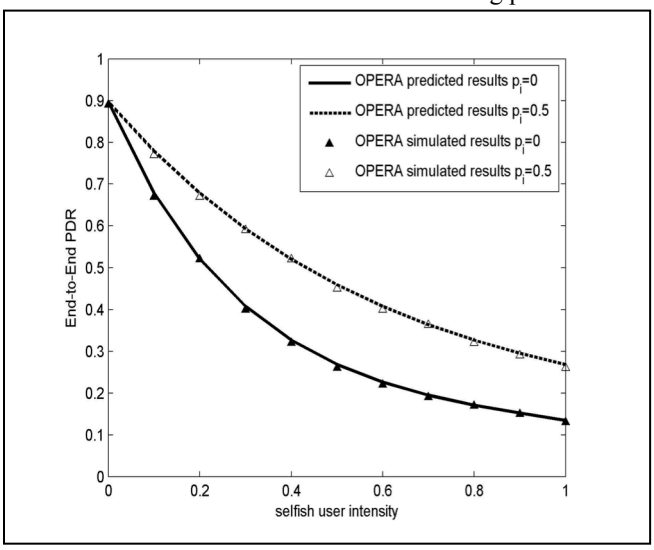

Figure 3. End-to-end PDR with OPERA routing v.s. selfish user intensity.

Moreover, through comparison between results of different routing protocols, we can find that OPERA is able to provide the best packet delivery ratio in cases with higher cooperative level (lower selfish SU intensity γ and higher cooperation value). But when the selfish SU intensity γ increase to almost 1 and the cooperation value becomes 0, SPF protocol performs better than OPERA.

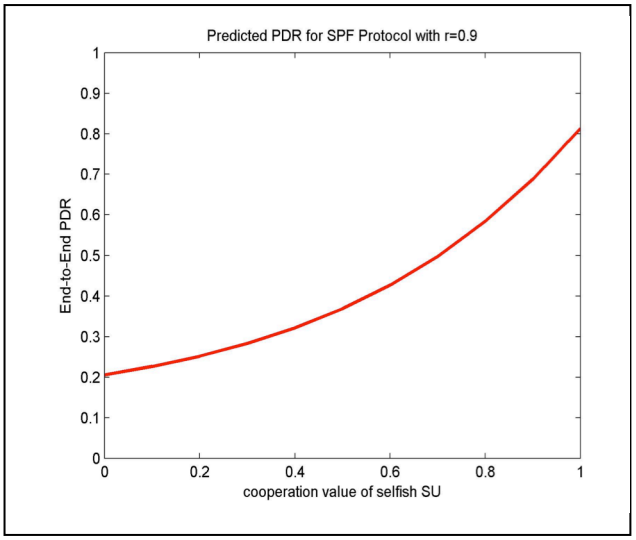

Figure 4. End-to-end PDR with OPERA routing v.s. coperation value.

We also give the results for SPF protocol with different values of ρ_i from 0.0 to 1.0 in Figure 4. From Figure 4, we also find that a modest level of increase in node cooperation is sufficient to achieve a considerable performance improvement in packet delivery ratio. Thus, it is essential to enhance the cooperation willingness of SUs in order to provide efficient routing performance, such as introduce some reward-and-penalty mechanism.

V. CONCLUSISON

In this paper, we characterized the performance of proactive routing protocols for CRNs under different levels of node cooperation. We also perform extensive simulations to validate our analysis. The simulation results give some insights into future routing protocol designs for CRNs, such as incorporate selfish node detection mechanisms and reward-and-penalty mechanism into routing protocols. In the future work, we will focus on applying our conclusions to CRNs.

ACKNOWLEDGMENT

The work described in this paper was fully supported by a grant from the Research Grants Council of the Hong Kong SAR, China (UGC/FDS16/E05/14).

REFERENCES

[1] S. Haykin, “Cognitive radio: brain-empowered wireless communications,”, IEEE Journal on Selected Areas in Communications, vol. 23, iss. 2, 2005, pp. 201–220.

[2] J. Mitola III and G. Q. Maguire, Jr., “Cognitive Radio: Making Software Radios More Personal,” IEEE Personal Commun., vol. 6, no. 4, Aug. 1999, pp. 13–18.

[3] M. Cesana, F. Cuomo, and E. Ekici, “Routing in cognitive radio networks: challenges and solutions,” Elsevier Ad Hoc Network Journal, vol. 9, no. 3, 2011, pp. 228–248.

[4] S. Bayhan and J. Kangasharju, “Extending cognitive radios with new perspectives,” Proc. Sixth International Conference on Ubiquitous and Future Networks (ICUFN’2014), July 2014, pp. 363-368.

[5] Y. Xing and R. Chandramouli, “Human behavior inspired cognitive radio network design,” IEEE Communications Magazine, vol. 46, iss. 12, 2008, pp. 122–127.

[6] K. C. How, M. Ma, and Y. Qin, “An altruistic differentiated service protocol in dynamic cognitive radio networks against selfish behaviors,” Elsevier Computer Networks, vol. 56, iss. 7, 2012, pp. 2068–2079.

[7] X. W. Zhou, L. Lin, J. P. Wang, and X. S. Zhang, “Cross-layer Routing Design in Cognitive Radio Networks by Colored Multigraph Model,” Wireless Personal Communications, vol. 49, no. 1, 2009, pp.123–131.

[8] I. Pefkianakis, et al., “SAMER: spectrum aware mesh routing in cognitive radio networks,” 3rd IEEE Symposium on New Frontiers in Dynamic Spectrum Access Networks (DySPAN 2008)., Chicago, IL, 14-17 Oct. 2008, pp. 1–5.

[9] M. Caleffi, I.F. Akyildiz, and L. Paura, “OPERA: Optimal Routing Metric for Cognitive Radio Ad Hoc Networks,” IEEE Transactions on Wireless Communications, vo1. 1, iss. 8, 2012, pp. 2884–2894.

[10] Y. B. Bai and L. Gong, “Link availability prediction with radio irregularity coverage for mobile multi-hop networks,” IEEE Communications Letters, vol. 14, iss. 1, 2010, pp. 518–520.

[11] T. Camp, J. Boleng, and V. Davies, “A survey of mobility models for ad hoc network research,” Wireless Communications Mobile Computing , vol. 25, 2002, pp. 483–502.

 ISBN: 978-1-61208-456-5

Optimal Action for Cognitive Radio User under Constrained Energy and Data Traffic Uncertainty

Hiep Vu-Van, Young-Doo Lee and Insoo Koo
School of Electrical Engineering
University of Ulsan, Ulsan, South Korea
Email: vvhiep@gmail.com, leeyd1004@naver.com and iskoo@ulsan.ac.kr

***Abstract*—In cognitive radio network, cognitive radios should operate with a small battery. Operation schedule for cognitive radio user (CU) strongly affects performance of a device with a finite capacity battery. An energy harvester that harvests energy from the environment to recharge the battery can be utilized to extend the lifetime of the CU. While the CU consumes a similar energy for sensing and transmitting data in all active slots, its reward (i.e., throughput) may not be the same because of different data traffic (i.e., the amount of data that needs to be transmitted). Therefore, in order to maximize performance of the cognitive radio network, the CU needs to consider the current data traffic to determine its optimal action policy in terms of sleeping or active. In this paper, we formulate the problem of choosing an action by the CU by using a partially observable Markov decision process (POMDP) in which the CU's three states in terms of data traffic, belief and remaining energy are utilized as main factors to decide an optimal action of the CU in current time slot, and the effect of current action to future reward will be considered through POMDP. Simulation results prove the efficiency of the proposed scheme.**

***Keywords*—cognitive radio; energy harvesting; energy efficiency; optimal action policy; POMDP.**

I. INTRODUCTION

Cognitive radio (CR) technology can improve spectrum utilization by allowing cognitive radio users (CU) to share the frequency assigned to a licensed user, called the primary user (PU). In order to avoid interference with the operation of the licensed user, the CU is allowed to be active only when the frequency is free. Otherwise, when the presence of the PU is detected, the CU has to vacate their occupied frequency.

In the CR network, the CU often has a small battery that can maintain operations of the CU in a short time. Therefore, the performance of the CR network strongly depends on how effectively the CU uses its electric power. The problem of optimal energy management has been considered previously in [1], [2] where an optimal energy management scheme for a sensor node with an energy harvester to maximize throughput was proposed. In [3], [4], a scheme to find an optimal action policy including sleeping to save energy or active to take opportunity of transmitting data is proposed. Due to the energy-constrained of the CU, the proposed scheme applies the partially observable Markov decision process (POMDP) [5], [6] to determine that optimal action policy.

In most of the previous works, data traffic (i.e., the amount of data that needs to be transmitted) was not considered in order to decide the optimal action for energy efficiency. It is often assumed that the CU always has data to transmit. However, this assumption may be not real in practice. For example, in wireless sensor network, in order to save energy, only the change of data (e.g., the change of monitoring environment) is tracked and reported. In this case, the data traffic varies in time. Therefore, the performance of CR network can be strongly affected by the data traffic. In order to maximize performance of the cognitive radio network, the CU needs to consider the current data traffic to determine its optimal action policy in terms of sleeping or active. In sleeping mode, the CU is silent and waits until the next time slot for another action round. In active mode, the CU first determines the status of the PU signal, if the PU signal is absent, the CU is allowed to access the considered channel to transmit data. If the CU wants to switch to active mode, it must have enough energy for all operations of the mode (i.e., spectrum sensing and data transmitting). In both sleeping and active mode, the CU can harvest energy from the environment to recharge the battery.

In this paper, we formulate the problem of choosing an action by the CU by using a partially observable Markov decision process (POMDP) in which the CU's three states in terms of data traffic, belief and remaining energy are utilized as main factors to decide an optimal action of the CU in current time slot, and the effect of current action to future reward will be considered through POMDP. It is expected that the proposed scheme based on POMDP theory will provide the CR system an improved performance.

This paper is organized as follows. Section 2 describes the system model that we consider in the paper. Section 3 details the proposed optimal action decision scheme based on POMDP. Section 4 introduces simulation models and simulation results of the proposed scheme. Finally, Section 5 concludes this paper.

II. SYSTEM MODEL

We consider a CR network and a PU that is assumed to operate in a time slotted model. The status of the PU changes between two states of the Markov chain model, that is, Presence (P) and Absence (A) as shown in Figure 1. The transition probability of the PU from state P to state A and from state A to itself are defined as P_{PA} and P_{AA}, respectively.

The data that needs to be transmitted is stored in a data buffer of the CU; the amount of data D in the buffer is defined as data traffic of the CU. The buffer can store maximum B_{max} units of data. At the time t, data traffic of the CU can be defined as,

 ISBN: 978-1-61208-456-5

$$D(t) \in \{c_1, c_2, ..., c_{\xi_d}\} \quad (\text{units of data}), \tag{1}$$

where $0 \leq c_1 < c_2 < ... < c_{\xi_d} \leq B_{max}$ and ξ_d is the number of possible states of data traffic.

At each time slot, there are uncertainty amount of data d^{in} coming the buffer. d^{in} can take its values from the set of possible coming data as,

$$d^{in}(t) \in \left\{c_1^{in}, c_2^{in}, ..., c_{\xi_{in}}^{in}\right\} \quad (\text{units of data}), \tag{2}$$

where $0 \leq c_1^{in} < c_2^{in} < ... < c_{\xi_{in}}^{in}$ and ξ_{in} is the number of possible states of coming data.

The probability mass function (PMF) of the coming data is given as follows:

$$P_{d^{in}}(k) = \Pr\left[d^{in}(t) = c_k^{in}\right], \ k = 1, 2, ..., \xi_{in}. \tag{3}$$

We assume that the coming data follows the stochastic process that is marked by the Poisson process. Subsequently, $d^{in}(t)$ is a Poisson random variable with mean d_{mean}^{in}. The PMF in (3) can be equivalent to:

$$P_{d^{in}}(k) \approx \frac{e^{-d_{mean}^{in}}\left(d_{mean}^{in}\right)^k}{k!}, \ k = 1, 2, ..., \xi_{in}. \tag{4}$$

In order to guarantee the security of the primary network, when the CU decides to utilize the channel of the PU, it firstly needs to check the status of the primary network by performing spectrum sensing. Only if no activity from the channel is captured, CU will be allowed to use the channel.

The CU utilizes an energy detector to monitor the activity of the PU. The Gaussian noise is considered in the sensing channel. Therefore, when the number of sensing samples is relatively large (e.g., $M \geq 200$), the received signal energy xE from the detector can be closely approximated as a Gaussian random variable under both hypotheses of the PU signal [7]. So that, we have,

$$xE \sim \begin{cases} \mathrm{N}(M, 2M), & \mathrm{A} \\ \mathrm{N}(M(\gamma+1), 2M(2\gamma+1)), & \mathrm{P} \end{cases}, \tag{5}$$

where γ is the signal-to-noise ratio (SNR) of the sensing channel between the CU and the PU.

According to the received signal energy xE, the decision on the PU status can be made as follows:

$$\begin{cases} G = 1 \,(\text{the PU signal is present}), & \text{if } xE \geq \lambda \\ G = 0 \,(\text{the PU signal is absent}), & \text{otherwise} \end{cases}, \tag{6}$$

where λ is the energy threshold for a local decision.

The sensing performance of the CU can be evaluated by the probability of detection (P_d) and the probability of false alarm (P_f), which are given, respectively, as:

$$P_d = Q\left(\frac{\lambda - M(\gamma+1)}{\sqrt{2M(2\gamma+1)}}\right) \tag{7}$$

and

$$P_f = Q\left(\frac{\lambda - M}{\sqrt{2M}}\right). \tag{8}$$

The main tasks that consume energy of the CU are spectrum sensing and data transmitting. The energy is provided by a rechargeable battery with a finite capacity E_{max} units of energy. The CU can be equipped with a separate energy harvester that can help the CU collect energy from ambient sources (e.g., solar, wind, thermal, vibration) concurrently with other operations. The harvested energy of the current time slot will recharge the battery for powering the CU in the next time slot.

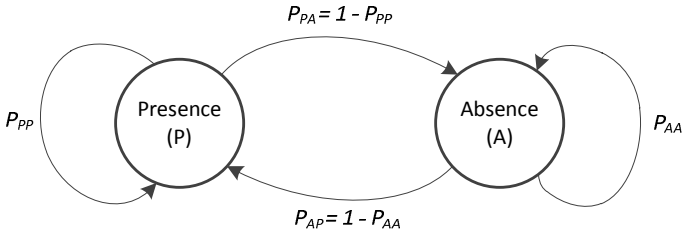

Fig. 1. Markov chain states of the PU.

At the time t, the harvested energy is either $e_h(t) = \{e|0 < e \leq E_{\max}\}$ with probability τ_h or no energy ($e_h(t) = 0$) is harvested with probability $(1 - \tau_h)$. The PMF of the harvested energy can be given as,

$$P_{e_h} = \begin{cases} \tau_h, & \text{if } \mathrm{e}_h = \{e|0 < e \leq E_{\max}\} \\ 1 - \tau_h, & \text{otherwise} \end{cases}. \tag{9}$$

In this paper, we focus on energy efficiency of the CU under uncertain data traffic. There are three main factors affecting the CU throughput in terms of data traffic D, absence probability of the PU signal p (that is defined as *belief* in this paper) and remaining energy e_r. Therefore, we use this information as main factors to decide the optimal action of the CU. At the beginning of the time slot, data traffic and remaining energy are available at the CU, and the information of belief p can be estimated based on statistics of sensing results history of the CU. We define the state of the CU as $S = \{D, p, e_r\}$. Based on the state S, the CU decides its action including silent to save energy or carry out spectrum sensing to take opportunity of transmitting data.

III. Action Decision Based on POMDP Under Uncertain Data Traffic of Cognitive Radio User

In this section, we propose a POMDP-based scheme to find an optimal action policy for the CU in order to maximize its throughout. The CU can take one of two actions as: $\Psi = \{\text{sleeping (S)}, \ \text{active (Ac)}\}$.

- Sleeping mode (S): as a normal device with limited energy resources, if the CU lacks energy for operations (i.e., spectrum sensing and data transmitting), it will keep sleeping and only harvest energy for operation in the next time slots.

- Active mode (Ac): the CU performs spectrum sensing to detect the state of the PU. If the state A of the PU is detected, the CU transmitter will send data to the CU receiver. At the same time, the harvester of the CU will also harvest energy from the environment.

In this paper, we define throughput R (units of data) of the CU as the amount of data successfully transmitting from the CU, then $0 \leq R \leq S_{max}$, where S_{max} is maximum transmission capacity per slot of the CU. The optimal mode

decision policy in terms of sleeping or active is formulated as the framework of POMDP. For POMDP, we define the value function $V(D, p, e_r)$ as the maximum total discounted throughput from the current time slot when the current state of the CU is $S(k) = \{D(k), p(k), e_r(k)\}$ where $D(k)$, $p(k)$ and $e_r(k)$ are data traffic, belief and the remaining energy at the beginning of the k^{th} time slot. The value function is given by:

$$V\left(S\left(k\right)\right) = \max_{a(k)} \mathrm{E}\left\{\sum_{t=k}^{\infty} \alpha^{t-k} R\left(S\left(t\right), a\left(t\right)\right) | S\left(k\right)\right\}, \tag{10}$$

where $0 \leq \alpha < 1$ is the discount factor, $S\left(k\right) = \{D\left(k\right), p\left(k\right), e_r\left(k\right)\}$. $R\left(S(t), a(t)\right)$ is the throughput of the CU achieved at the t^{th} time slot, which is mainly dependent on state $S(t)$ and action decision $a(t)$.

A. Sleeping Mode (ϕ_1)

If the CU decides to remain sleeping, no throughput is achieved, then $R\left(S(t), S\left|\phi_1\right.\right) = 0$.

State $S(t+1) = \{D(t+1), p(t+1), e_r(t+1)\}$ of the CU will be updated for the next time slot. Firstly, data traffic will be updated as,

$$D(t+1) = min\left(D\left(t\right) + d^{in}\left(t\right), S_{\max}\right), \tag{11}$$

with transition probability

$$\Pr\left(D(t) \rightarrow D(t+1) \left|\phi_1\right.\right) = \Pr\left[d^{in}\left(t\right) = c_k^{in}\right], \tag{12}$$

where $k = 1, 2, ..., \xi_{in}$.

Secondly, the belief p is updated as follows,

$$p(t+1) = p(t)P_{AA} + \left(1 - p(t)\right) P_{PA}. \tag{13}$$

Finally, the remaining energy of the battery will be increased as,

$$e_r(t+1) = e_r(t) + e_h\left(t\right), \tag{14}$$

with transition probability

$$\Pr\left(e_r(t) \rightarrow e_r(t+1) \left|\phi_1\right.\right) = \Pr\left[e_h\left(t\right)\right]. \tag{15}$$

B. Active mode

When the CU has enough energy for spectrum sensing and data transmitting (i.e., $e_r > e_s + e_t$), it may decide to be active. In this action mode, the achieved throughput of the system depends on the observations of the CU. In this paper, we define 3 observations for the active mode of the CU as,

Observation 1 *(ϕ_2):* The CU detects that the PU is present (the channel is used by the PU). Then, the CU is not allowed to access the channel and there is no achieved throughput $R\left(S(t), Ac\left|\phi_2\right.\right) = 0$. The probability that ϕ_2 happens is:

$$\Pr\left(\phi_2\right) = p(t)P_f + (1 - p(t))P_d. \tag{16}$$

Data traffic for the next time slot will be updated similarly to the case of observation ϕ_1.

The sensing result can be used to correct belief p in the current time slot as,

$$p^u(t) = \frac{p(t)P_f}{p(t)P_f + (1 - p(t))P_d}. \tag{17}$$

As a result, the updated belief for the next time slot is given by:

$$p(t+1) = p^u(t)P_{AA} + (1 - p^u(t))P_{PA}. \tag{18}$$

The updated remaining energy is obtained as:

$$e(t+1) = e(t) + e_h\left(t\right) - e_s, \tag{19}$$

with transition probability

$$\Pr\left(e_r(t) \rightarrow e_r(t+1) \left|\phi_1\right.\right) = \Pr\left[e_h\left(t\right)\right]. \tag{20}$$

Observation 2 *(ϕ_3):* The CU does not detect any signal from the PU. The CU is allowed to use the channel to transmit data and receive an ACK message. This means that the sensing result is correct (the PU signal is absent) and the CU successfully transmits data. The throughput is achieved as:

$$R\left(S(t), Ac\left|\phi_3\right.\right) = \begin{cases} S_{\max}, & \text{if } D\left(t\right) \geq S_{\max} \\ D\left(t\right), & \text{otherwise.} \end{cases}. \tag{21}$$

The probability that ϕ_3 happens is:

$$\Pr\left(\phi_3\right) = p\left(t\right)\left(1 - P_f\right). \tag{22}$$

Data traffic for the next time slot will be updated as,

$$D(t+1) = min\left(D\left(t\right) + d^{in}\left(t\right) - R\left(S\left(t\right), Ac\left|\phi_3\right.\right), S_{\max}\right), \tag{23}$$

with transition probability

$$\Pr\left(D(t) \rightarrow D(t+1) \left|\phi_1\right.\right) = \Pr\left[d^{in}\left(t\right) = c_k^{in}\right]. \tag{24}$$

where $k = 1, 2, ..., \xi_{in}$.

The belief and remaining energy for the next time slot can be updated, respectively, as:

$$p(t+1) = P_{AA} \tag{25}$$

and

$$e(t+1) = e(t) + e_h\left(t\right) - e_s - e_t, \tag{26}$$

with transition probability

$$\Pr\left(e_r(t) \rightarrow e_r(t+1) \left|\phi_1\right.\right) = \Pr\left[e_h\left(t\right)\right]. \tag{27}$$

Observation 3 *(ϕ_4):* This observation is similar to the observation ϕ_3, state A of the PU is detected and the CU transmits its data. However, the CU can not receive ACK message. This means that the sensing result is incorrect (the PU signal is present), and the transmission data fails, no throughput is achieved, $R\left(S(t), Ac\left|\phi_4\right.\right) = 0$. The probability that ϕ_4 is obtained is:

$$\Pr\left(\phi_4\right) = \left(1 - p\left(t\right)\right)\left(1 - P_d\right). \tag{28}$$

Data traffic for the next time slot will be updated similarly to the case of observations ϕ_1 and ϕ_2.

The belief that the PU in state A at the next time slot is:

$$p(t+1) = P_{PA}. \tag{29}$$

$$V\left(S\left(k\right)\right)=\max_{a_k}\{\sum_{t=k}^{\infty}\alpha^{t-k}\sum_{\phi_i\in a(t)}\Pr\left(\phi_i\right)\sum_{e(t+1)}\Pr\left(e\left(t\right)\rightarrow e\left(t+1\right)|\phi_i\right)\sum_{D(t+1)}\Pr\left(D(t)\rightarrow D(t+1)\,|\phi_i\right)R\left(S\left(t\right),a\left(t\right)|\phi_i\right)|S\left(k\right)\}\,. \tag{30}$$

TABLE I. SIMULATION PARAMETERS

Symbol	Description	Value
γ	SNR of the sensing channel	-10 dB
$\Pr(H_0)$	Average absence probability of the PU	0.5
P_{AA}	Transition probability from state A to itself	0.8
P_{PA}	Transition probability from state P to state A	0.2
E_{ca}	Total capacity of battery	10 units of energy
e_h	Harvested energy	1 units of energy
τ_h	Success probability of energy harvester	0.8
e_t	Transmission energy	2 units of energy
e_s	Sensing energy	1 units of energy
B_{max}	Capacity of data buffer	10 units of data
s_{max}	Transmission capacity	5 units of data
d^{in}_{mean}	Mean value of coming data	1 units of data

The remaining energy of the CU for the next time slot can be updated similar to the case of observation ϕ_3.

According to those observations, the value function in (10) can be expressed as (30). In order to find an optimal mode policy for maximizing throughput, the optimization problem in (30) will be solved by using the *value iterations* method [8].

IV. Simulation Results

In this section, we present simulation results to prove the efficiency of the proposed scheme. *Myopic* scheme only considers the current time slot for the *value function* (i.e., $\alpha = 0$) to decide the CU's action. This means that unless the CU has not enough energy for spectrum sensing and data transmitting or there is no data in the data buffer, *Myopic* scheme will always allow the CU to be active. Simulation results of *Myopic* will be provided for reference. The parameters for simulations are shown in Table I.

In order to evaluate the performance of the proposed scheme, we define *Reward* of the CU as the average number of units of data successfully transmitted in each time slot.

Figure 2 shows the *Reward* of the considered schemes according to the capacity of the CU battery E_{max}. It can be seen that the increase of battery capacity may help the CU achieve higher *Reward*. However, when the battery is big enough (i.e., it has enough space to store all harvested energy), the increase of battery will not affect the *Reward*.

Figure 3 presents the relation between *Reward* and harvested energy e_h of the CU. Higher amount of e_h provide more energy for active mode of the CU, so that the CU can get more *Reward*. However, when e_h is high enough for active mode of the CU in all time, e_h has no more effect on the CU's *Reward*. In this case, the energy constraint will disappear; and then the action of the proposed scheme and *Myopic* scheme will be the same. That is the reason why they have the same performance when the harvested energy is high.

Transmission energy e_t may give strong effect to the *Reward* of the proposed scheme, as shown in Figure 4. More energy is consumed by transmitting data, less *Reward* the CU achieves.

Figures 5 and 6 illustrate the *Reward* according to the change of maximum transmission capacity s_{max} of the CU (i.e., the maximum amount of data that the CU can transmit in whole duration of a time slot) and the change of SNR in the sensing channel, respectively. These figures show that better transmission capacity or better SNR will improve the performance of the proposed scheme.

The simulations results shown in all figures prove that the proposed scheme can offer the CU better performance than the conventional *Myopic* scheme. That benefit of the proposed scheme is achieved by considering future *Reward* on deciding current action.

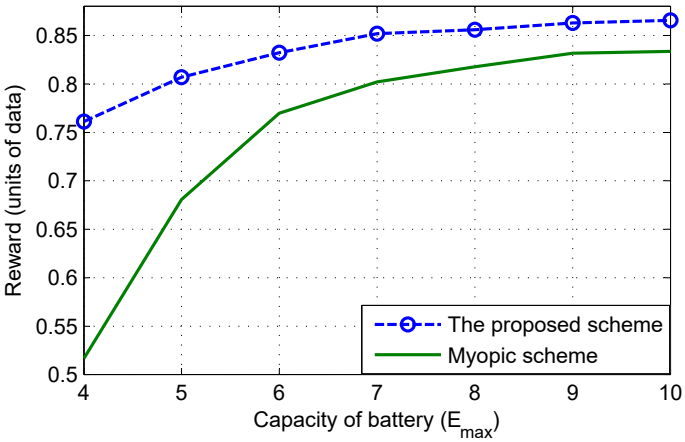

Fig. 2. *Reward* versus battery capacity E_{max}.

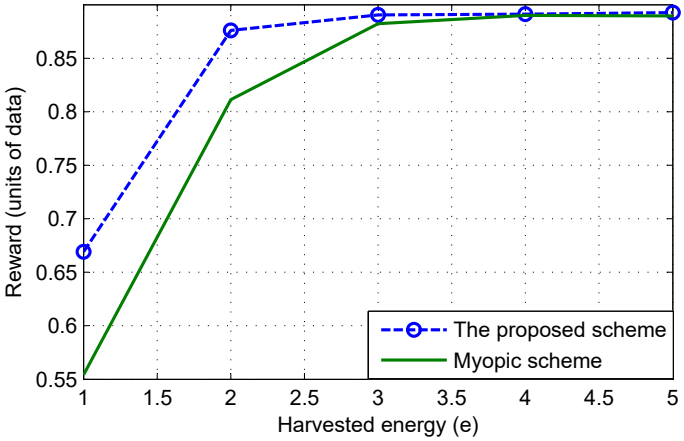

Fig. 3. *Reward* versus harvested energy e_h.

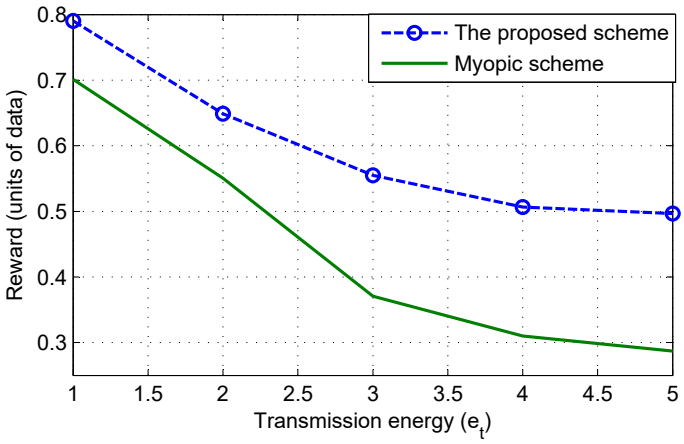

Fig. 4. *Reward* versus transmission energy e_t.

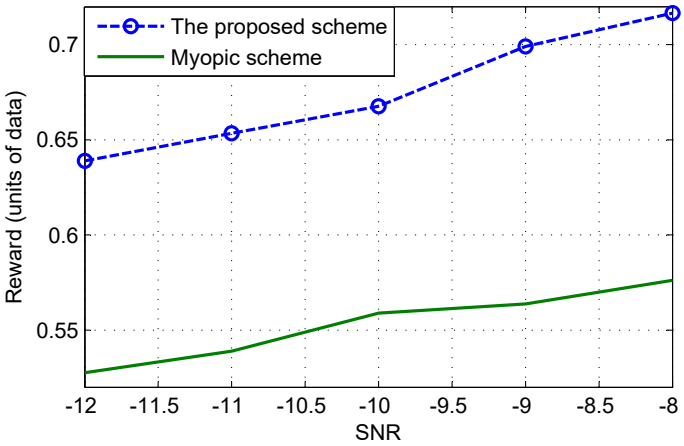

Fig. 6. *Reward* versus SNR of the sensing channel γ.

V. Conclusion

In this paper, we proposed a scheme to decide an optimal action to maximize *Reward* of the CU on energy-constrained and uncertainty data traffic manner. By focusing on uncertainty data traffic, the proposed scheme is more practical than in the previous studies. On the other hand, the proposed scheme can take consideration into the effect of the future *Reward* on current action of the CU by applying POMDP theory. Simulation results show that the proposed scheme can obtain better performance than conventional *Myopic* scheme.

Acknowledgement

This work was supported by the KRF funded by the MEST (NRF-2014R1A1A2005378).

References

[1] V. Sharma, U. Mukherji, V. Joseph, and S. Gupta, "Optimal energy management policies for energy harvesting sensor nodes," *IEEE Transactions on Wireless Communications,*, vol. 9, no. 4, pp. 1326–1336, 2010.

[2] S. Mao, M. H. Cheung, and V. Wong, "An optimal energy allocation algorithm for energy harvesting wireless sensor networks," in *Communications (ICC), 2012 IEEE International Conference on*, 2012, pp. 265–270.

[3] A. Sultan, "Sensing and transmit energy optimization for an energy harvesting cognitive radio," *Wireless Communications Letters, IEEE*, vol. 1, no. 5, pp. 500–503, 2012.

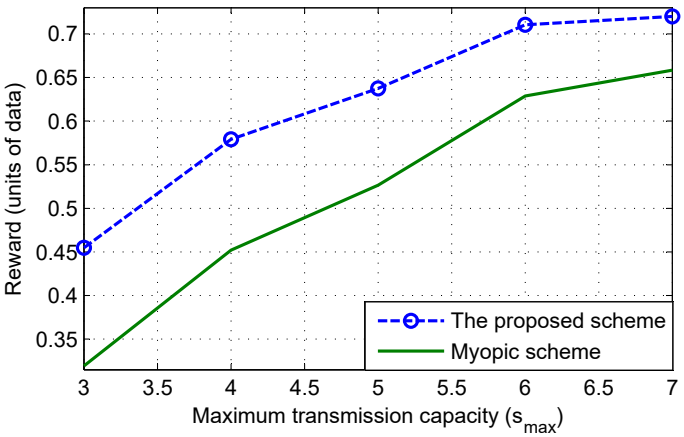

Fig. 5. *Reward* versus maximum transmission capacity s_{max}.

[4] S. Park, J. Heo, B. Kim, W. Chung, H. Wang, and D. Hong, "Optimal mode selection for cognitive radio sensor networks with rf energy harvesting," in *Personal Indoor and Mobile Radio Communications (PIMRC), 2012 IEEE 23rd International Symposium on*, 2012, pp. 2155–2159.

[5] X. Cao and X. Guo, "Partially observable markov decision processes with reward information," in *Decision and Control, 2004. CDC. 43rd IEEE Conference on*, vol. 4, 2004, pp. 4393–4398.

[6] L. P. Kaelbling, M. L. Littman, and A. R. Cassandra, "Planning and acting in partially observable stochastic domains," *ARTIFICIAL INTELLIGENCE*, vol. 101, pp. 99–134, 1998.

[7] J. Ma and Y. Li, "Soft combination and detection for cooperative spectrum sensing in cognitive radio networks," in *IEEE Global Telecommunications Conference (GLOBECOM)*, 2007, pp. 3139–3143.

[8] D. P. Bertsekas, *Dynamic Programming and Optimal Control*. Athena Scientic, 2nd edition, 2001, vol. 1 and 2.

 ISBN: 978-1-61208-456-5

Multi-Antenna Energy Detector Under Unknown Primary User Traffic

Pawan Dhakal and Daniel Riviello
Department of Electronics and Telecommunications
Politecnico di Torino
Torino, Italy
Email: {pawan.dhakal, daniel.riviello}@polito.it

***Abstract*—In cognitive radio (CR) networks, the knowledge of primary user (PU) traffic plays a crucial role in designing the sensing slot duration and synchronization with PU traffic. However, the secondary user (SU) sensing unit usually does not have the knowledge of the exact time slot structure in the primary network. Moreover, it is also possible that the communication among PUs are not based on synchronous schemes at all. In this paper, the effect of unknown primary user (PU) traffic on the performance of multi-antenna spectrum sensing is evaluated under a flat fading channel. In contrast to the commonly used continuous time Markov model of the existing literature, a realistic and simple PU traffic model is proposed which is based only on the discrete time distribution of PU free and busy periods. Furthermore, in order to assess the effect of PU traffic on the detection performance, analytical expressions for the probability density functions of the decision statistic are derived considering Energy Detection (ED) test as spectrum sensing method. It is shown that the time varying PU traffic severely affects the spectrum sensing performance. Most importantly, our results show that the performance gain due to multiple antennas in the sensing unit is significantly reduced by the effect of PU traffic when the mean lengths of free and busy periods are of the same order of magnitude of the sensing slot.**

***Index Terms*—Energy Detection, Unknown Primary Traffic, Spectrum Sensing, Cognitive Radio**

I. INTRODUCTION

By accessing the unoccupied spectrum of licensed band, cognitive radio (CR) based dynamic spectrum sharing (DSS) is initially intended to alleviate the most challenging problems of future wireless communications, namely, spectrum scarcity. With real-time perception of surroundings and bandwidth availability and with the help of spectrum sensing functionality of CR, secondary users (unlicensed users) may dynamically use the vacant spectrum and perform opportunistic transmissions, by adapting the functionality intelligently to accommodate current wireless environments [1]. Thus, the domain of spectrum sensing techniques has long been investigated by many researchers: a detailed bibliography of the contributions in this area can be found in [2], [3]. Despite the significant volume of available literature on spectrum sensing under ideal scenarios, investigation under practical constraints and imperfections are still lacking [3]. Thus, recent research efforts are devoted to improve the accuracy and efficiency of sensing techniques under practical constraints and imperfections.

Currently, most of the existing research on cognitive radio spectrum sensing has been conducted based on the assumption that SUs are perfectly synchronized with PUs, thus providing a solid basis for guaranteeing that PU traffic transitions occur only at the beginning of the SU sensing frames. However, the SUs may not have the knowledge of the exact time slot structure in the primary network. Moreover, it is also possible that the communications among PUs are not based on synchronous schemes at all [5], [6]. Thus, under practical scenarios, the primary traffic transition may occur during the sensing period, especially when a long sensing period is used to achieve a good sensing performance, or when spectrum sensing is performed for a network with high traffic load.

Among a limited number of literature including [9]–[14] that deal with unknown primary traffic scenario, [9] was the first one to study the performance of well known semi-blind spectrum sensing algorithms including Energy Detection (ED) and Roy's Largest Root Test (RLRT) under bursty primary traffic, in which the burst interval is comparable to or smaller than the spectrum sensing interval. The traffic model used is limited to constant length bursts of the PU data, whose length is smaller than the SU sensing duration. However, the burst length of the PU may be varying with time following some stochastic models [7], [8]. A more general scenario, in which the PUs traffic transition is completely random, may affect the spectrum sensing performance. The analysis of the spectrum sensing performance has been presented in [11]–[14] by modeling the PU traffic as an independent and identically distributed two state Markov's model. Using this primary traffic model, authors in [11], [13], [14] analyzed the effect of PU traffic on the sensing performance and the sensing-throughput trade-off considering ED as a sensing technique under the half duplex scenario. Moreover, the effect of multiple PUs traffic on the sensing-throughput trade-off of the secondary system has been studied in [12]. Although all the aforementioned contributions recognized the fact that the PU traffic might affect the sensing performance including sensing-throughput trade-off, none of them considered the realistic scenario of multi-antenna spectrum sensing in a complex signal sample domain.

In this paper, the effect of PU traffic on the performance of multi-antenna spectrum sensing is evaluated under the complex domain of PU signal, noise and channel considering ED as a sensing technique. In contrast to the commonly used continuous time Markov model in the existing literature, a

 ISBN: 978-1-61208-456-5

novel technique of modeling PU traffic is proposed which is only based on the discrete time distribution of PU free and busy periods. The proposed model is more realistic and simple compared to the continuous time Markov model proposed in the previous literature [11]–[14]. Moreover, an analytical performance evaluation of the decision statistic under the considered scenario is carried out. It is shown that the time varying PU traffic severely affects the performance of ED. More importantly, it is shown that the performance gain due to multiple antennas in the sensing unit is significantly suppressed by the effect of PU traffic when the mean lengths of free and busy periods are small.

The rest of the paper is organized as follows: A system model is presented in Section II. Simple characterization of the PU traffic model is described in Section III. The sensing performance is derived in Section IV. The simulation results are discussed in Section V and finally, the conclusion in Section VI.

II. System Model

We consider a scenario where multiple antennas are employed by an SU. Suppose the SU has K antennas and each antenna receives N samples in each sensing slot. We focus on a single source scenario (single primary transmitter), which is of particular interest in many detection problems in CRNs. In a given sensing frame, the detector calculates its decision statistic T_D by collecting N samples from each one of the K antennas. Subsequently, the received samples are stored by the detector in the $K \times N$ matrix $\boldsymbol{Y}$.

As described in Section I, when the primary transmissions are not based on some synchronous schemes or the sensing unit at the SU does not have any information about the primary traffic structure, the received vector at the sensing unit may consist of partly the samples from one PU state and the remaining from alternate PU state as shown in Figure 1. To simplify the scenario, we begin with the following classification of the sensing slots based on the PU traffic status,

1) Steady State (SS) sensing slot: In such type of sensing slot, all the received samples in one sensing slot are obtained from the same PU state.
2) Transient State (TS) sensing slot: In such type of sensing slot, a part of the received samples within the sensing slot are obtained from one PU state and the remaining from the next PU state.

In general, the probabilities of receiving SS and TS sensing slots are dependent on the PUs traffic model. At the end of the sensing interval, based on the received samples, the detector must distinguish between null and alternate hypothesis.

$\mathcal{H}_0$: the channel is going to be free,
$\mathcal{H}_1$: the channel is going to be busy.

This hypothesis formulation implies that in a TS sensing slot, a transition from the PU busy state to the PU free state is considered $\mathcal{H}_0$, while a transition from the PU free state to the PU busy state is considered $\mathcal{H}_1$.

In the considered scenario, in an SS sensing interval, the generic received signal matrix under each hypothesis can be written as,

$$\boldsymbol{Y}_{SS} = \begin{cases} \boldsymbol{V} & (\mathcal{H}_0), \\ \boldsymbol{hs} + \boldsymbol{V} & (\mathcal{H}_1), \end{cases} \tag{1}$$

where $\boldsymbol{V} \triangleq [\boldsymbol{v}(1) \cdots \boldsymbol{v}(n) \cdots \boldsymbol{v}(N)]$ is the $K \times N$ noise matrix , $\boldsymbol{h} = [h_1 \cdots h_K]^T$ is the channel vector and $\boldsymbol{s} \triangleq [s(1) \cdots s(n) \cdots s(N)]$ is a $1 \times N$ signal vector.

And in the TS sensing interval, the generic received signal matrix under each hypothesis can be written as,

$$\boldsymbol{Y}_{TS} = \begin{cases} \boldsymbol{h}\boldsymbol{s}_{N-D_0} + \boldsymbol{V} & (\mathcal{H}_0), \\ \boldsymbol{h}\boldsymbol{s}_{D_1} + \boldsymbol{V} & (\mathcal{H}_1), \end{cases} \tag{2}$$

where D_0 represents the number of pure noise samples in TS sensing slot under $\mathcal{H}_0$, D_1 represents the number of noise plus PU signal samples in TS sensing slot under $\mathcal{H}_1$, $\boldsymbol{s}_{D_0} \triangleq [\boldsymbol{s}_{1\times(N-D_0)} | \boldsymbol{0}_{1\times D_0}]$ with $\boldsymbol{s}_{1\times(N-D_0)}$ a $1 \times (N - D_0)$ signal vector and $\boldsymbol{0}_{1\times D_0}$ a $1 \times D_0$ zero vector. Similarly, $\boldsymbol{s}_{D_1} \triangleq [\boldsymbol{0}_{1\times(N-D_1)} | \boldsymbol{s}_{1\times(D_1)}]$ with $\boldsymbol{0}_{1\times(N-D_1)}$ a $1\times(N-D_1)$ zero vector and $\boldsymbol{s}_{1\times D_1}$ a $1\times D_1$ signal vector. In each of these, the unknown primary transmitted signal $s(n)$ at time instant n is modeled as independent and identically distributed (i.i.d.) complex Gaussian with zero mean and variance $\sigma_s^2 : s(n) \sim \mathcal{N}_{\mathbb{C}}(0, \sigma_s^2)$. The noise sample $v_k(n)$ at the k^{th} antenna of the SU at the time instant n is also modeled as complex Gaussian with mean zero and variance $\sigma_v^2 : v_k(n) \sim \mathcal{N}_{\mathbb{C}}(0, \sigma_v^2)$. The channel coefficient h_k of k^{th} antenna is assumed to be constant and memory-less during the sensing interval.

III. Characterization of Primary user traffic

In this paper, the PU traffic is modeled as an i.i.d. on-off random process with geometrically distributed busy and free periods. To be in-line with the binary hypothesis testing of a spectrum sensing problem, a two state on-off modeling of the PU traffic is rather realistic especially when we are more concerned only about if the PU is transmitting or not. Furthermore, we are actually dealing with the discrete set of samples with a fixed sensing interval, thus the geometrically distributed busy and free periods are perfectly relevant in our considered scenario.

Let N_b be the geometrically distributed random variable denoting the number of consecutive busy samples with a parameter p_b. Similarly, let N_f be another identical and independent geometrically distributed random variable denoting the number of consecutive free samples with a parameter p_f. Then, the probability mass function (pmf) for each of them can be written as,

$$f_{N_b}(N_b = n_b) = (1 - p_b)^{n_b - 1} p_b, \quad \text{for } n_b = 1, 2, .., \infty \tag{3}$$
$$f_{N_f}(N_f = n_f) = (1 - p_f)^{n_f - 1} p_f, \quad \text{for } n_f = 1, 2, .., \infty \tag{4}$$

In the TS sensing slot, depending on the length of the free period or the busy period, the PU state can change anywhere within the sensing slot resulting the random variables (RVs) D_0 and D_1. For instance, suppose the PU is previously in

 ISBN: 978-1-61208-456-5

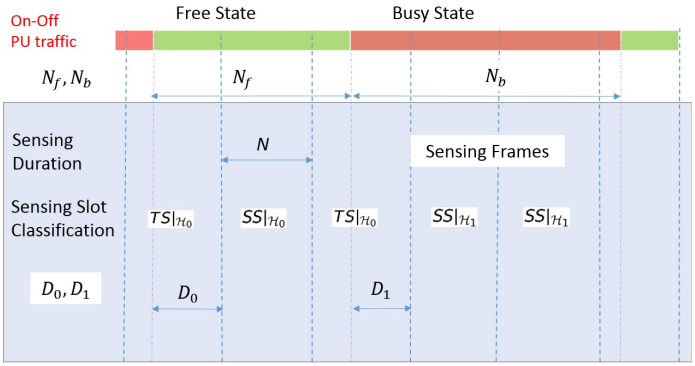

Fig. 1. Primary user traffic scenario and sensing slot classification

the busy state. The PU state transition from busy to the free state may occur anywhere, let's say after $(N - D_0)$ samples within the sensing slot. Thus, in each PU state transition from busy state to free state, the sensing unit has to decide based on D_0 pure noise samples and $(N - D_0)$ noise plus primary signal samples, which actually affects the overall sensing performance. The following Lemmas compute the pmfs of D_0 and D_1 respectively, based on the distribution of the busy period N_b, free period N_f and the sensing length N.

Lemma 1. Given the number of samples in a sensing duration N, the length of PU busy period N_b distributed as in (4), the probability of having D_0 noise only (PU signal free) samples in a TS sensing slot under $\mathcal{H}_0$ is given by,

$$P_{D_0}(D_0 = d_0)|_{\mathcal{H}_0} = \frac{p_b(1-p_b)^{N-d_0-1}}{1-(1-p_b)^N}. \tag{5}$$

Proof. As mentioned earlier during binary hypothesis formulation, the PU state transition from busy state to the free state corresponds to $\mathcal{H}_0$ sensing slot. We consider thus, without loss of generality, while dealing TS sensing slot under $\mathcal{H}_0$, PU state transition from busy to free state depends only on PU busy period N_b. Thus, for given N_b, the additional number of noise only samples D_0 which is required to complete a TS sensing slot under $\mathcal{H}_0$ is given by,

$$D_0 = \left\lceil \frac{N_b}{N} \right\rceil N - N_b. \tag{6}$$

Using the pmf of N_b, the probability of D_0 can be written as,

$$P_{D_0} = p_b(1-p_b)^{aN-D_0-1}, \tag{7}$$

where $a = \left\lceil \frac{N_f}{N} \right\rceil$. Now, from (6) and (7), it is clear that D_0 can be obtained from many different values of N_b. To be more precise, we obtain D_0 for all N_b such that $N_b = aN - D_0$. Thus, in order to evaluate the pmf of D_0, we need to sum the probability of occurrence of all the instances of N_b, i.e., $N_b = aN - D_0$, obtaining

$$P_{D_0}(D_0 = d_0) = \sum_{a=1}^{+\infty} p_b(1-p_b)^{aN-d_0-1}. \tag{8}$$

After some algebra and the truncation of infinite sum of geometric series, we obtain the pmf of D_0 as in (5). □

Lemma 2. Given the number of samples in a sensing duration N, the length of PU free period N_f distributed as in (3), the probability of having D_1 noise plus primary signal samples in a TS sensing slot under $\mathcal{H}_1$ is given by,

$$P_{D_1}(D_1 = d_1)|_{\mathcal{H}_1} = \frac{p_f(1-p_f)^{N-d_1-1}}{1-(1-p_f)^N} \tag{9}$$

Proof. Using the same line of reasoning as in the proof of Lemma 1, the proof of Lemma 2 is straightforward. □

As depicted from (1) and (2), to find the distribution of the decision statistic under different hypotheses, the prior deduction of the chances of occurrence of SS sensing interval, TS sensing interval, pmf of D_0 and pmf of D_1 is inevitable. The following proposition computes the probability of occurrence of SS sensing slot $p_{SS}|_{\mathcal{H}_0}$ under $\mathcal{H}_0$ and the probability of occurrence of TS sensing slot is normally the complementary of $p_{SS}|_{\mathcal{H}_0}$, i.e., $p_{TS}|_{\mathcal{H}_0} = 1 - p_{SS}|_{\mathcal{H}_0}$.

Proposition 1. Given the sample length of a sensing interval N, the length of PU free period N_f distributed as in (3), the probability of receiving SS sensing slot under $\mathcal{H}_0$ is given by,

$$p_{SS}|_{\mathcal{H}_0} = \frac{\sum_{s_0=0}^{+\infty} s_0 P(s_0)}{\sum_{s_0=0}^{+\infty}(s_0+1)P(s_0)}, \tag{10}$$

where $P(s_0) = \left[(1-p_f)^{s_0 N-1} - (1-p_f)^{N(s_0+1)-1}\right]$.

Proof. Under $\mathcal{H}_0$, the probability of receiving s_0 number of SS sensing slot is given by,

$$\begin{aligned} P(s_0) &= P(s_0 N \le N_f < (s_0+1)N) \\ &= F_{N_f}(N(s_0+1)-1) - F_{N_F}(Ns_0-1) \\ &= \left[(1-p_f)^{s_0 N-1} - (1-p_f)^{N(s_0+1)-1}\right], \end{aligned} \tag{11}$$

where $F_{N_f}(\cdot)$ denotes the Cumulative Distribution Function (CDF) of N_f.

For each free period N_f, there occurs one TS sensing slot unless the free period N_f is a perfect multiple of the sensing

 ISBN: 978-1-61208-456-5

period N. Thus, the probability of receiving an SS sensing slot can be written as the ratio of the average number of SS sensing slot that can be received for a given distribution of N_f to the total number of sensing slots under consideration,

$$p_{SS}|\mathcal{H}_0 = \frac{\sum_{s_0=0}^{+\infty} s_0 P(s_0)}{\sum_{s_0=0}^{+\infty}(s_0+1)P(s_0) - \sum_{m=1}^{+\infty} p_{N_f}(N_F = mN)}. \quad (12)$$

Since the second summation in the denominator of (12) is negligibly small compared to the first summation, we can neglect this summation leading to (10). □

The following proposition computes the probability of occurrence of SS sensing slot $p_{SS}|\mathcal{H}_1$ under $\mathcal{H}_1$ and the probability of occurrence of TS sensing slot is normally the complementary of $p_{SS}|\mathcal{H}_1$, i.e., $p_{TS}|\mathcal{H}_1 = 1 - p_{SS}|\mathcal{H}_1$.

Proposition 2. Given the sample length of a sensing interval N, the length of PU busy period N_b distributed as in (4), the probability of receiving SS sensing slot under $\mathcal{H}_1$ is given by,

$$p_{SS}|\mathcal{H}_1 = \frac{\sum_{s_1=0}^{+\infty} s_1 P(s_1)}{\sum_{s_1=0}^{+\infty}(s_1+1)P(s_1)}, \quad (13)$$

where $P(s_1) = \left[(1-p_b)^{s_1 N - 1} - (1-p_b)^{N(s_1+1)-1}\right]$.

Proof. Using the same line of reasoning as in the proof of Proposition 1, the proof of Proposition 2 is straightforward. □

IV. Sensing Performance Analysis

Energy detection computes the average energy of the received signal matrix $\boldsymbol{Y}$ normalized by the noise variance σ_v^2 and compares it with a predefined threshold T_{ED} is given by,

$$T_{ED} = \frac{1}{\sigma_v^2} \sum_{k=1}^{K} \sum_{n=1}^{N} |y_k(n)|^2. \quad (14)$$

To analyze ED performance, it is necessary to express the probability density function (pdf) of the decision statistic in case of unknown primary traffic. The following theorem computes the pdf of the ED decision statistic under both the hypotheses using the PU traffic characterization presented in Section III.

Theorem 1. Given a multi-antenna sensing unit with K receiving antennas, N received samples in each slot and the random PU traffic with geometrically distributed free state duration, the pdf of the ED decision statistic under $\mathcal{H}_0$ and $\mathcal{H}_1$ is given by (15) and (16) (shown at the top of the next page), respectively, where $f_{\mathcal{G}}(x, \alpha, \beta)$ is a pdf of Gamma distribution with shape parameter α & rate parameter β and $f_{\mathcal{N}}(x, \mu, \sigma^2)$ is the pdf of Gaussian distribution with mean μ and variance σ^2.

Proof. As noted from Section II, the term within the summation in (14) is different for the SS sensing slot and TS sensing slot. Under the null hypothesis $\mathcal{H}_0$, the ED decision statistic in (14) can be decomposed as a probabilistic sum of $T_{ED}^{SS}|\mathcal{H}_0$ and $T_{ED}^{TS}|\mathcal{H}_0$.

$$T_{ED}|\mathcal{H}_0 = \frac{p_{SS}|\mathcal{H}_0}{2} \sum_{k=1}^{K}\sum_{n=1}^{N} \left|\frac{v_k(n)}{\sigma_v/\sqrt{2}}\right|^2 + \frac{p_{TS}|\mathcal{H}_0}{2} \left[\sum_{k=1}^{K}\sum_{n=1}^{D_0} \left|\frac{v_k(n)}{\sigma_v/\sqrt{2}}\right|^2 + \sum_{k=1}^{K}\sum_{n=N-D_0+1}^{N} \left|\frac{h_k s(n) + v_k(n)}{\sigma_v/\sqrt{2}}\right|^2\right]. \quad (17)$$

Next, the distribution of each sum in (17) can be derived as [15],

$$T_{ED}|\mathcal{H}_0 = \frac{p_{SS}|\mathcal{H}_0}{2}\chi^2_{2KN} + \frac{p_{TS}|\mathcal{H}_0}{2} \sum_{d_0=1}^{N-1} P_{D_0}(d_0) \left[\chi^2_{2Kd_0} + K\rho\chi^2_{2(N-d_0)} + \chi^2_{2K(N-d_0)} + \mathcal{N}(0, 2\rho(N-d_0)K)\right] \quad (18)$$

where χ^2_A represents a Chi-squared random variable with A degrees of freedom. and $\mathcal{N}(\mu, \sigma^2)$ represents the Normal random variable with mean μ and variance σ^2.

In fact, the product of a Chi-squared RV with a constant is a Gamma RV, thus, with this replacement we obtain,

$$T_{ED}|\mathcal{H}_0 = p_{SS}|\mathcal{H}_0 \mathcal{G}(KN, 1) + p_{TS}|\mathcal{H}_0 \sum_{d_0=1}^{N-1} P_{D_0}(d_0) \left[\mathcal{G}(Kd_0, 1) + \mathcal{G}(N-d_0, K\rho) + \mathcal{G}(K(N-d_0), 1) + \mathcal{N}(0, 2\rho(N-d_0)K)\right] \quad (19)$$

In addition, $\mathcal{G}(\alpha, \beta)$ represents a Gamma random variable with a shape parameter α and a rate parameter β. Since the goal is to find the pdf of the sum in (14) under $\mathcal{H}_0$, we replace the random variables in (19) with their respective pdfs to obtain (15).

In the similar manner, under the alternate hypothesis $\mathcal{H}_1$, the ED decision statistic in (14) can be decomposed as a probabilistic sum of $T_{ED}^{SS}|\mathcal{H}_1$ and $T_{ED}^{TS}|\mathcal{H}_1$.

$$T_{ED}|\mathcal{H}_1 = \frac{p_{SS}|\mathcal{H}_1}{2} \sum_{k=1}^{K}\sum_{n=1}^{N} \left|\frac{h_k s(n) + v_k(n)}{\sigma_v/\sqrt{2}}\right|^2 + \frac{p_{TS}|\mathcal{H}_1}{2} \cdot \left[\sum_{k=1}^{K}\sum_{n=1}^{D_1} \left|\frac{h_k s(n) + v_k(n)}{\sigma_v/\sqrt{2}}\right|^2 + \sum_{k=1}^{K}\sum_{n=N-D_1+1}^{N} \left|\frac{v_k(n)}{\sigma_v/\sqrt{2}}\right|^2\right] \quad (20)$$

Using the fact that D_1 is a random variable,

$$T_{ED}|\mathcal{H}_1 = \frac{p_{SS}|\mathcal{H}_1}{2} \sum_{k=1}^{K}\sum_{n=1}^{N} \left|\frac{h_k s(n) + v_k(n)}{\sigma_v/\sqrt{2}}\right|^2 + \frac{p_{TS}|\mathcal{H}_1}{2} \sum_{d_1=1}^{N-1} P_{D_1}(d_1) \cdot \left[\sum_{k=1}^{K}\sum_{n=1}^{d_1} \left|\frac{h_k s(n) + v_k(n)}{\sigma_v/\sqrt{2}}\right|^2 + \sum_{k=1}^{K}\sum_{n=N-d_1+1}^{N} \left|\frac{v_k(n)}{\sigma_v/\sqrt{2}}\right|^2\right]. \quad (21)$$

Deriving the distribution of each sum in (21) using [15],

$$T_{ED}|\mathcal{H}_1 = p_{SS}|\mathcal{H}_1 \left(\mathcal{G}(N, K\rho) + \mathcal{G}(KN, 1) + \mathcal{N}(0, 2\rho KN)\right) + p_{TS}|\mathcal{H}_1 \sum_{d_1=1}^{N-1} P_{D_1}(d_1) \left[\mathcal{G}(d_1, K\rho) + \mathcal{G}(Kd_1, 1) + \mathcal{N}(0, 2\rho K d_1) + \mathcal{G}(K(N-d_1), 1)\right]. \quad (22)$$

$$f_{T_{ED}|_{H_0}}(x) = p_{SS}|_{H_0} f_{\mathcal{G}}(x, KN, 1) + p_{TS}|_{H_0} \sum_{d_0=1}^{N-1} P_{D_0}(d_0) \left[f_{\mathcal{G}}(x, 2Kd_0, 1) + f_{\mathcal{G}}(x, N-d_0, K\rho) + f_{\mathcal{G}}(x, K(N-d_0), 1) + f_{\mathcal{N}}(x, 0, 2\rho K(N-d_0)) \right], \quad (15)$$

$$f_{T_{ED}|_{H_1}}(x) = p_{SS}|_{\mathcal{H}_1} \left(f_{\mathcal{G}}(x, N, K\rho) + f_{\mathcal{G}}(x, KN, 1) + f_{\mathcal{N}}(x, 0, 2\rho KN) \right) + p_{TS}|_{\mathcal{H}_1} \sum_{d_1=1}^{N-1} P_{D_1}(d_1) \left[f_{\mathcal{G}}(x, d_1, K\rho) + f_{\mathcal{G}}(x, Kd_1, 1) + f_{\mathcal{N}}(x, 0, 2\rho Kd_1) + f_{\mathcal{G}}(x, K(N-d_1), 1) \right]. \quad (16)$$

Finally, we replace the random variables in (22) with their respective pdfs to obtain (16). □

In essence, the pdfs in (15) and (16) consist of the sum of independent random variables. From a statistical point of view, the sum of two independent pdfs can be realized as a convolution of these pdfs [16]. Thus, the sum of pdfs can be computed using convolution or as an alternative, we can exploit the characteristic function approach by computing Fourier transform. In conclusion, (15) and (16) can be easily evaluated by using standard Fast Fourier Transform (FFT) techniques.

A. Probability of False Alarm: Given the pdf of the decision statistic in (15), we can compute the false-alarm probability. Under $\mathcal{H}_0$, the PU is in free state at the end of the sensing interval, but the decision statistic is erroneously above the threshold τ and the PU signal is declared present. For defining the probability of false-alarm P_F in our case, the following Corollary of Theorem 1 holds.

Corollary 1. The false-alarm probability of the ED test under unknown PU traffic and complex signal space scenario is:

$$P_F = P(T_{ED}|_{\mathcal{H}_0} \geq \tau) \equiv \int_{\tau}^{+\infty} f_{T_{ED}|_{H_0}}(x)dx. \quad (23)$$

B. Probability of Detection: Given the pdf of the decision statistic in (16), we can compute the detection probability. Under $\mathcal{H}_1$, i.e., the PU is in busy state at the end of the sensing interval. Under this scenario, if the decision statistic is above the threshold, the PU signal is declared present. The following Corollary of Theorem 1 holds for defining the probability of detection P_D.

Corollary 2. The detection probability of the ED test under unknown PU traffic and the complex signal space scenario is:

$$P_D = P(T_{ED}|_{\mathcal{H}_1} \geq \tau) \equiv \int_{\tau}^{+\infty} f_{T_{ED}|_{H_1}}(x)dx. \quad (24)$$

V. Numerical Results and Discussion

In this section, the effect of PU traffic on the multi-antenna ED is analyzed based on the the traffic model developed in Section II. The length of the free and busy periods of the PU traffic are measured in terms of the discrete number of samples where each of them has Geometric distribution with probability of success parameters p_f and p_b, respectively. In this section, more often we use mean and busy period denoting

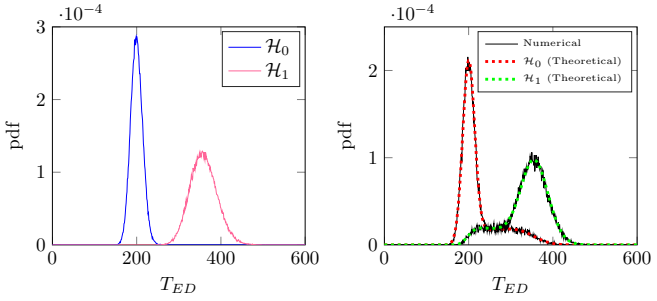

(a) Known PU Traffic (thus, synchronized PU-SU sensing slots)

(b) Unknown PU Traffic

Fig. 2. Pdfs of the ED decision statistic: Parameters: $N = 50$, $K = 4$, $M_f = 150$, $M_b = 150$ and SNR $= -6$ dB

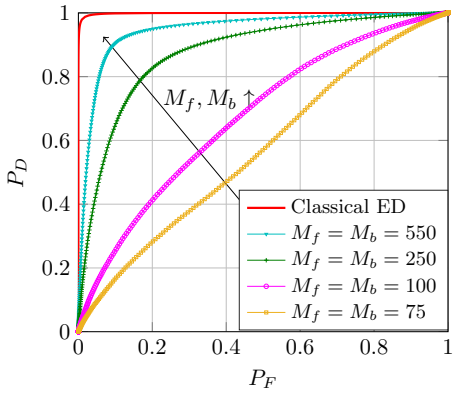

Fig. 3. ROC performance for the considered scenario, Parameters: $N = 100$, $K = 4$ and SNR $= -6$ dB

$M_f = \frac{1}{p_f}$ and $M_b = \frac{1}{p_b}$, respectively. Under multiple antenna sensing scenario, the average SNR at the receiver is defined as, $\rho = \frac{\sigma_s^2 \|\boldsymbol{h}\|^2}{K\sigma_v^2}$, where $||.||$ denotes the Euclidean norm. The analytical expressions derived in Section III are validated via numerical simulation.

In Figure 2, the pdf of the decision statistic under ideal PU-SU sensing slot synchronization is compared with the pdf of the decision statistic under unknown PU traffic considering both hypotheses. In addition, the accuracy of derived analytical expressions of the pdfs is confirmed by the results presented in Fig. 1(b), where the theoretical formulas are compared against the numerical results obtained by Monte-Carlo simulation. The perfect match of the theoretical and the numerical pdfs validates the derived analytical expressions. Figure 3 illustrates

 ISBN: 978-1-61208-456-5

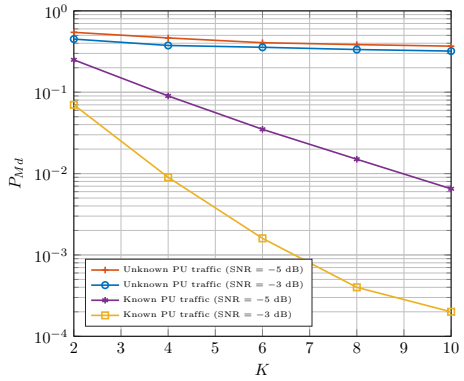

Fig. 4. Probability of missed detection vs. the number of Antennas, Parameters: $N = 25$, $M_f = 62$, $M_b = 62$ and $P_F = 0.1$

the Receiver Operating Characteristic (ROC) performance of the ED for different values of the mean free and busy period of the PU traffic. It shows that as the mean free and busy periods of the primary traffic increases, the detection performance of SU also increases. The conventional model with perfect synchronization of the PU-SU sensing slots performs better than the one with unknown PU traffic.

The variation of the sensing performance of the detector for different number of receiving antennas is plotted in Figure 4. It can be observed that unlike the rapid increase in sensing performance with the increasing number of receiving antennas under synchronized PU-SU sensing slot scenario (rapid decrease in missed-detection probability with the increasing number of receiving antennas), the sensing performance is almost constant even if we increase the number of antennas under unknown PU traffic. During a TS sensing slot, from each receiving antenna, the received signal samples are the mixture of pure noise samples and the samples with both noise and PU signal. Thus, even if we use multiple antennas, the nature of the received signal doesn't change much which is the reason the sensing performance improvement is suppressed by the unknown PU traffic (more specifically, the TS sensing performance) when the length of the free and busy periods of PU traffic are quite small (a few multiples of the length of the sensing window).

VI. Conclusion

In this paper, the effect of PU traffic on the performance of multi-antenna Energy Detector has been studied under a flat fading channel. A realistic and simple PU traffic model has been considered which is based only on the discrete time distribution of PU free and busy periods. Moreover, an analytical evaluation of the spectrum sensing performance under the considered scenario has been carried out. It has been shown that the performance gain due to multiple antenna in the sensing unit is significantly reduced by the effect of PU traffic when the mean lengths of free and busy periods are small (in the range of a few multiples of the sensing period).

Acknowledgments

This work was supported by the European Commission in the framework of the FP7 Network of Excellence in Wireless COMmunications NEWCOM# (Grant agreement no. 318306).

References

[1] S. Haykin, "Cognitive radio: Brain-empowered wireless communications", IEEE Journal on Selected Areas in Communications, , Feb. 2005, vol. 23, no. 2, pp. 201-220.

[2] E. Axell, G. Leus, E. G. Larsson, and H. V. Poor, "Spectrum sensing for cognitive radio:State-of-the-art and recent advances,"IEEE Signal Processing Magazine May 2012, vol. 29, no. 3, pp. 101-116.

[3] S. K. Sharma et al., "Cognitive Radio Techniques under Practical Imperfections: A Survey", IEEE Commun. Surveys Tutorials, Jul. 2015, vol. PP, pp. 1.

[4] S. K. Sharma, S. Chatzinotas, and B. Ottersten, "A hybrid cognitive transceiver architecture: Sensing-throughput tradeoff", 9th International Conference on Cognitive Radio Oriented Wireless Networks and Communications (CROWNCOM), Jun. 2014, pp. 143-149.

[5] Consultative Committee for Space Data Systems, "TC synchronization and channel coding", CCSDS 231.0-B-2 Blue Book, Sep. 2010.

[6] M. Zorzi, A. Gluhak, S. Lange and A. Bassi, "From today's INTRAnet of things to a future INTERnet of things: a wireless- and mobility-related view", IEEE Wireless Communications Dec. 2010, vol. 17, no. 6, pp. 44-51.

[7] R. Palit, K. Naik and A. Singh, "Anatomy of WiFi access traffic of smartphones and implications for energy saving techniques", International Journal of Energy, Information and Communication Feb. 2012, vol. 3, no. 1, pp. 1-16.

[8] A. Ghosh, R. Jana, V. Ramaswami, J. Rowland and N. K. Shankaranarayanan, "Modeling and characterization of large-scale Wi-Fi traffic in public hot-spots", IEEE INFOCOM, April 2011, pp. 2921-2929.

[9] F. Penna and R. Garello, "Detection of Discontinuous Signals for Cognitive Radio Applications", IET Communications, Jan. 2011, vol. 5, no. 10, pp. 1453-1461.

[10] S. L. MacDonald and D. C. Popescu, "Impact of primary user activity on the performance of energy-based spectrum sensing in cognitive radio systems", IEEE GLOBECOM, Dec. 2013, pp. 3224-3228.

[11] T. Wang, Y. Chen, E. Hines, and B. Zhao, "Analysis of effect of primary user traffic on spectrum sensing performance", Fourth International Conference on Communications and Networking in China, ChinaCOM 2009, pp. 1-5.

[12] H. Pradhan, A. S. Kalamkar and A. Banerjee, "Sensing-throughput tradeoff in cognitive radio with random arrivals and departures of multiple primary users", IEEE Communications Letters, Mar. 2015, vol. 19, no. 3, pp. 415-418.

[13] J. Y. Wu, P. H. Huang, T. Y. Wang and V. W. S. Wong, "Energy detection based spectrum sensing with random arrival and departure of primary user's signal", IEEE Globecom Workshops (GC Wkshps), Dec. 2013, pp. 380-384.

[14] L. Tang, Y. Chen, E. L. Hines and M. S. Alouini, "Effect of primary user traffic on sensing-throughput tradeoff for cognitive radios',, IEEE Transactions on Wireless Communications, Apr. 2011, vol. 10, no. 4, pp. 1063-1068.

[15] P. Dhakal, D. Riviello, F. Penna and R. Garello, "Impact of noise estimation on energy detection and eigenvalue based spectrum sensing algorithms", IEEE International Conference on Communications (ICC), Jun. 2014, pp. 1367-1372.

[16] Hwei P. Hsu, Schaum's outline of theory and problems of probability, random variables, and random processes, McGraw-Hill Education (India) Pvt Limited, 2004.

 ISBN: 978-1-61208-456-5

Underlay Cognitive Radio Wireless Networks using Repetition Coding and Spread Spectrum

Saed Daoud, David Haccoun, and Christian Cardinal

Department of Electrical Engineering
École Polytechnique de Montréal
Montréal, QC, Canada
Email: saed.daoud@polymtl.ca, david.haccoun@polymtl.ca, christian.cardinal@polymtl.ca

***Abstract*—In this paper, we investigate the use of repetition coding (RC) in conjunction with code division multiple access (CDMA) spread spectrum (SS), as a means to spread the signal power of a secondary (cognitive) underlay system, operating at the same time and on the same frequency band with a primary system. First, we consider single user (SU) systems, where we find the bit error rate (BER) at the secondary receiver (SR), satisfying a given quality of service (QoS) requirement for the primary system. Then, we find the maximum coding rate required to satisfy the QoS of both systems. Also, we investigate the combination of RC and SS in multiuser (MU) systems, where SS is used as a means to separate the signals from each others. Simulation results show that, using RC with low coding rate, can maintain the interference level at the primary receiver (PR) below the maximum allowed level, while, at the same time, improving the BER performance of the secondary system. Furthermore, the largest coding rate required to satisfy both systems' QoS grows fast, as the transmit power of the primary system gets larger than the minimum value for the secondary system to operate. Finally, it is shown that, in some cases, dividing the bandwidth between RC and SS is a better option than allocating the whole bandwidth to SS only.**

Keywords–Bit error rate, cognitive radio, repetition coding, quality of service, spread spectrum.

I. INTRODUCTION

Future wireless communication systems will require ever increased data rate (or equivalently, bandwidth), required by the demanding multimedia applications. This is challenging as most of the electromagnetic (EM) spectrum is licensed to primary users. However, close investigations reveal that, the EM spectrum can be utilized more efficiently, by making the transmissions' parameters adaptable to the surrounding environment, as well as to the users' demands [1]–[4].

These findings have triggered huge research activities on developing techniques on how to access the spectrum more efficiently, resulting in the so-called *dynamic spectrum access* (DSA) techniques. In the literature, two models of DSA are mainly studied: interweave and underlay models [5]. In the interweave model, a cognitive secondary unlicensed system uses only the white spaces, i.e., the portions of the spectrum that are not currently utilized by the primary system, to whom the spectrum is licensed, and hence has priority in using it. This model, however, involves detection and tracking of the white spaces, which are complex to implement, and could lead to false detection. As a consequence, the quality of service (QoS) of the primary system is sometimes jeopardized, or white spaces can be gone unused by ready-to transmit secondary users. Furthermore, the required white spaces are not guaranteed to be found at the time a secondary system is ready to transmit. On the other hand, in underlay model, which is our focus, there are no temporal or spatial constraints, but there are interference power constraints imposed by the primary users, which has to be maintained below a given noise floor, in order to maintain a given QoS. These interference constraints can be met in one of two ways: using beamforming in multiple antenna systems by focusing the signal power toward the secondary receivers, and away from the primary receivers, or spreading the signal power over large bandwidth, to decrease the interference level within the primary users' bandwidth of interest [5].

In this paper, our focus is on the underlay model, where we investigate the usage of repetition codes (RC) as a means to spread the signal power, with possibly spread spectrum (SS) techniques for multiuser systems, i.e., code division multiple access (CDMA) [6]. In particular, we consider a secondary system operating at the same time and on the same frequency band with a primary system. First, we consider single user (SU) systems, and we set a QoS limit on the primary system in terms of the largest bit error rate (BER) allowed at the primary receiver (PR), and derive the BER performance at the secondary receiver (SR) for different coding rates. Then, we set a QoS requirement at the secondary system in terms of the maximum BER tolerable at the SR for a satisfying service, and find the maximum coding rate required to satisfy the QoS of both systems. We then consider multiuser (MU) systems, where the primary system uses orthogonal spreading codes such as Walsh-Hadamard (WH) codes [7], where the cross-correlation between the spreading codes is zero, as a means to spread and separate the primary signals, while the secondary system uses a combination of RC and WH codes to spread and distinguish the secondary signals. Simulation results show that RC with low coding rate can be used as a simple means to spread the signal power to satisfy the QoS of both the primary and secondary systems. Furthermore, in MU systems, it is shown that, in some cases, dividing the total available bandwidth between RC and SS is a better option in terms of BER at SRs than allocating the whole available bandwidth to SS only.

To the best of the authors' knowledge, the above proposed systems haven't been considered in the literature. The rest of the paper is organized as follows: In Section II, the system and channel model are presented, in Section III, the performances

 ISBN: 978-1-61208-456-5

of SU and MU systems are investigated, in Section IV, simulation results are presented and discussed, and finally in Section V, a conclusion is provided.

II. System Model

A. SU Systems

First, we consider a secondary (cognitive) system consisting of one secondary transmitter (ST) and one SR, which operates at the same time and over the same frequency band as a primary system consisting of one primary transmitter (PT) and one PR. All channels are assumed to be additive white Gaussian noise (AWGN) channels, where the additive noise at the front-end receivers is assumed to have a single-sided power spectral density (PSD) N_0 Watts/Hz, and both systems use binary phase shift keying (BPSK) modulation with the same bit rate R_b bits/sesond, and thus both systems have the same baseband bandwidth, $W = R_b$ Hz, where rectangular pulse shaping is assumed, and null-to-null bandwidth is considered. Both systems are assumed to be synchronous. The power received at the front-end receivers is noted to be P from the PT and S from the ST. The QoS of the primary system is protected by setting a maximum BER value τ_p allowable at the PR. This implies that the minimum data bit energy-to-interference-plus-noise PSD allowed at the PR, denoted by $\eta_{p,\min}$, is given by [8]

$$\eta_{p,\min} = \frac{Q^{-1}(\tau_p)^2}{2}, \tag{1}$$

where $Q(.)$ is the Q-function given by $Q(x) = \frac{1}{\sqrt{2\pi}} \int_x^\infty e^{-u^2/2}\, du$, and $Q^{-1}(.)$ is its inverse. From (1), it is implied that the interference is approximated as a white Gaussian random process. The secondary system uses a RC scheme with coding rate $R_c = 1/N$, as a means to spread its signal power over a wider bandwidth. At the SR, the majority logic detection is used for decoding, where a bit is declared $1(0)$, if the majority of decoded bits are 1s$(0$s$)$. The secondary system might have its own QoS requirement in terms of maximum allowable BER at the SR, denoted by τ_s.

B. MU Systems

In multiuser systems, we consider a secondary system with N_s transmitter-receiver (Tx-Rx) pairs operating simultaneously with a primary system with N_p Tx-Rx pairs, where all transmissions are assumed to be synchronous at both the bit and chip levels. WH codes are used in both systems as a means to spread and separate the signals from different transmitters in a given system. It is assumed that the primary signals are spread over the entire available bandwidth, with a spreading factor (SF) G_p. For the secondary system, first a RC with coding rate $R_c = 1/M_s$ is used, and then each coded bit is spread by a SF Q_s, where $Q_s = G_p/M_s$, such that the signal after coding and SS occupies the total available bandwidth, i.e., $M_s Q_s = G_p$. The above description implies that, each user, whether in the primary or secondary system, has a transmission rate of $G_p R_b$ chips/second at the channel input, where R_b is the information bit rate measured in bits/second. Since WH code matrices are squared matrices with dimensions of power 2, and for mathematical convenience, we assume that the parameters G_p, N_p, and M_s are also variables of power 2, i.e., $G_p = 2^{g_p}$, $N_p = 2^{n_p}$, and $M_s = 2^{m_s}$, where g_p, n_p, and m_s are all non-negative integers. Also, it is assumed implicitly that $N_p \leq G_p$ and $N_s \leq Q_s$. Finally, all receivers are assumed to receive a power P from all PTs, and power S from all STs. The other parameters are the same as in SU systems.

III. Performance Analysis

A. SU Systems

Let that the PSD of the primary signal be denoted J_p, and that of the secondary signal J_s. Then we have $P = J_p W$ and $S = J_s W$. In SU case, since RC coding with coding rate $R_c = 1/N$ is used, the secondary signal is spread by a factor N, i.e., the bandwidth and PSD after coding are given by NW and J_s/N, respectively. Thus, the signal-to-interference-plus-noise ratio (SINR) at the PR is given by

$$\frac{J_p W}{\frac{J_s}{N} \times W + N_0 W} = \frac{P}{\frac{S}{N} + N_0\, W}, \tag{2}$$

where $N_0 W$ is the noise power within the primary signal's bandwidth, and the corresponding data bit energy-to-interference-plus-noise PSD is given by [9]

$$\eta_p = \frac{\gamma_p}{\frac{\gamma_s}{N} + 1}, \tag{3}$$

where $\gamma_p = (E_b)_p/N_0$ and $\gamma_s = (E_b)_s/N_0$ are the interference-free signal-to-noise ratio (SNR) at PR and SR, respectively, where $(E_b)_p = P/W$ and $(E_b)_s = S/W$. To satisfy the QoS requirement of the primary system, we need

$$\eta_p = \frac{\gamma_p}{\frac{\gamma_s}{N} + 1} \geq \eta_{p,\min}, \tag{4}$$

which results in

$$\frac{\gamma_s}{N} \leq \frac{\gamma_p}{\eta_{p,\min}} - 1. \tag{5}$$

At the input of the SR, and following the same logic as done above for the PR, the SINR can be found to be

$$\frac{S}{P + N_0 NW}, \tag{6}$$

and the corresponding coded bit energy-to-interference-plus-noise PSD is given by

$$\eta_{s,c} = \frac{\gamma_s/N}{\frac{\gamma_p}{N} + 1}. \tag{7}$$

For the majority logic detector at the SR, the BER is given by

$$\mathtt{BER}_s = \sum_{k=L}^{N} \binom{N}{k} \mathtt{BER}_{s,c}^k \left(1 - \mathtt{BER}_{s,c}\right)^{N-k}, \tag{8}$$

where $L = \lfloor N/2 \rfloor + 1$, and

$$\mathtt{BER}_{s,c} = Q\left[\sqrt{2\,\eta_{s,c}}\right], \tag{9}$$

is the BER per coded bit.

If the secondary system also has a QoS requirement, then we aim to find the largest coding rate, or equivalently, the smallest value of N that is required to satisfy the QoS of both systems. Toward that end, the BER at the SR needs to be simplified as a function of N. It can be upper bounded, for $\mathtt{BER}_{s,c} \ll 1$, by [10]

$$\mathtt{BER}_s \leq \left[2\sqrt{\mathtt{BER}_{s,c}}\right]^N \leq 2^{N/2} \exp\left(-\frac{N}{2}\eta_{s,c}\right), \tag{10}$$

where the second inequality is due to the Chernoff upper bound of the Q-function: $Q(x) \leq \frac{1}{2}\exp\left(-\frac{x^2}{2}\right)$. To make sure that BER_s is less than a predefined maximum BER τ_s, we need to satisfy the following inequality

$$2^{N/2}\exp\left(-\frac{N}{2}\eta_{s,c}\right) \leq \tau_s, \tag{11}$$

or equivalently

$$\frac{N}{2}\ln 2 - \frac{\gamma_s}{2\left[\frac{\gamma_p}{N}+1\right]} \leq \ln \tau_s, \tag{12}$$

where $\ln(.)$ is the natural logarithm. Solving (12) for γ_s yields

$$\gamma_s \geq 2\left[\frac{\gamma_p}{N}+1\right]\left[\frac{N}{2}\ln 2 - \ln \tau_s\right]. \tag{13}$$

Combining (5) and (13) results in

$$2\left[\frac{\gamma_p}{N}+1\right]\left[\frac{N}{2}\ln 2 - \ln \tau_s\right] \leq \gamma_s \leq N\left[\frac{\gamma_p}{\eta_{p,\min}}-1\right]. \tag{14}$$

Since

$$2\left[\frac{\gamma_p}{N}+1\right]\left[\frac{N}{2}\ln 2 - \ln \tau_s\right] \leq N\left[\frac{\gamma_p}{\eta_{p,\min}}-1\right], \tag{15}$$

and assuming that $N \geq 1$, we can solve (15) for N, which yields the following quadratic function

$$N^2\underbrace{\left[\frac{\gamma_p}{\eta_{p,\min}} - 1 - \ln 2\right]}_{A} + N\underbrace{\left[2\ln\tau_s - \gamma_p \ln 2\right]}_{B} + \underbrace{2\gamma_p \ln \tau_s}_{C} \geq 0. \tag{16}$$

Using the general quadratic solution formula, N can be found to be

$$N \geq \frac{-B \pm \sqrt{B^2 - 4AC}}{2A}, \tag{17}$$

and thus, denoting the minimum *real* value in the right hand side of (17) that is grater than or equal to 1 by $N_{\min}$, the maximum RC coding rate that satisfies the QoS of both the primary and secondary systems is given by $R_{c,\max} = 1/N_{\min}$.

B. MU Systems

In MU systems, it can be shown that the SINR at each PR is given by [11]

$$\frac{P}{N_s S + \sigma_{n,p}^2}, \tag{18}$$

where $\sigma_{n,p}^2 = N_0 G_p W$ is total noise power at the front-end of the PR. Then, the bit-energy-to-interference-plus-noise PSD at each PR after despreading is given by [11]

$$\eta_p = \frac{\gamma_p}{\frac{N_s}{G_p}\gamma_s + 1}. \tag{19}$$

Hence, we need that

$$\eta_p = \frac{\gamma_p}{\frac{N_s}{G_p}\gamma_s + 1} \geq \eta_{p,\min}, \tag{20}$$

to satisfy the QoS of the primary system, which, when solved for γ_s, yields

$$\gamma_s \leq \frac{G_p}{N_s}\left[\frac{\gamma_p}{\eta_{p,\min}} - 1\right]. \tag{21}$$

In (21), we have found the maximum allowable power that each SR can receive from the corresponding STs, which will be used next to evaluate the BER at each secondary receiver for different values of M_s, and N_s. Using the majority logic detection for $(M_s,\, 1)$ RC, the BER at each SR is given by

$$\mathrm{BER}_{s,\mathrm{RCSS}} = \sum_{k=\lfloor \frac{M_s}{2} \rfloor + 1}^{M_s} \binom{M_s}{k} \varepsilon_{s,\mathrm{RC}}^{k}\left(1-\varepsilon_{s,\mathrm{RC}}\right)^{M_s-k}, \tag{22}$$

where $\varepsilon_{s,\mathrm{RC}}$ is the BER per coded bit, which is given by [8]

$$\varepsilon_{s,\mathrm{RC}} = Q\left[\sqrt{2\eta_{s,\mathrm{RC}}}\right], \tag{23}$$

where $\eta_{s,\mathrm{RC}}$ is the secondary system's coded bit energy to interference-plus-noise PSD, and can be shown to be [9]

$$\eta_{s,\mathrm{RC}} = \frac{\gamma_s/M_s}{\frac{N_p}{G_p}\gamma_p + 1}. \tag{24}$$

Note that if the secondary users are spread the same way as the primary users, i.e., if $N_s \leq G_p$ secondary users are spread over the entire bandwidth using a WH code matrix of dimension $G_p \times G_p$, then nothing would change for the primary receivers. However, the BER at the secondary receivers will differ, as the BER in this case will be given by

$$\mathrm{BER}_{s,\mathrm{SS}} = Q\left[\sqrt{\frac{2\gamma_s}{\frac{N_p}{G_p}\gamma_p + 1}}\right]. \tag{25}$$

In next section, we will compare the performance of coded SS (using RC and WH codes), and uncoded SS (when only WH codes are used).

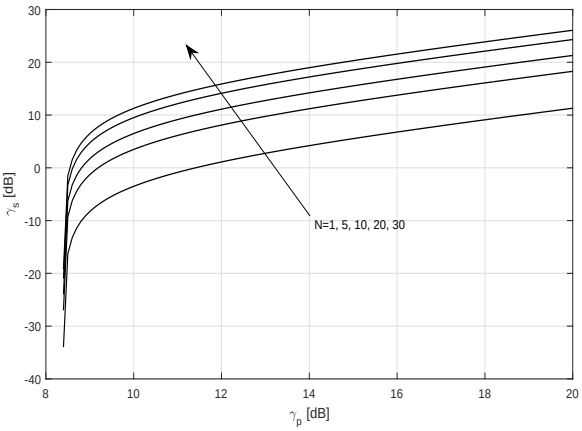

Figure 1. SNR at SR γ_s in dB vs. SNR at PR γ_p in dB for $\tau_p = 10^{-4}$ and $N = 1,\ 5,\ 10,\ 20,\ 30$.

IV. Simulation Results

In this section we evaluate the analytical results we derived in the previous sections. First we show the results for SU systems, when only the primary system has to meet a QoS requirement, and then when both the primary and secondary systems have to meet their respective QoSs. Then we illustrate the performance of MU systems, and compare coded SS with uncoded SS systems. All simulations were conducted using MATLAB program version R2015a.

 ISBN: 978-1-61208-456-5

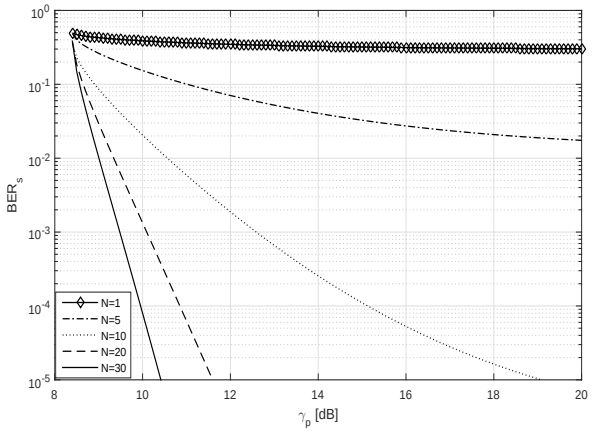

Figure 2. BER at SR $\mathtt{BER}_s$ vs. SNR at PR γ_p in dB for $\tau_p = 10^{-4}$ and $N = 1, 5, 10, 20, 30$.

A. SU Systems

First we consider the following parameters: $\tau_p = 10^{-4}$ and $N = 1, 5, 10, 20, 30$. In Figure 1, the interference-free SNR at the SR, γ_s, in dB vs. the interference-free SNR at the PR, γ_p, in dB is shown. It is shown that as N increases, i.e., the rate decreses, the allowed power from the secondary system increases as well. This is because the interference margin at PR is constant, while at the same time, increasing N decreases the actual interference from the ST. The corresponding BER at the SR, $\mathtt{BER}_s$, vs. the interference-free SNR at the PR, γ_p, in dB is shown in Figure 2, where we can see that, as N increases, the BER decreases for a given value of γ_p. This improvement is attributed to coding gain, where as N increases, each bit is repeated a larger number of times, while the SNR per coded bit, γ_s/N, is kept constant, because of the increased power allowed by the low coding rate, as it is shown in (5).

We now examine the case when both the primary and secondary systems have a QoS requirements, we consider the following parameters: $\tau_p = 10^{-2}, 10^{-3}, 10^{-4}, 10^{-5}$ and $\tau_s = 10^{-4}$. In Figure 3, the minimum number of repetitions per bit to satisfy the QoS of both systems $N_{\min}$ in dB vs. the interference-free SNR at the PR γ_p in dB is shown. We can observe two things here: first, as the QoS requirement at the PR becomes more stringent, the secondary system requires higher power from the PT, to create enough interference margin to start operating. Second, when γ_p is high enough for a given τ_p for the secondary system to start operating satisfactory, the coding rate required to satisfy both systems' QoS is very low, i.e., $N_{\min}$ is very large. This is because the interference margin is very low at the PR. However, $N_{\min}$ decays fast as γ_p gets larger than the minimum value required for the secondary system to operate, and then it becomes almost constant at yet higher γ_p. For example, if we want the secondary system to operate immediately at $\gamma_p \simeq 12$ dB for $\tau_p = 10^{-5}$, then we would need $N_{\min}$ as large as 1000. However, $N_{\min} \simeq 100$ at $\gamma_p \simeq 12.5$ dB, and $N_{\min} \simeq 25$ for $\gamma_p \geq 16$ dB. In Figure 4 the corresponding interference-free SNR at the SR normalized by $N_{\min}$, i.e., $\gamma_s/N_{\min}$ in dB is shown versus the interference-free SNR at the PR γ_p in dB, where it is apparent that ST can transmit at higher power for lower QoS requirements at the PR.

It is worth mentioning here that, using RC to spread the secondary system's power, decreases the secondary system bandwidth efficiency, because we transmit the same bit several times. This is the cost the secondary system has to pay, in exchange of accessing the channel, in the presence of a primary system, with QoS constraints on the secondary and/or primary systems. However, RC serves as a very simple coding scheme, where all we have to do, is just to repeat each data bit at the transmitter, and use the majority logic detection principle at the receiver, and thus, *very low* coding rates can be realized with reasonable complexity. More complex low coding rate codes require increased hardware and computational complexities for the encoding and decoding processes, although they may offer better performance.

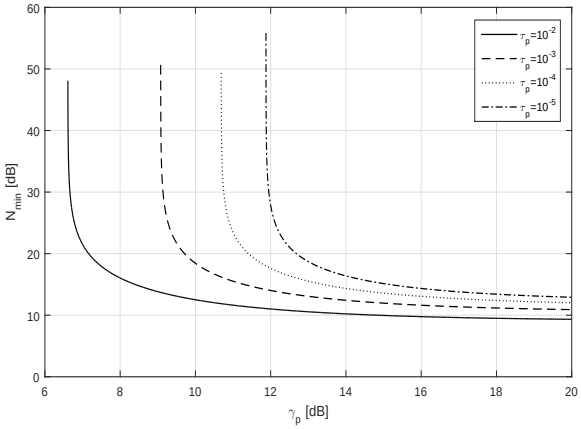

Figure 3. The value $N_{\min}$ in dB vs. SNR at PR γ_p in dB for $\tau_p = 10^{-2}, 10^{-3}, 10^{-4}, 10^{-5}$ and $\tau_s = 10^{-4}$.

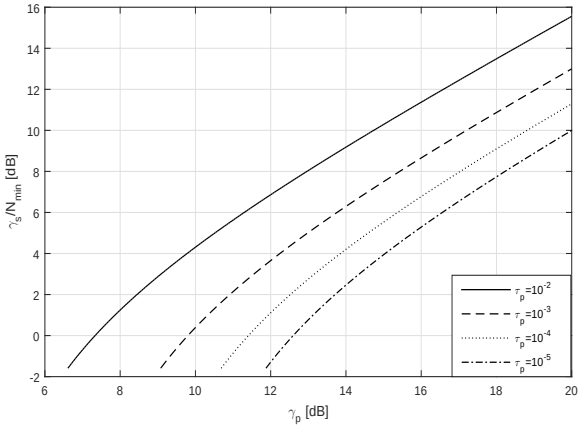

Figure 4. SNR at SR normalized by $N_{\min}$ $\gamma_s/N_{\min}$ in dB vs. SNR at PR γ_p in dB for $\tau_p = 10^{-2}, 10^{-3}, 10^{-4}, 10^{-5}$ and $\tau_s = 10^{-4}$.

B. MU Systems

In the MU case, we consider the following parameters for the numerical simulations: the total available bandwidth, normalized by the baseband bandwidth is $G_p = 2^{10} = 1024$, and the number of primary users is $N_p = 2^9 = 512$. The maximum allowable BER at each PR is set to be 10^{-4}.

 ISBN: 978-1-61208-456-5

In Figure 5, the interference-free SNR at each SR γ_s in dB vs. the interference-free SNR at each PR γ_p in dB, is shown for $M_s = 2^1 = 2$ repetitions per bit, and the number of secondary users (SUs) is $N_s = 2^{n_s}$ for $n_s = 4, 5, 6, 7, 9$. We can see that as the number of SUs increases, the allowed transmit power at each ST decreases for a given γ_p. This is natural, since as N_s increases, the interference at each PR increases, and thus to maintain the maximum allowed interference power at each PR, the transmit power at each ST must be decreased. In Figure 6, the coded SS BER $\mathrm{BER}_{s,\mathrm{RCSS}}$ vs. interference-free SNR at each PR in dB, is shown for $N_s = 64$ and $M_s = [1, 2, 4, 8, 16]$. For each value of M_s, a WH matrix of dimensions $Q_s \times Q_s$ is used for SS, where $Q_s = G_p/M_s$. Also shown the case when the whole available bandwidth is allocated to SS only (i.e., no coding is used), where a WH matrix of dimensions 1024×1024 is used. We can see that for $M_s = 2, 4$ coded SS outperforms uncoded SS, significantly so for $M_s = 2$. However, for $M_s = 8, 16$, coded SS has inferior performance compared to uncoded SS. This trend holds true for different values of N_s. The implication from this figure is that, dividing the total available bandwidth between coding and SS, is more beneficial in some cases compared to uncoded SS.

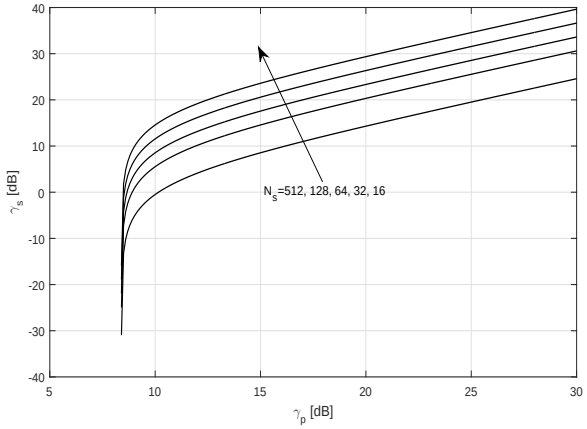

Figure 5. SNR at each SR γ_s in dB vs. SNR at each PR γ_p in dB for $G_p = 1024$, $N_p = 512$, $M_s = 2$, $N_s = [16, 32, 64, 128, 512]$, and maximum BER of $\tau_p = 10^{-4}$.

V. Conclusions and Future Works

In this paper, we investigated the use of repetition coding, as a means to spread the signal power, possibly in conjunction with other spreading techniques such as spread spectrum, in an underlay cognitive radio system. We considered single user and multiuser systems. In single user systems, we considered two cases: when the primary system only has a QoS requirement, and when both the primary and secondary systems have QoS requirements. In multiuser systems, we incorporated Walsh-Hadamard coding as an a means to distinguish the signals from each others, while deploying repetition coding at each secondary transmitter. Simulation results showed that, in single user systems, repetition codes with low enough coding rate, can decrease the interference level at the primary receiver effectively, only by repeating each data bit, instead of using more complex spreading techniques, while at the same time

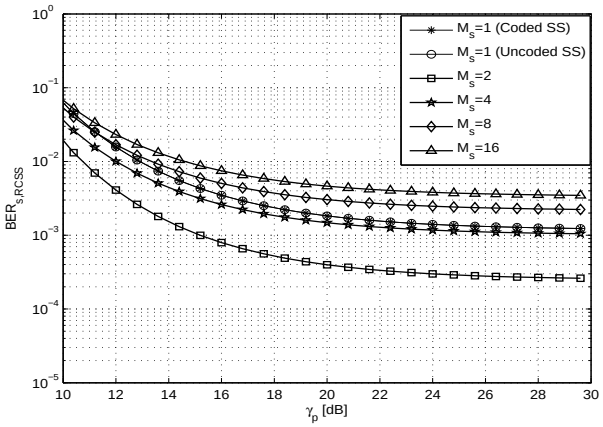

Figure 6. BER at each SR $\mathrm{BER}_{s,\mathrm{RCSS}}$ vs. SNR at each PR γ_p in dB for $G_p = 1024$, $N_p = 512$, $M_s = [1, 2, 4, 8, 16]$, $N_s = 64$, and maximum BER of $\tau_p = 10^{-4}$.

enhancing the bit error rate at the secondary receiver due to coding gain. In multiuser systems, it is shown that, in some cases, dividing the total bandwidth between coding and spread spectrum, is more beneficial, in terms of bit error rate performance at each secondary receiver, than allocating the total available bandwidth to spread spectrum only. As a future work, convolutional codes will be investigated and compared with RC in terms of performance, as well as complexity requirements.

References

[1] J. Ma, G. Li, and B. H. Juang, "Signal processing in cognitive radio," Proc. IEEE, vol. 97, no. 5, May 2009, pp. 805–823.

[2] M. Buddhikot, "Understanding dynamic spectrum access: Models,taxonomy and challenges," in 2nd IEEE International Symposium on New Frontiers in Dynamic Spectrum Access Networks, 2007. DySPAN 2007., April 2007, pp. 649–663.

[3] S. Haykin, D. Thomson, and J. Reed, "Spectrum sensing for cognitive radio," Proc. IEEE, vol. 97, no. 5, May 2009, pp. 849–877.

[4] Q. Zhao and B. Sadler, "A survey of dynamic spectrum access," IEEE Signal Processing Mag., vol. 24, no. 3, May 2007, pp. 79–89.

[5] A. Goldsmith, S. Jafar, I. Maric, and S. Srinivasa, "Breaking spectrum gridlock with cognitive radios: An information theoretic perspective," Proc. IEEE, vol. 97, no. 5, May 2009, pp. 894–914.

[6] R. Pickholtz, D. Schilling, and L. Milstein, "Theory of spread-spectrum communications–a tutorial," IEEE Trans. Commun., vol. 30, no. 5, May 1982, pp. 855–884.

[7] A. Viterbi, "Very low rate convolution codes for maximum theoretical performance of spread-spectrum multiple-access channels," IEEE J. Select. Areas Commun., vol. 8, no. 4, 1990, pp. 641–649.

[8] J. Proakis, Digital Communications, 4th ed. McGraw-Hill, 2000.

[9] A. Viterbi, "When not to spread spectrum - a sequel," IEEE Commun. Mag., vol. 23, no. 4, April 1985, pp. 12–17.

[10] P. Azmi, "The effect of channel coding rate on the resistance of direct-sequence spread-spectrum communication systems to narrow-band interference," Prog. Electromagn. Res., vol. 7, 2008, pp. 89–103.

[11] K. Gilhousen, I. Jacobs, R. Padovani, A. Viterbi, J. Weaver, L.A., and C. Wheatley, E. III, "On the capacity of a cellular CDMA system," IEEE Trans. Veh. Technol., vol. 40, no. 2, May 1991, pp. 303–312.

 ISBN: 978-1-61208-456-5

Analyzing the Effect of Spectrum Mobility on Mobile IPv6 in Cognitive Radio Networks

Manoj Kumar Rana
SMCC
Jadavpur University
Kolkata, India
e-mail:
manoj24.rana@gmail.com

Bhaskar Sardar
Dept of IT
Jadavpur University
Kolkata, India
e-mail:
bhaskargit@yahoo.co.in

Swarup Mandal
Delivery Head
Wipro Limited
Kolkata, India
e-mail:
swarup.mandal@wipro.com

Debashis Saha
MIS Group,
Indian Institute of
Management (IIM)
Calcutta, Kolkata, India
e-mail: ds@iimcal.ac.in

***Abstract*— In cognitive radio (CR) networks, the secondary users (SUs) may encounter frequent IP handoffs due to high *spectrum mobility*, even if they remain static spatially i.e., their network attachment does not change. However, mobile IPv6 (MIPv6) was not originally designed to deal gracefully with such handoffs induced by spectrum mobility only. As a result, the performance of the data applications running in SUs may degrade severely. This paper presents a simulation based investigation to gauge the seriousness of the issue and to suggest possible solutions. We have developed a CR Attribute Model, and implemented MIPv6 over it in the well-known simulator ns-3. For SUs, we have considered three spectrum selection strategies, namely Greedy (GDY), Most Recently Used (MRU), and Least Frequently Used (LFU). In each case, we have analyzed how the number of IP handoffs increases with rise in spectrum mobility, resulting in degraded throughput performance in SUs. Our study reveals that MIPv6 is unable to work properly in CR networks mainly due to *high default values* of router advertisement (RA) interval, lifetime period of care-of-address (CoA), and duplicate address detection (DAD) period. So, we need to customize MIPv6 – in terms of appropriating the pre-set values of RA interval, lifetime for CoA, and DAD period – to make it work properly in CR networks, where spectrum mobility is high.**

Keywords- Cognitive Radio Network; Spectrum Mobility; IP handoff; MIPv6; Throughput; Simulation; ns-3.

I. INTRODUCTION

Recent studies have revealed that significant parts of licensed spectrums remain underutilized for long duration; the Federal Communications Commission (FCC) reported that the utilization of licensed spectrum ranges from as low as 15% to 85% [1]. To improve the spectrum utilization maximally [1], cognitive radio (CR) networks harp on dynamic spectrum allocation, permitting opportunistic access to the unused spectrum by the unlicensed users [2][3], known as *secondary users* (SUs), when subscribed customers, known as *primary users* (PUs) are not using the spectrum. SUs are equipped with cognitive capability as well as re-configurability that enable them to figure out currently unused spectrum *holes*, decide the best spectrum hole to utilize, and exploit that spectrum. SUs have the ability to detect reappearance of PUs. As soon as the presence of PU is detected, SU evacuates the spectrum immediately and moves to another currently unused spectrum, if available. This process of switching from one spectrum to another is called *spectrum mobility*/handoff [4] by SUs.

Today, the wireless environment is highly heterogeneous, where multiple wireless access systems coexist over a certain area. If we assume that they all implement CR technology in their own spectrum [5][6], the spectrum handoff in such heterogeneous environments may give rise to two scenarios: (1) if the SU switches spectrum within the same system, only spectrum handoff occurs (which is referred to as *intra-system* spectrum handoff), (2) if the SU switches to a spectrum of a completely different system, a spectrum handoff is followed by IP handoff (which is referred to as *inter-system* spectrum handoff) [7]. Figure 1 illustrates these two types of handoffs, where dotted lines indicate only spectrum handoff and solid lines indicate spectrum handoff as well as IP handoff. Conventionally, it has been assumed that IP handoffs occur only due to spatial mobility of users in wireless networks. But, in CR networks, spectrum handoff may result in IP handoff even in absence of spatial mobility. From Figure 1, it is clear that the unavailability of unused spectrum in SU's current wireless network during spectrum mobility results into inter-system spectrum handoff that leads to an IP handoff. It is to be noted that the number of IP handoffs may be very high in case of high spectrum mobility, and so, IP handoff becomes a more common event in CR environments. This work mainly focusses on inter-system

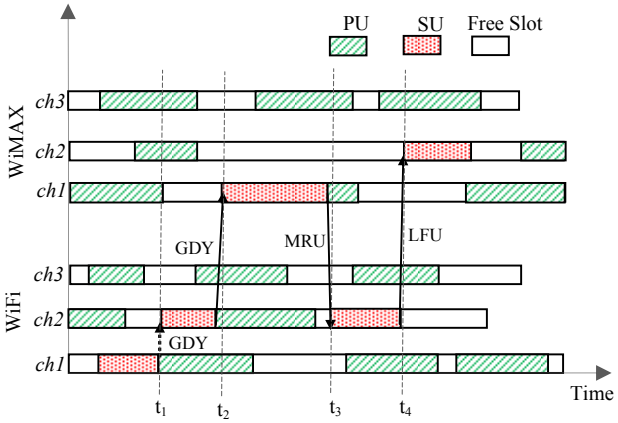

Figure 1. Spectrum mobility in CR networks

spectrum handoff.

The number of IP handoffs depends on the network parameters, such as PU arrival rate, PU channel holding time, and the number of SUs. In CR networks, the number of IP handoffs for an SU may be quiet high even when the SU is stationary. In modern wireless LAN (WLAN) and Long Term Evolution (LTE) or LTE-Advanced (LTE-A) networks, the channel usage occurs in discontinuous reception mode, where a PU uses a channel for a transmission and immediately releases the channel for the transmissions from other users [8]. For instance, for data rate of 20 kbps and transmission size 1000 byte, the average channel holding time is (1000*8/20000)=0.4 sec. So, for such small PU channel holding time with significant PU arrival rate, the duration of each spectrum hole becomes very small and SU interruption frequency becomes very high. It makes the CR network environment very dynamic for the SUs. This, in turn, poses a new set of challenges for the mobile IPv6 (MIPv6) protocol [9], the de-facto standard for IP handoff management. Even if the SUs are static, they have to invoke MIPv6 to handle IP handoff triggered by spectrum mobility. MIPv6 was originally designed for handling spatial mobility only, and so is not optimized for frequent IP handoffs due to inter-system spectrum mobility. It is well known that the handoff procedure in MIPv6 takes a significant amount of time, approximately 1.896 sec to 2.47 sec [10]. So, the net temporal overhead due to multiple IP handoffs becomes very high during the complete lifetime of a data connection for an SU, which degrades the data throughput significantly, giving rise to several new issues for CR networks. Recent research works on CR networks mainly focus on reducing the spectrum handoff latency [11][12], not exploring the IP handoff issues much.

Hence, the objective of this paper is to investigate the performance of the standard MIPv6 [9] in CR networks, in particular, the effect of spectrum mobility on MIPv6. To this end, we have developed the following modules in network simulator ns-3 [13]: (1) a cognitive radio attribute module (CRAM) to simulate a typical CR network consisting of IEEE 802.11 WLAN and WiMAX, (2) three basic spectrum selection algorithms, namely greedy (GDY), most recently used (MRU), and least frequently used (LFU), (3) our own MIPv6 according to the descriptions given in RFC 6275 [9].

In the first set of simulations, our objective is to identify the issues of MIPv6 when used in CR networks. We have investigated the simulation traces and observed that the high values of router advertisement (RA) interval, lifetime of care-of-address (CoA), and duplicate address detection (DAD) timers are responsible for poor performance of MIPv6. In the second set of simulations, we have set RA interval, lifetime of CoA, and DAD timer to sufficiently small values (as deemed fit by us). Then, we have measured the number of IP handoffs and throughput performance of SUs for different spectrum selection algorithms by varying the PU arrival rate, PU channel holding time, and the number of SUs in the CR networks.

The rest of the paper is organized as follows. In Section II, we discuss recent research works on spectrum mobility and IP mobility in CR networks. Section III provides a brief description of our model implementation in ns-3. Section IV illustrates the MIPv6 issues noted in CR networks. In Section V, we analyze the number of IP handoffs and its impact on throughput performance of the SUs. Finally, Section VI concludes the paper.

II. RELATED WORKS

To access the Internet services using CR networks, the SUs cycle through three phases: *spectrum handoff* phase, *IP handoff* phase, and *data transmission* phase. The spectrum handoff phase consists of channel sensing, handoff decision, pause, and channel switching functions [4]. Similarly, IP handoff phase consists of RA, CoA formation, and tunnel setup [9]. The phase transition is illustrated in Figure 2. During data transmission, if reappearance of PU occurs, then SU moves to channel sensing phase where the SU attempts to find spectrum holes to switch to another empty channel. If an empty channel is unavailable, the SU continues sensing the busy set of channels, repeating channel sensing and pause phases continuously. In spectrum decision phase, the SU decides the best channel to switch to, based on available channels. The selection logic is closely related to the channel characteristics, and the operations of the PUs and the SUs. In the channel switch phase, SU changes its operating channel. If the channel switch occurs in the same system, data transmission begins immediately; otherwise, the SU encounters an additional MIPv6 handoff.

Though many recent research works focus on spectrum mobility in CR networks, only a few research works focus on the resulting IP handoff and problems thereof faced by SUs.

A. Spectrum Handoff

Wang et al. [11][12] have proposed a dynamic programming based greedy algorithm to determine the optimal target channel sequence, and proved that greedy algorithm provides better results in terms of time complexity.

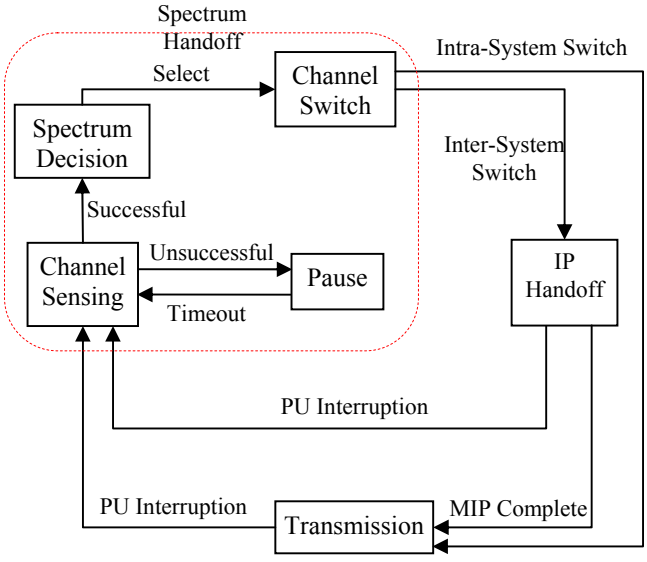

Figure 2. Mobility phase diagram in CR networks

To optimize the data delivery time, a traffic-adaptive spectrum handoff mechanism is proposed in [12]. It changes the target channel sequence of spectrum handoffs based on traffic conditions. Southwell et al. [14] analyzed spectrum handoff delay, considering the cost of channel switching and congestion due to multiple SUs, with prior knowledge of heterogeneous channels. They have proposed a fast algorithm to determine the best single-user decision, depending on other user's plans without communicating with each other.

B. IP Handoff

In [7], M. Kataoka et al. have proposed a MIP protocol based Cognitive Radio system architecture to reduce the handoff delay. The system architecture follows a hierarchical structure consisting of a wired and a wireless part. However, the downside of this protocol is that the control node becomes a bottleneck and may result in a single point failure. Chen et al. [15] have proposed a cross-layer protocol to optimize the data transmission time in Cognitive Radio LTE networks. Since the authors assumed homogeneous LTE network, they did not use MIPv6. Instead they used Standard LTE handoff mechanism which takes only a few milliseconds and so, there is no such noticeable impact of IP handoff in the transmission time.

The above proposals have been made to reduce the IP handoff latency in CR networks. To the best of our knowledge, no efforts have been reported thus far in the literature to investigate the issues of network layer mobility management protocols, such as MIPv6 in CR networks. Also, no prior works exist to show the impact of spectrum mobility on MIPv6. These observations call for a detailed analysis of MIPv6 in CR networks which may give us an insight into the practical design issues of MIPv6 and the impact of spectrum mobility on IP handoffs. In this paper, we have attempted to identify those issues in MIPv6 and shown that MIPv6 must be customized to work properly in CR networks.

III. COGNITIVE RADIO ATTRIBUTE MODEL (CRAM)

We have implemented CRAM in ns-3 [13]. It takes traffic parameters and spectrum selection strategy as input. We describe CRAM in the following three subsections.

A. Traffic Parameter

We consider one WLAN network with C_1 number of channels and one WiMAX network with C_2 number of channels. At any point in time, each of these channels can be occupied by a PU or a SU or remains empty. For simplicity, we have assumed homogeneous traffic parameters for all channels. Let us assume that the arrival rate of both PU and SU is Poisson. Let λ_p (arrival/second) be the arrival rate of PUs and λ_s (arrival/second) be the arrival rate of SUs. Let the service time for PUs and SUs be X_p (second/arrival) and X_s (second/arrival), respectively; both follow exponential distribution. If ρ_p and ρ_s denote the channel utilization for the transmissions of PUs and SUs, respectively, then the overall utilization is:

$$\rho = \rho_p + \rho_s \tag{1}$$

It is to be noted that $\rho \leq 1$. We denote by I_p the inter arrival time of the PUs. Due to memory less property, it follows exponential distribution with rate λ_p. As given in [12], we have,

$$E[I_p] = \frac{1}{\lambda_p} \cdot \tag{2}$$

I_p is the sum of $E[X_p]$ and spectrum hole duration. The mean spectrum hole duration $E[X_S]$ is the mean service time for the SU, i.e.,

$$E[X_S] = E[I_p] - E[X_p] \tag{3}$$

To allow the SU to utilize the channel, the spectrum hole duration must be greater than 0, i.e,

$$E[X_{SH}] > 0 \tag{4}$$

$$or, \ \frac{1}{\lambda_p} - E[X_p] > 0 \tag{5}$$

$$or, \ \lambda_p E[X_p] < 1 \tag{6}$$

The CRAM model takes C_1, C_2, λ_p, and $E[X_p]$ as input parameters. To obtain ρ_s we use M/M/C queuing model, where C denotes number of channels being used to serve the SUs. According to the definition of the M/M/C queue, the average number of SUs in the system can be written as [16]:

$$E[N_S] = C\rho_s + \frac{\rho_s}{1-\rho_s} D\left(C, \frac{\lambda_s}{\mu_s}\right) \tag{7}$$

where,

$$C = C_1 + C_2 \tag{8}$$

and

$$D\left(C, \frac{\lambda_s}{\mu_s}\right) = \frac{\frac{(C\rho_s)^C}{C!}\frac{1}{1-\rho_s}}{\sum_{k=0}^{C-1}\frac{(C\rho_s)^k}{k!} + \frac{(C\rho_s)^C}{C!}\frac{1}{1-\rho_s}} \tag{9}$$

Using the above formula, we can compute ρ_s, taking C and $E[N_S]$ as inputs.

B. Spectrum Selection Strategies

We have implemented three spectrum selection strategies: *Greedy* (GDY) [11][17], *Most Recently Used* (MRU) [18], and *Least Frequently Used* (LFU) [19]. These

strategies are implemented based on the statistical information of the channels. In GDY strategy, the SU selects the first empty channel without any pre-estimation of its freeness. Typically, the works [12][17] on modeling and analysis of spectrum mobility events assume GDY strategy (called first-come-first-served in their system model). The GDY strategy is an opportunistic one; it selects the empty channel at random, not targeting to utilize the spectrum holes optimally [11]. In contrast, several other research works [11][15][18][19] adopt selection strategies to utilize spectrum holes efficiently for the purpose of load balancing among channels as well as reducing data transmission time and improving throughput of SUs. These works consider the typical heterogeneous CR network environment [15] with multiple PUs and SUs [11][18][19]. We also assume this type of scenario in this work. MRU and LFU are selected as two efficient spectrum selection strategies based on the concept applied in [18] and [19], respectively. In MRU strategy, the SU selects the channel which has been used most recently by a PU, expecting a lengthy absence of PUs in that channel in near future. In LFU strategy, the SU selects the channel which has been least used by the PUs thus far, hoping that it will remain so in near future too.

In Figure 1, we have illustrated spectrum selection by a SU using these three strategies. At the time t_1 and t_2, the SU follows the GDY strategy to switch channel. At time t_1, the SU selects the spectrum hole of the first channel even though channel 3 is also empty. Similarly, at time t_2, the SU selects the spectrum hole of the first channel of WiMAX network. At time t_3, the SU follows MRU strategy and selects the spectrum hole of channel 2 of the WiFi network as it is used most currently among the free channels. At time t_4, the SU uses LFU strategy to switch to channel 2 of WiMAX network as the usage percentage of the channel by PU is less than other free channels.

C. CRAM Implementation in ns-3 [13]

We used the *Time*, *Timer*, *Simulator*, and *RandomVariable* classes to implement CRAM. The *Time* and *Timer* classes are used to schedule a task, such as assigning a channel to a SU/PU for a particular time interval and cancel it after completion of the task. The *Simulator* class is used for initial scheduling of the entire task in the simulation, i.e., it starts the PU and SU transmissions. The *RandomVariable* class is used to generate exponentially distributed random numbers. We used two schedulers: channel scheduler (Figure 3) and SU scheduler. The channel scheduler takes the mean value of λ_p and $E[X_p]$ as input. Following the distribution, the sequence generator generates a large number of sequences (over 1000). Each sequence consists of PU service time and duration of spectrum holes. During simulation, it makes the state of the channel either *busy* or *free*, based on the generated values. In the PU *busy* state, the channel scheduler starts the PU timer and makes the state as busy. After expiration of the PU timer, the free timer starts and the channel state becomes *free*. It would remain free up to the spectrum hole duration of the current sequence unless an SU sends a busy trigger. The SU busy trigger changes the channel state into busy. After expiration, it queries for the next sequence. A channel sensor database is designed that acquires the channel information.

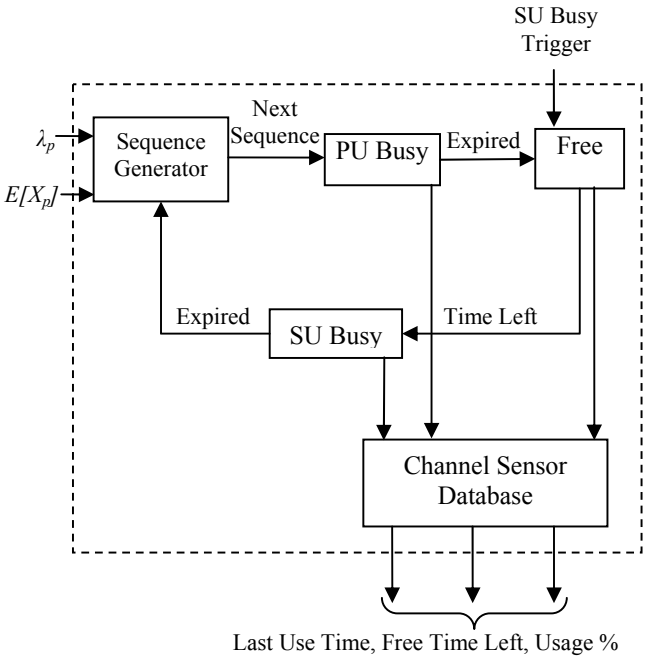

Figure 3. CRAM Channel Scheduler

In SU scheduler (Figure 4), user inputs its data transmission time and the spectrum selection strategy. The spectrum selection strategy acquires the channel information from all channels of all systems and makes a decision. It outputs the next channel number (k) and the remaining free time. If it gets the free time slot, it starts transmission timer, giving a busy trigger to the k^{th} channel scheduler. The start transmission functionality makes the SU's WiFi or, WiMAX netdevice state into 'UP'. The Stop Transmission function makes the SU's corresponding state into 'Down' state. If anytime the spectrum selection strategy cannot find a free channel, it pauses for a predefined timer value. After

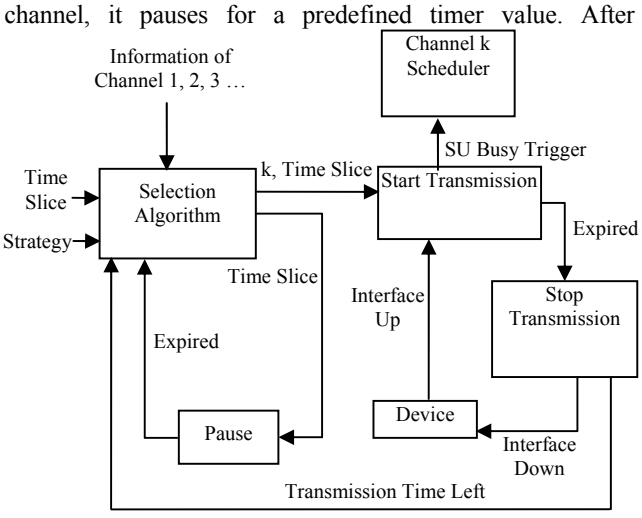

Figure 4. CRAM SU Scheduler

expiration of the pause timer, it again runs the spectrum selection strategy.

IV. MIPv6 ISSUES IN CR NETWORKS

We have developed our own MIPv6 module for ns-3 (as it is not available currently) on top of CRAM.

A. Simulation setup

We have considered a WLAN with 10 channels and a WiMAX network with 20 channels. SU is opportunistic to WLAN. We used constant position mobility model for the SUs because we are not interested in spatial mobility. We used λ_p=1.5 and $E[N_S]$=4. The average connection length is 480 bytes for exponentially distributed connections [20]. So, when the data rate of primary connection is 19.2 Kbps, we have $E[X_p]$=(480*8)/(19.2*10^3)=0.2 sec. The Pause timeout value and spectrum handoff delay are set as 0.05 sec and 0.01 sec, respectively. Correspondent node (CN) and SU are running '*UDP Echo*' application and transferring packets at the rate of 80 Kbps. The whole simulation is run for 1000 sec. However, we present only the results selected from 100 sec to 200 sec to highlight the design issues.

B. High RA Interval and Lifetime Period

If the duration of spectrum holes is very small, an SU may switch from one network (say WLAN) to another (say WiMAX), reside there for a very short time, and then may return to WLAN again. When the SU switches to WiMAX, the address configured in WLAN still remains valid for some more time. If it returns to WLAN quickly, it could use the previously configured CoA in WLAN, giving rise to two issues. *First*, when the SU is in WiMAX, another SU in WLAN may configure the same CoA and execute DAD procedure. The DAD procedure detects the address as valid for obvious reasons. So, when the SU returns to WLAN quickly, duplicate addresses would exist in WLAN even if DAD procedure detects no duplicity. *Second*, the binding update and tunnel setup procedures in MIPv6 are always triggered after the completion of DAD procedure. So, if the SU uses previously configured CoA in WLAN, those procedures are skipped. Since MIPv6 is not triggered, the tunnel set up between the SU and its home agent (HA) would still be the older one and the traffic would not be redirected towards the SU. As a result, the performance of the SU degrades drastically.

In Figure 5, we illustrate the impact of high RA interval and lifetime duration on packet flow in CR networks. First, we used MaxRAInterval=3 sec and MinRAInterval=1 sec as given in [10]. So, after switching back to WLAN, the SU does not perform MIPv6 operations for a long time due to high RA interval and lifetime period. This is evident from long gaps in packet sequence number in Figure 5. Next, we decreased the values of RA interval to MaxRAInterval=0.07 sec and MinRAInterval=0.03 sec. The corresponding simulation result (Figure 5) shows that MIPv6 is unable to work gracefully, resulting in long gaps in packet sequence number. So, we further reduced the values of RA intervals to 7ms (MaxRAInterval) and 3ms (MinRAInterval), and then we found that all MIPv6 operations are completed

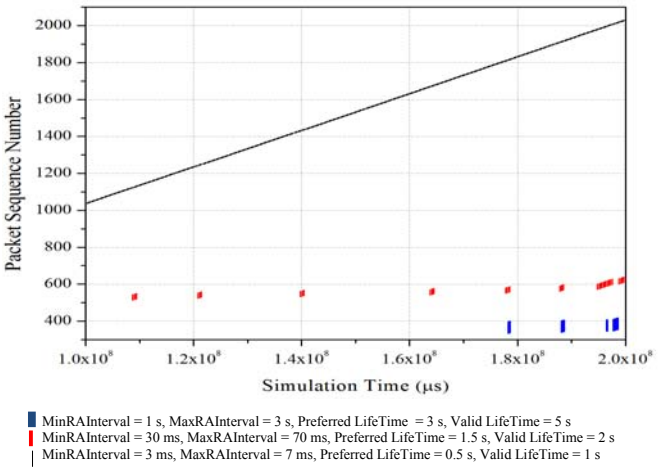

Figure 5. Behaviour under High and Low RA Intervals

successfully (Figure 5). We also observed that, under this circumstance, a large number of control packets are being generated, leading to congestion. So, we argue that the *RA interval and lifetime period must be set considerably low in order to be appropriate for use in CR networks*.

C. High DAD Period

RFC 6275 [9] has mentioned the default DAD period as 1 sec. It may be higher than the considered duration of spectrum holes in CR networks. Whenever an SU switches to a new network, the address configuration procedure – in particular, the DAD procedure – consumes almost the entire time, and hence, the spectrum hole cannot be used for data transmission (Figure 6). So, the throughput of SUs degrades in CR networks. For this reason, the DAD period must also be reduced to make MIPv6 more effective in CR networks.

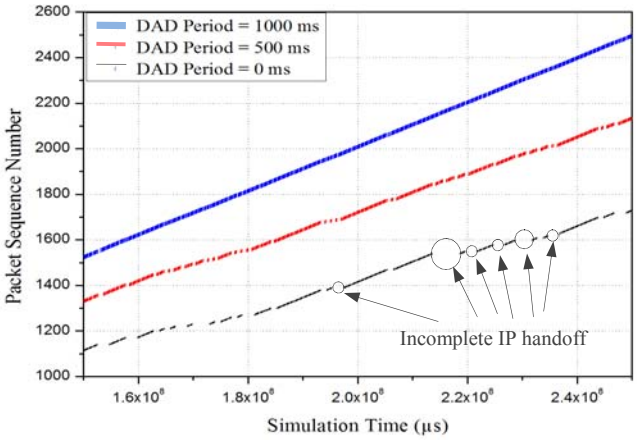

Figure 6. Behaviour under High and Low DAD Values

V. ANALYSIS OF IMPACT OF SPECTRUM MOBILITY

We have made some changes in the simulation setup, described in Section IV-A, to bring in more randomness in the availability of spectrum holes. The channels of CRAM are characterized as high usage and low usage to benefit

from LFU and MRU strategies. We used λ_p, $E[Xp]$, and $E[N_S]$ variables to control the emptiness of the channels (Table I). Also, to alleviate the problems explained in Section IV, we have taken 7 msec and 3 msec for MaxRAInterval and MinRAInterval, respectively. The preferred and valid lifetime values are assumed to be 0.5 sec and 1 sec, respectively.

TABLE I. SIMULATION PARAMETER VALUES

Variable Parameter	Other Parameter Values
λ_p	$(E[X_P])_{LOW}$=0.1, $(E[X_P])_{HIGH}$=0.3, $E[N_S]$=4
$E[X_p]$	$(\lambda_p)_{LOW}$=1, $(\lambda_p)_{HIGH}$=1.5, $E[N_S]$=4
$E[N_S]$	$(\lambda_p)_{LOW}$=2.0, $(\lambda_p)_{HIGH}$=2.5, $(E[X_P])_{LOW}$=0.1, $(E[X_P])_{HIGH}$=0.3

We have randomly assigned either $(E[X_p])_{HIGH}$ or $(E[X_p])_{LOW}$ values in all 30 channels, while keeping $E[N_S]$=4. Increasing λ_p, increases the frequency of spectrum holes but with reduced duration of each. From Figure 7, we observe that (i) up to $\lambda_p \leq 2.8$, the number of IP handoffs increases, (ii) for $0.1 \leq \lambda_p \leq 2.2$, all IP handoffs complete successfully due to sufficiently large spectrum holes. As a result, the throughput of the SU is reduced due to the lengthy handoff operation of Simulation Parameter Values MIPv6 as shown in Figure 8. For $2.2 < \lambda_p \leq 2.8$, only few IP handoffs were not completed due to the small duration of the spectrum holes. As a result, there was not such a drastic degradation in the throughput of the SUs as shown in Figure 8. But, for $\lambda_p > 2.8$, the spectrum holes became very small. So, the SUs could not get the opportunity to perform spectrum handoff as well as IP handoff for most of the time. In this case, SUs cycle between pause and channel sensing phases (Figure 2), thereby reducing the throughput performance of the SUs drastically (Figure 8).

For $\lambda_p \leq 2.2$, the MRU strategy performs better than LFU and GDY strategies (Figure 8) because the MRU strategy always finds the freest channel, i.e., the SU can use the channel for a long time without needing to perform frequent

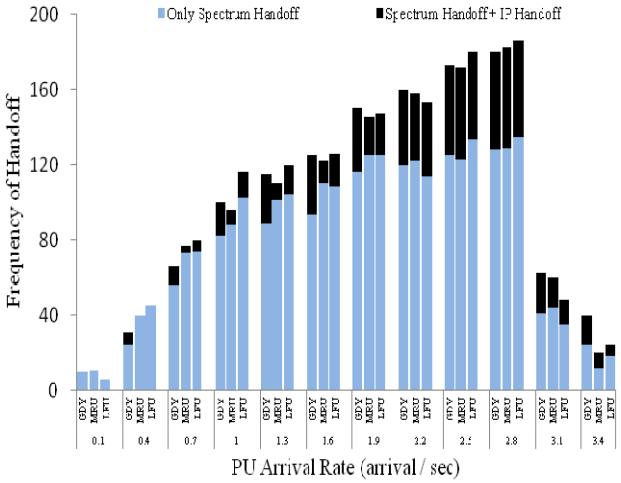

Figure 7. Variation of IP handoff with PU arrival rate

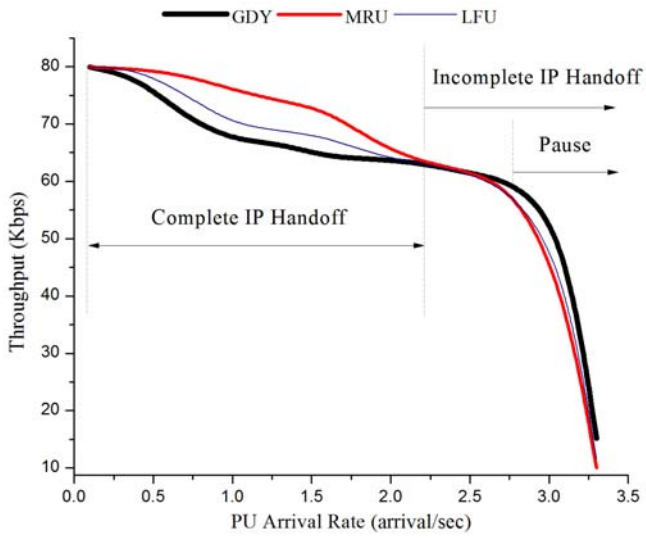

Figure 8. Effect of PU arrival rate on throughput of SU

IP handoffs. But that is not true for the other two strategies. However, for the range $\lambda_p > 2.2$, the spectrum hole duration becomes very small and is consumed by the MIPv6 handoff procedure in all the three spectrum selection strategies. In this case, since MRU always selects the longest spectrum hole, it wastes more time than the other two strategies. For $0.1 \leq E[X_p] \leq 0.4$, the number of IP handoffs was increasing. In particular, for $0.1 \leq E[X_p] \leq 0.3$, all IP handoffs were completed successfully leading to throughput degradation due to lengthy MIPv6 handoff operation (Figure 9). But, for $0.3 < E[X_p] \leq 0.4$, most of the IP handoffs were incomplete. As a result, the throughput of the SUs dropped quickly (Figure 9). Also, for $E[X_p] > 0.4$, the number of IP handoffs was reduced because the SUs were mostly cycling between channel sensing and pause phases (Figure 2). As a result, the throughput of the SUs degraded sharply (Figure 9).

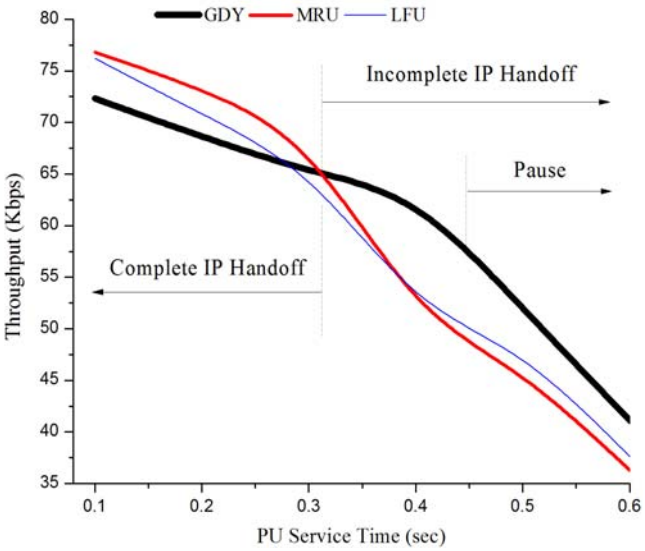

Figure 9. Impact of PU service time on throughput of SU

 ISBN: 978-1-61208-456-5

VI. CONCLUSION AND FUTURE WORK

Our study reveals that MIPv6 cannot work properly in CR networks due to high values of RA interval, lifetime period of CoA, and DAD period – especially when the spectrum holes are becoming smaller. So, the values for these parameters must be reduced to appropriate levels for use in CR environment. We have also analyzed the number of IP handoffs resulting from spectrum mobility in the absence of spatial mobility. Those results indicate that, unless the afore-mentioned parameters are properly tuned, the number of IP handoffs escalates with increase in the number of spectrum handoffs, resulting in severe degradation of data throughput. Also, the throughput of an SU (irrespective of the GDY, MRU or LFU strategy used) depends upon various values of the PU arrival rate and the PU service time. For lower values of these traffic parameters, MRU and LFU have better performance than GDY has; but, for higher values of the traffic parameters, GDY is better than MRU and LFU. So, in dynamic spectrum availability scenario, designing *an adaptive spectrum selection strategy* would be a good approach to enhance the overall throughput of the SU. Thus, in effect, our analyses clearly indicate that more research efforts are needed to optimize MIPv6 before it is used in CR networks.

REFERENCES

[1] FCC, ET Docket No 03-222, 2003, Retrieved from http://web.cs.ucdavis.edu/~liu/289I/Material/FCC-03-322A1.pdf, January, 2016.

[2] J. Xiao, R. Q. Hu, Y. Qian, L. Gong, and B. Wang, "Expanding LTE network spectrum with cognitive radios: From concept to implementation", IEEE Wireless Communications, vol. 20, no. 2, April 2013, pp. 12-19.

[3] B. Sayrac, H. Uryga, W. Bocquet, P. Cordier, and S. Grimoud, "Cognitive radio systems specific for IMT systems: Operator's view and perspectives", Telecommunication Policy, vol. 37, March-April 2013, pp. 154-166.

[4] I. Christian, S. Moh, I. Chung, and J. Lee, "Spectrum mobility in cognitive radio networks", IEEE Communications Magazine, vol. 50, June 2012, pp. 114 – 121.

[5] K. -C. Chen, Y. -J. Peng, N. Prasad, Y.-C. Liang, and S. Sun, "Cognitive radio network architecture: part I -general structure", Proc. Intl conf Ubiquitous Information Management and Commun, January 2008, pp. 114-119.

[6] K.-C. Chen, Y.-J. Peng, N. Prasad, Y.-C. Liang, and S. Sun, "Cognitive radio network architecture: part II - trusted network layer structure", Proc. Intl conf Ubiquitous Info Mngmnt and Commun, January 2008, pp. 120-124.

[7] M. Kataoka, T. Ishikawa, S. Hanaoka, M. Yano, and S. Nishimura, "Evaluation of inter base station handover for cognitive radio", Proceeding on IEEE Radio and Wireless Symposium, January 2008, pp. 251-254.

[8] J. F. Weng, B. H. Ku, J. C. Chen, and W. T. Chen, "Channel holding time of packet sessions in all-IP cellular networks", Proc. IEEE ICPADS, December 2014, pp. 404-411.

[9] C. Perkins, D. Johnson, and J. Arkko, "Mobility support in IPv6", RFC 6275, IETF, 2011.

[10] J. S. Lee, S. J. Koh, and S. -H. Kim, "Analysis of handoff delay for Mobile IPv6", Proc. IEEE VTC, vol. 4, September 2004, pp. 2967-2969.

[11] L.-C. Wang, C.-W. Wang, and C.-J. Chang, "Optimal target channel sequence for multiple spectrum handoffs in cognitive radio networks", IEEE Transactions on Communication", vol. 60, September 2012, pp. 2444-2455.

[12] L.-C. Wang, C.-W. Wang, and C.-J. Chang, "Modeling and Analysis for Spectrum Handoffs in Cognitive Radio Networks", IEEE Transactions on Mobile Computing", vol. 11, July 2012, pp. 1499-1513.

[13] Network simulator (ns), version 3, Retrieved from http://www.nsnam.org/, January 2016.

[14] R. Southwell, J. Huang, and X. Liu, "Spectrum mobility games", INFOCOM, 2012 Proceedings IEEE, March 2012, pp. 37-45.

[15] Y. –S. Chen, C. -H. Cho, I. You, and H. -C. Chao, "A cross-layer protocol of spectrum mobility and handover in cognitive LTE networks", Simulation Modelling Practice and Theory, vol. 19, September 2011, pp. 1723-1744.

[16] J. Sztrik, "Basic queueing theory", University of Debrecen, Faculty of Informatics, 2011.

[17] C. –W. Wang, L. –C. Wang, and Adachi F., "Modeling and Analysis for Reactive-Decision Spectrum Handoff in Cognitive Radio Networks", Proc. IEEE Global Telecommunications Conference (GLOBECOM 2010), December 2010, pp. 1-6.

[18] S. –U. Yoon, and E. Ekici, "Voluntary Spectrum Handoff: A Novel Approach to Spectrum Management in CRNs", IEEE International Conference on Communications (ICC), May 2010, pp. 1-5, 23-27.

[19] G. Yuan, R. C. G.rammenos, Y. Yang, and W. Wang, "Performance Analysis of Selective Opportunistic Spectrum Access With Traffic Prediction", IEEE Transactions on Vehicular Technology, vol. 59, no. 4, May 2010, pp. 1949-1959.

[20] ETSI, "Universal Mobile Telecommunications System (UMTS): Selection Procedures for the Choice of Radio Transmission Technologies of the UMTS", Technical Report UMTS 30.03, version 3.2.0, April 1998.

 ISBN: 978-1-61208-456-5

LTE and WLAN Interference Suppression in CR Applications

Johanna Vartiainen and Risto Vuohtoniemi
Centre for Wireless Communications
University of Oulu
Oulu, Finland
Email: firstname.lastname@ee.oulu.fi

***Abstract*—In traditional cognitive radio approach, spectrum is divided into black and white spaces. Black space is reserved to primary users (PU) as secondary users (SU) are able to transmit in white space. A modern approach is that the black space is divided into black and grey spaces to get more capacity. Grey space leads to novel type of interference environment because of interfering signals coming from PUs and other SUs. In addition, novel CR applications like long term evolution advanced (LTE-A) and internet of things (IoT) generate interfering signals. Thus, interference suppression is needed. In this paper, the performance of the forward consecutive mean excision algorithm (FCME) interference suppression method is studied in the presence of relatively narrowband interfering signals existing in the novel CR networks. Real-world LTE and WLAN signal measurements were used to verify the usability of the FCME IS method in future CR applications.**

Keywords–interference suppression; grey zone; cognitive radio; LTE; WLAN; measurements.

I. INTRODUCTION

Heavily used spectrum calls for new technologies and innovations. Cognitive radio (CR) [1] [2] offers possibility to effective spectrum usage allowing secondary users (SU) to transmit at unreserved frequencies if they guarantee that primary users (PU) transmissions are not disturbed. Earlier, spectrum was divided into two zones (spaces): black and white zone. As black zone was fully reserved to PUs and off limits to secondary users, their transmission was allowed in white zones where there were no PU transmissions. The problem in this classification is that if the spectrum is not totally unused, secondary users are not able to transmit. Thus, the spectrum usage is not as efficient as it could be. Instead, spectra can be divided into three zones: white, grey (or gray) and black zone [3]. In this model, the SU transmission is allowed in white and grey spaces, as black spaces are reserved for PUs.

Cognitive radio has several novel applications. Long Term Evolution Advanced (LTE-A) is a 4G mobile communication technology [4]. LTE-A exploits cognitive radio technology and utilizes flexible and intelligent spectrum usage. Its focus is on high capacity. LTE-A enables one of the newest topics called Wide Area IoT (Internet of Things), where sensors, systems and other smart devices are connected to internet. Therein, long-range communication, long battery life and minimal amount of data, as well as narrow bandwidth are key issues. In addition, Cognitive IoT (CIoT) has been proposed to highlight required intelligence [5].

As cognitive radio technology offers more efficient spectrum use, there are many challenges. One of those is that the cognitive world is an interference-intensive environment. Especially in-band interfering signals cause problems. There are three main types of interference in CR: from SU to PU (SU-PU interference), from PU to SU (PU-SU interference), and interference among SUs (SU-SU interference) [6] [7]. The basic idea in CR is that SU must not interfere PUs. Instead, SU may be interfered by PUs or other SUs. When there are multiple PUs and SUs with different applications and technologies, cumulative interference is a problematic task [8]. In grey spaces, there is interference from PU (and possible other SU) transmissions. It is efficient to mitigate unknown interference in order to achieve higher capacity. Therefore, interference suppression (IS) methods are needed.

Interference suppression exploits the characteristics of desired / interfering signal by filtering the received signal [9]. IS techniques include, for example, filters, cyclostationarity, transform-domain methods like wavelets and short-time Fourier transform (STFT), high order statistics, spatial processing like beamforming and joint detection / multiuser detection [10]. Filter-based IS is performed in the time domain. Optimal filter (Wiener filter) can be defined only if the interference and signal of interest Power Spectral Densities (PSDs) are known. Usually, those are not known, so adaptive filtering is an option. In filter-based IS, both computational complexity and hardware costs are low but co-channel interference cannot be suppressed, and no interference with similar waveforms to signals can be suppressed. Cyclostationarity based interference suppression has low hardware complexity but medium computational complexity. This may cause challenges in real-time low-power applications. In transform domain IS, computational complexity is medium, but transform domain IS cannot be used when interference and signal-of-interest have the same kind of waveforms. However, waveform design may be used. Transform domain IS has medium computational complexity and low hardware complexity. High-order statistics based interference suppression is computationally complex, and multiple antennas/samplers are needed, so its hardware cost is high and computational complexity too. In beamforming, co-channel interference as well as interference with similar waveforms to the signal of interest can be suppressed, but because of multiple antennas, the hardware cost is high. Its computational complexity is medium.

The less about the interfering signal characteristics is known, the more demanding the IS task will be. As most of the IS methods need some information about the suppressed signals and/or noise, there are some methods that are able to operate blindly. Blind IS methods do not need any *a priori* information

 ISBN: 978-1-61208-456-5

about the interfering signals, their modulations or other characteristics. Also the noise level can be unknown, so it has to be estimated. Blind IS methods are well suited for demanding and varying environments.

It is crystal clear that when operating in real-world with mobile devices and varying environment, computational complexity is one of the key issues. Fast and reliable as well as cost-effective, powersave and adaptive methods are needed. In this paper, a transform domain IS method called the forward consecutive mean excision (FCME) algorithm [11] [12] is proposed to be used for interfering signal suppression (IS) in cognitive radio applications. The FCME algorithm is a blind constant false alarm rate (CFAR) -type interference suppression method that is able to suppress all kind of relatively narrowband (RNB) signals in all kind of environments and in all kind of frequency areas. Here, RNB means that the suppressed signal is narrowband with respect to the studied bandwidth. The wider the studied band is the wider the suppressed signal can be. First, cognitive radio applications and interference environment are considered. Focus is on IS in SU receiver interfered by PUs and other SUs. A scenario that clarifies the interference environment is presented. The FCME algorithm is presented and its feasibility is considered. Measurement results for LTE and WLAN signals are used to verify the performance of the FCME IS method.

This paper is organized as follows. Section II considers future cognitive applications as in Section III, interference environment in cognitive radios is studied. The FCME algorithm is presented and its feasibility is considered in Section IV. Measurement results are presented in Section V, and conclusions are drawn in Section VI.

II. Future Cognitive Applications

Future applications that use cognitive approach include, for example, LTE-A and cognitive IoT. LTE-A is an advanced version of LTE. Therein, orthogonal Frequency Division Multiplex (OFDM) signal is used. In OFDM systems, data is divided between several closely spaced carriers. LTE downlink uses OFDM signal as uplink uses Single Carrier Frequency Division Multiple Access (SC-FDMA). Downlink signal has more power than uplink signal. Thus, its interference distance is larger than uplink signals. OFDM offers high data bandwidths and tolerance to interference. As LTE uses 6 bandwidths up to 20 MHz, LTE-A may offer even 100 MHz bandwidth. LTE-A offers about three times greater spectrum efficiency when compared to LTE. In addition, some kind of cognitive characteristics are expected [13] [14] [15]. RNB interfering signals exist especially at grey zones. This calls for IS.

In the network ecosystem, it is expected that cognitive IoT [5] [16] will be the next 'big' thing to focus on. Wide-area IoT is a network of nodes like sensors and it offers connections between/to/from systems and smart devices (i.e., objects) [17] [18]. Cognitive IoT enables objects to learn, think and understand both the physical and social world. Connected objects are intelligent and autonomous and they are able to interact with environment and networks so that the amount of human intervention is minimized. Therein, the long-range (even tens of kilometers) connection of nodes via cellular connections is expected. Data sent by nodes is minimal and transmissions may seldom occur. Thus, there is no need to use wide bandwidths for a transmission. This saves power consumption but also spectrum resources. Proposed technologies include, e.g., LoRa [19], Neul [20], GSM, SigFox [21], and LTE-M [22]. As Neul is able to operate in bands below 1 GHz and LoRa as well as SigFox operate in ISM band, LTE-M operates in LTE frequencies. A common thing is that the ultra-narrowband (UNB) signals are proposed to be used. For example, in LTE-M, 200 kHz BW is to be studied. Maximum transmit power is of the order of 20 dBm. In Neul, 180 kHz band is needed. Most of those technologies are on the phase of development. In any case, it is expected that the amount of narrowband signals is growing. Thus, IS is required, especially when it is operated in mobile bands.

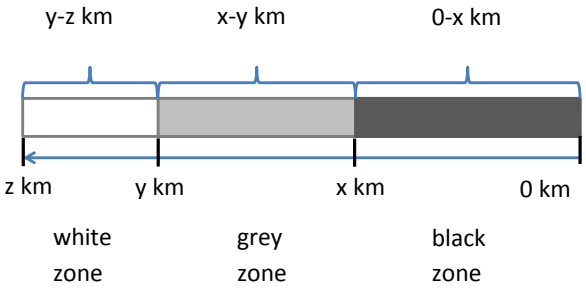

Figure 1. White, grey and black zones.

III. Interference Environment in CR

In modern CR, the spectrum is divided into three zones - white, grey and black. In Figure 1, zone classification is presented. It is assumed that PU-SU distance is >y km in the white zone, <x km in the black zone, and in the grey zone it holds that x km <PU-SU-distance <y km [23]. It means that if SU is more than y km from the PU, SU is allowed to transmit. If SU is closer than y km but further than x km from the PU, SU may be able to transmit with low power. Spectrum sensing is required before transmission and there are interfering signals so IS is needed to ensure SU transmissions. If PU-SU distance is less than x km, SU transmission is not allowed.

Interference environment differs between the zones. White space contains only noise. Therein, the noise is most commonly additive white Gaussian (AWGN) noise at the receiver's front-end, and man-made noise. This is related to the used frequency band. Grey space contains interfering signals within the noise which causes challenges. Grey space is occupied by PU (and possible other SU) signals with low to medium power that means interference with low to medium power. IS is required especially is this zone. Black space includes communications signals, possible interfering signals, and noise. In black space, there are PU signals with high power and SUs have no access.

There must be some rules that enable SUs to transmit in grey zone without causing any harm to PUs. According to [24], SU can transmit at the same time as PU if the limit of interference temperature at the desired receiver is not reached. In [2],

 ISBN: 978-1-61208-456-5

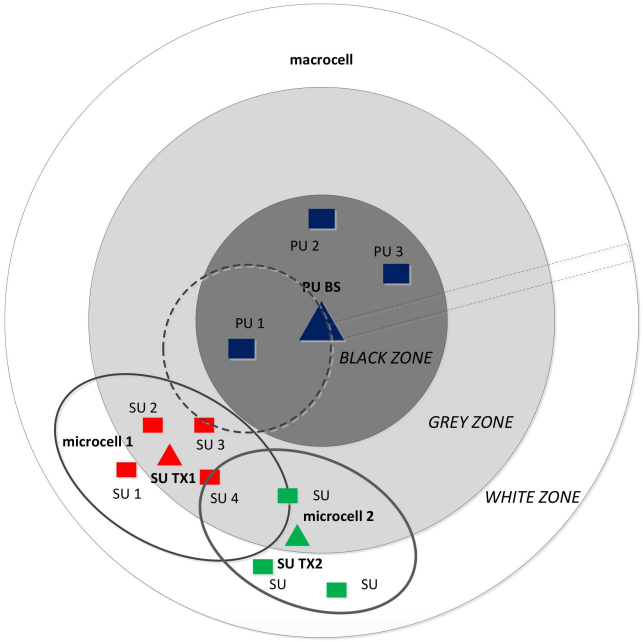

Figure 2. Scenario with one macrocell and two microcells.

it is considered the maximum amount of interference that a receiver is able to tolerate, i.e., an interference temperature model. This can be used when studying interference from SU to PU network. In [25], primary radio network (PRN) defines some interference margin. This can be done based on channel conditions and target performance metric. Interference margin is broadcasted to the cognitive radio network. In any case, the maximum transmit power of SUs is limited.

In our scenario presented in Figure 2, it is assumed that we have one PU base station (BS), several PU mobile stations and several SUs. SU terminals form microcells. Part or all of SUs are mobile and part of SUs may be intelligent devices or sensors (i.e., IoT). Between SUs, weak signal powers are needed for a transmission. One microcell can consist of, for example, devices in an office room. They can use the same or different signal types than PU. For example, in the office room case, a wireless local area network (WLAN) can be used. Between the intelligent devices (IoT), UNB signals are used. It is assumed that SUs operate at grey zone, so IS is required to ensure the quality of SU transmissions.

SUs measure signals transmitted by PU base stations and estimate relative distance to them. Using this information, SUs know whether their short range communication will cause harmful interference to the PU base station. To enable secondary transmissions under continuous interference caused by the PU base station this interference is attenuated by interference suppression.

The secondary access point knows the locations of PU terminals or SUs measure the power levels of the signals coming from PU mobile terminals in the uplink. If it is assumed that SUs know the locations of PUs, SUs do not interfere with PUs. If SUs do not know PUs locations, their transmission is allowed when received PU signal power is below some predetermined threshold. If the level of the power coming from a certain primary terminal is small, it is assumed that secondary transmission generates negligible interference towards primary terminal. However, it may happen that SUs don't sense closely spaced silent PUs.

Let us consider microcell 1 in Figure 2. There are one SU transmitter SU TX1 and four terminals SU $i, i = 1, \cdots, 4$. In addition to the intended signal from SU TX1, SU 1 receives the noise η, SU 2 receives PU downlink (PU BS) signal and the noise η, SU 3 receives PU downlink (PU BS) and PU uplink (PU 1) signals and the noise η, and SU 4 receives PU downlink (PU BS) signal, signal from other microcell's SU, and the noise η. For example, if it is assumed that PUs are in the LTE-A network and SUs use WLAN signals, receiver SU 2 has to suppress OFDM signal, receiver SU 3 has to suppress OFDM and SC-FDMA signals, and receiver SU 4 has to suppress OFDM and WLAN signals.

In addition, interfering and communication signals have to be separated from each other. The receiver has to know which signals are interfering signals to be suppressed and which signals are of interest. An easy way to separate an interfering signal from the intended signal is to use different bandwidths. For example, in LTE networks, it is known that there are 6 different signal bandwidths between 1.4 and 20 MHz that are used [4]. Especially if different signal type is used, it is easy to separate interfering signals from our information signal. It can also be assumed that interfering signal has higher power than the desired signal. However, this consideration is out of the scope of this paper.

IV. THE FCME METHOD

The adaptively operating FCME method [11] was originally proposed for impulsive interference suppression in the time domain. It was noticed later that the method is practical also in the frequency domain [12]. Earlier, the FCME method has mainly been studied against sinusoidal and impulsive signals which are narrowband ones. The computational complexity of the FCME method is $N \log_2(N)$ due to the sorting [12]. Analysis of the FCME method has been presented in [12].

The FCME method adapts according to the noise level, so no information about the noise level is required. Because the noise is used as a basis of calculation, there is no need for information about the suppressed signals. Even though it is assumed in the calculation that the noise is Gaussian, the FCME method operates even if the noise is not purely Gaussian [12]. In fact, it is sufficient that the noise differs from the signal. When it is assumed that the noise is Gaussian, $\overline{x^2}$ (=the energy of samples) has a chi-squared distribution with two degrees of freedom. Thus, the used IS threshold is calculated using [11]

$$T_h = -ln(P_{FA,DES})\overline{x^2} = T_{CME}\overline{x^2}, \quad (1)$$

where $T_{CME} = -ln(P_{FA,DES})$ is the used pre-determined threshold parameter [12], $P_{FA,DES}$ is the desired false alarm rate used in constant false alarm rate (CFAR) methods, $\overline{x^2} = \frac{1}{Q}\sum_{i=1}^{Q}|x_i|^2$ denotes the average sample mean, and

 ISBN: 978-1-61208-456-5

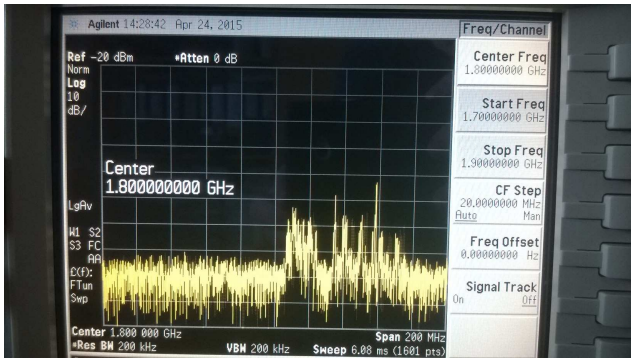

Figure 3. Agilent E4446. LTE1800 network downlink signals.

Q is the size of the set. For example, when it is selected that $P_{FA,DES} = 0.1$ (=10% of the samples are above the threshold in the noise-only case), the threshold parameter $T_{CME} = -ln(0.1) = 2.3$. The FCME method rearranges the frequency-domain samples in an ascending order according to the sample energy, selects 10% of the smallest samples to form the set Q, and calculates the mean of Q. After that, (1) is used to calculate the first threshold. Then, Q is updated to include all the samples below the threshold, a new mean is calculated, and a new threshold is computed. This is continued until there are no new samples below the threshold. Finally, samples above the threshold are from interfering signal(s) and suppressed.

The FCME algorithm is blind and it is independent of modulation methods, signal types and amounts of signals. It can be used in all frequency areas, from kHz to GHz. The only requirements are that (1) the signal(s) can not cover the whole bandwidth under consideration, and (2) the signal(s) are above the noise level. The first requirement means that the FCME method can be used against RNB signals. For example, 10 MHz signal is wideband when the studied bandwidth is that 10 MHz, but RNB when the studied bandwidth is, e.g., 100 MHz. In fact, it is enough that the interfering signal does not cover more than 80% of the studied bandwidth. However, the narrower the interference is, the better the FCME method operates [26].

V. MEASUREMENTS

The interference suppression performance of the FCME method against RNB signals was studied using real-world wireless data. The results are based on real-life measurements. Measurements were performed using spectrum analyzer Agilent E4446 [27] (Figure 3). Three types of signals were studied, namely the LTE uplink, LTE downlink, and WLAN signals. All those signals are commonly used wireless signals. Both LTE1800 network frequencies and WLAN signals were measured at the University of Oulu, Finland. IS was performed using the FCME method with threshold parameter 4.6, i.e., desired false alarm rate $P_{FA,DES} = 1\% = 0.01$ [12].

LTE1800 network operates at 2×75 MHz band so that uplink is on $1.710 - 1.785$ GHz and downlink is on $1.805 - 1.880$ GHz [28]. LTE downlink uses OFDM signal as uplink

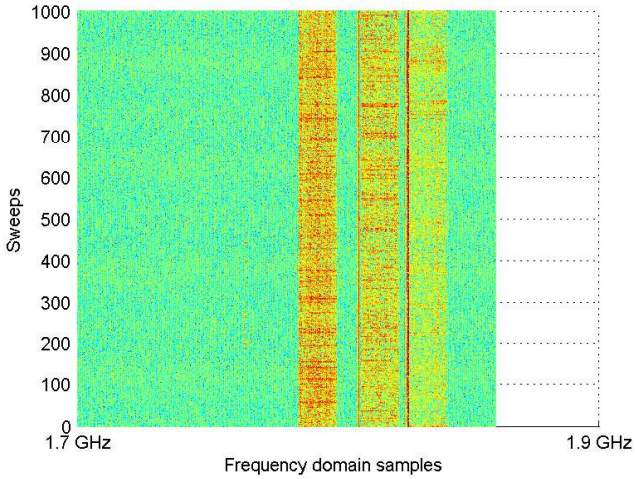

Figure 4. LTE1800 network frequencies. Spectrogram of downlink signals present.

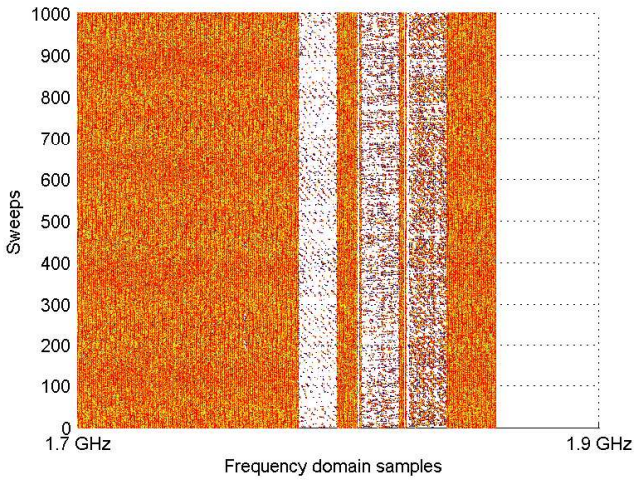

Figure 5. LTE1800 network frequencies. Spectrogram of suppressed downlink signals. The FCME method was used.

uses SC-FDMA. LTE assumes a small nominal guard band (10% of the band, excluding 1.4 MHz case).

One measurement at $1.7 - 1.9$ GHz containing 1000 time domain sweeps and 1601 frequency domain points is seen in Figure 4. Therein, only downlink signaling is present. Downlink signals have larger interference distance than uplink signals. Interfering signals cover about 30% of the studied bandwidth. In Figure 5, situation after the FCME IS is presented. It can be seen that the signals have been suppressed. On uplink signal frequencies where no signals are present (600 first frequency domain samples), average noise value is -99 dBm before and after IS.

In Figure 6, first line (sweep) of the previous case is presented more closely. The FCME thresholds after two cases are presented. In the first case, the FCME is calculated using

 ISBN: 978-1-61208-456-5

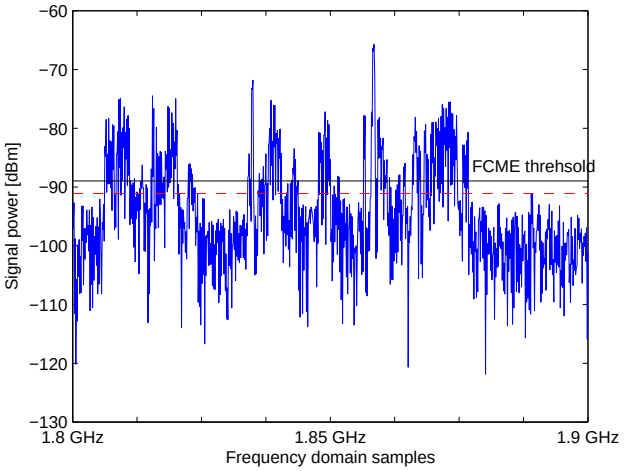

Figure 6. IS using the FCME method for LTE downlink signals. Upper threshold when the FCME calculated on $1.8 - 1.9$ GHz, lower threshold (dashed line) when the FCME calculated on $1.7 - 1.9$ GHz.

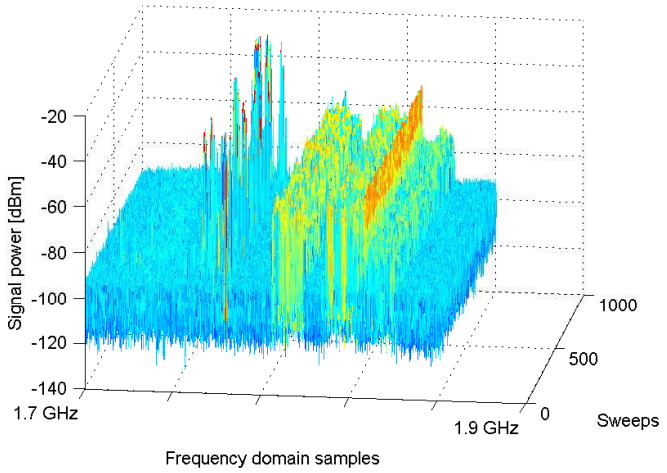

Figure 7. LTE1800 network frequencies. Uplink and downlink signals present.

frequencies $1.8 - 1.9$ GHz (downlink). Interfering signals cover about 60% of the studied bandwidth. The threshold is -89 dBm (upper line). In the second case, the threshold is calculated using both uplink and downlink frequencies $1.7-1.9$ GHz when there is no uplink signals (like case in Figure 4), i.e., SU is so far away from PU that only downlink signals are present. Interfering signals cover about 30% of the studied bandwidth. In that case, the threshold is -91 dBm (lower dashed threshold). It can be noticed that when the studied bandwidth is doubled and this extra band contains only noise, we get 2 dB gain.

Next, both uplink and downlink signals are present. There were 2001 frequency domain points and 1000 time sweeps. Figure 7 presents one measurement at $1.7 - 1.9$ GHz. Both uplink and downlink signals are present. In Figure 8, one snapshot when both uplink and downlink signals are present is presented. Therein, both signals are suppressed.

In the WLAN measurements, $2.4 - 2.5$ GHz frequency area was used. There were 1000 sweeps and 1201 frequency domain data points. In Figure 9, one snapshot is presented when there is a WLAN signal present and the FCME algorithm is used to perform IS. As can be seen, the WLAN signal is found.

Next, the desired false alarm rate ($P_{FA,DES}$) values are compared to the achieved false alarm rate (P_{FA}) values in the noise-only case. Figure 10 presents one situation when there is only noise present. According to the definition of the FCME method, threshold parameter 4.6 means that 1% of the samples is above the threshold when there is only noise present. Here, there are 1201 samples so $P_{FA,DES} = 1\% = 12$ samples. In Figure 10, 12 samples are over the threshold, so $P_{FA,DES} = P_{FA}$. We had 896 measurement sweeps in the noise-only case at WLAN frequencies. Therein, minimum 1 sample and maximum 19 samples were over the threshold as the mean was 10 samples and median value was 9 samples. Those were close of required 12 samples. Note that the definition has been made for pure AWGN noise.

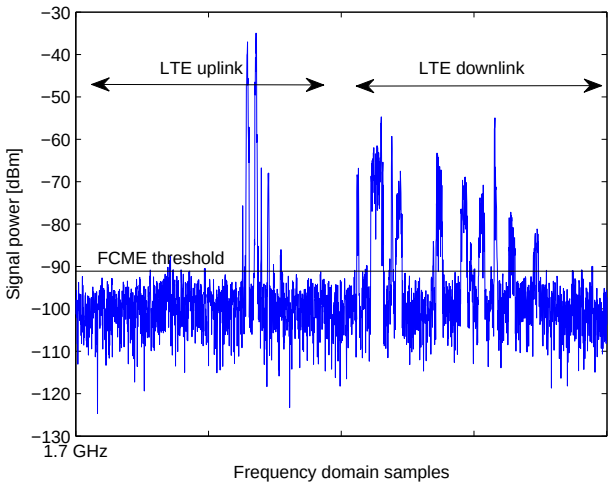

Figure 8. LTE1800 network frequencies. Uplink and downlink signals present. IS using the FCME method.

VI. CONCLUSION

In this paper, the performance of the forward consecutive mean excision (FCME) interference suppression method was studied against relatively narrowband interfering signals existing in the novel cognitive radio networks. Focus was on interference suppression in secondary user receiver suffering interfering signals caused by primary and other secondary users. Real-world LTE and WLAN measurements were performed in order to verify the performance of the FCME method. It was noted that the FCME method is able to suppress LTE OFDM and SC-FDMA signals as well as WLAN signals.

 ISBN: 978-1-61208-456-5

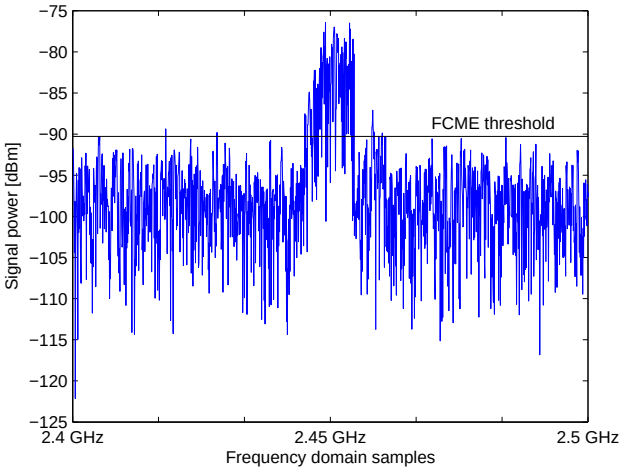

Figure 9. IS using the FCME method at frequencies 2.4-2.5 GHz where WLAN signals exist. Threshold is -90 dBm.

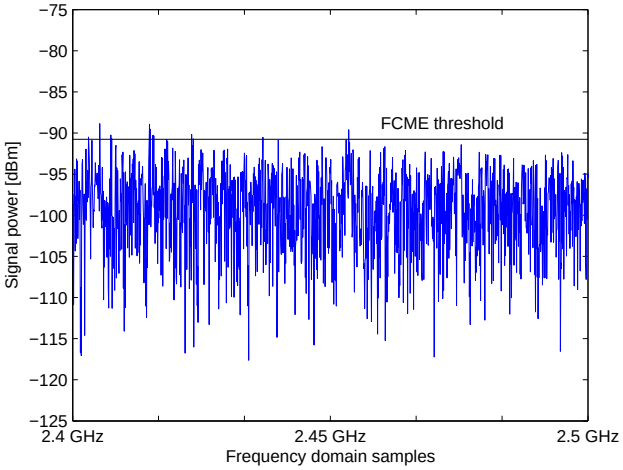

Figure 10. IS using the FCME method at frequencies 2.4-2.5 GHz where are no signals present. Threshold is -91 dBm. $1\% = 12$ samples are above the threshold, as expected.

ACKNOWLEDGMENT

The research of Johanna Vartiainen was funded by the Academy of Finland.

REFERENCES

[1] J. Mitola III and G. Q. M. Jr., “Cognitive radio: making software radios more personal,” IEEE Pers. Commun., vol. 6, no. 4, 1999, pp. 13–18.

[2] S. Haykin, “Cognitive radio: Brain-empowered wireless communications,” IEEE J. Select. Areas Commun., vol. 23, no. 2, Feb. 2005, pp. 201–220.

[3] S. Haykin, D. J. Thomson, and J. H. Reed, “Spectrum sensing for cognitive radio - the utility of the multitaper method and cyclostationarity for sensing the radio spectrum, including the digital tv spectrum, is studied theoretically and experimentally,” Proc. of the IEEE, vol. 97, no. 5, May 2009, pp. 849–877.

[4] 3GPP, “The mobile broadband standard,” (2013), http://www.3gpp.org [retrieved: Apr, 2015].

[5] Q. Wu et al., “Cognitive internet of things: A new paradigm beyond connection,” IEEE Journal of Internet of Things, vol. 1, no. 2, 2014, pp. 1–15, [retrieved: Jan, 2016].

[6] Z. Chen, “Interference modelling and management for cognitive radio networks,” Ph.D. dissertation, Doctoral Thesis (submitted), Apr. 2011, http://www.ros.hw.ac.uk/bitstream/10399/2421/1/ChenZ_0511_eps.pdf [retrieved: Jan, 2016].

[7] K. Nishimori, H. Yomo, and P. Popovski, “Distributed interference cancellation for cognitive radios using periodic signals of the primary system,” IEEE Trans. Wirel. Commun., vol. 10, no. 9, 2011, pp. 2971 – 2981.

[8] J. Peha, “Spectrum sharing in the gray space,” Telecommunications Policy Journal, vol. 37, no. 2-3, 2013, pp. 167–177.

[9] J. Andrews, “Interference cancelation for cellular systems: a contemporary overview,” IEEE Wireless Comm., vol. 12, no. 2, Apr. 2005, pp. 19–29.

[10] X. Hong, Z. Chen, C.-X. Wang, S. A. Vorobyov, and J. S. Thompson, “Cognitive radio networks - interference cancelation and management techniques,” IEEE Veh. Technol. Magazine, Dec. 2009, pp. 76–84.

[11] H. Saarnisaari, P. Henttu, and M. Juntti, “Iterative multidimensional impulse detectors for communications based on the classical diagnostic methods,” IEEE Trans. Commun., vol. 53, no. 3, Mar. 2005, pp. 395–398.

[12] J. Vartiainen, “Concentrated signal extraction using consecutive mean excision algorithms,” Ph.D. dissertation, Acta Univ Oul Technica C 368. Faculty of Technology, University of Oulu, Finland, Nov. 2010, http://jultika.oulu.fi/Record/isbn978-951-42-6349-1 [retrieved: Jan, 2016].

[13] P. Karunakaran, T. Wagner, A. Scherb, and W. Gerstacker, “Sensing for spectrum sharing in cognitive LTE-A cellular networks,” cornell University Library. http://arxiv.org/abs/1401.8226 [retrieved: Jan, 2016].

[14] L. Zhang, L. Yang, and T. Yang, “Cognitive interference management for LTE-A femtocells with distributed carrier selection,” in Vehicular Technology Conference Fall (VTC), 2010, pp. 1–5.

[15] V. Osa, C. Hearranz, J. F. Monserrat, and X. Gelabert, “Implementing opportunistic spectrum access in LTE-advanced,” EURASIP Journal on Wireless Communications and Networking, vol. 99, 2012.

[16] J. Tervonen, K.Mikhaylov, S. Pieska, J. Jamsa, and M.Heikkila, “Cognitive internet-of-things solutions enabled by wireless sensor and actuator networks,” in IEEE Conf. on Cognitive Infocommun. (CogInfoCom), 2014, pp. 97–102.

[17] K. Ashton, “That ’internet of things’ thing,” RFID Journal, June 2009.

[18] F. Xia, L. T. Yang, L. Wang, and A. Vine, “Internet of things,” Int. Journal of Commun. Systems, vol. 25, 2012, pp. 1101–1102.

[19] LoRa, http://lora-alliance.org/ [retrieved: Jan, 2016].

[20] Neul, www.neul.com [retrieved: Jan, 2016].

[21] SigFox, www.sigfox.com [retrieved: Jan, 2016].

[22] Nokia, “LTE M2M - optimizing LTE for the internet of things,” in White paper, 2014, http://networks.nokia.com/file/34496/lte-m-optimizing-lte-for-the-internet-of-things [retrieved: Jan, 2016].

[23] Z. Feng and Y. Xu, “Cognitive TD -LTE system operating in tv white space in china,” 2013, iTU-R WP 5A, Geneva, Switzerland.

[24] J. Mitra and L. Lampe, “Sensing and suppression of impulsive interference,” in Canadian Conference on Electrical and Computer Engineering (CCECE), Canada, May 2009, pp. 219–224.

[25] Y. Ma, D. I. Kim, and Z. Wu, “Optimization of OFDMA-based cellular cognitive radio networks,” IEEE Transactions on Communications, vol. 58, no. 8, 2010, pp. 2265–2276.

[26] J. Vartiainen, J. J. Lehtomäki, H. Saarnisaari, and M. Juntti, “Analysis of the consecutive mean excision algorithms,” J. Elect. Comp. Eng., 2011, pp. 1–13.

[27] Agilent, http://www.agilent.com [retrieved: Jan, 2016].

[28] Nokia Siemens Networks, “Introducing LTE with maximum reuse of GSM assets,” in White paper, 2011.

 ISBN: 978-1-61208-456-5

Citizens Broadband Radio Service Spectrum Sharing Framework - A Path to New Business Opportunity for Mobile Network Operators?

Seppo Yrjölä
Nokia Networks
Oulu, Finland
email: seppo.yrjola@nokia.com

***Abstract*—The paper seeks to identify mobile network operators' business opportunities in the new Citizens Broadband Radio Service (CBRS) shared spectrum access framework. More flexible and scalable use of the 3.5GHz spectrum aims to increase the efficiency of spectrum use in delivering fast growing and converging mobile broadband and media services while paving way to new innovations, e.g., in the area of Internet of Things and 5G. The opportunity analysis indicated that the mobile network operators could benefit significantly from the new, shared CBRS bands enabling to cope with increasing asymmetric media data traffic and to offer differentiation through improved quality and personalization of services. Heterogeneous network assets leveraging 3GPP LTE evolution were found to be the key enabler while regulatory actions may frame the availability of spectrum and limit the economic value for an operator. The concept of co-opetition was found useful to characterize the business environment regarding CBRS spectrum sharing.**

Keywords-business opportunity; mobile network operator; mobile broadband; cognitive radio; Citizens Broadband Radio Service.

I. INTRODUCTION

We have witnessed the rapid growth of wireless services with a large range of diverse devices, applications and services requiring connectivity. The number of mobile broadband (MBB) data subscribers, connected 'things' and the amount of data used per user is set to grow significantly [1] leading to increasing spectrum demand. The US President's Council of Advanced Science & Technology (PCAST) report [2] emphasized the need for novel thinking within wireless industry to meet the growing spectrum crisis in spectrum allocation, utilization and management. The essential role of spectrum sharing and dynamic spectrum access were underlined to find a balance between the different systems and services with their different spectrum requirements and system dynamics. For any spectrum sharing framework, where several radio systems operate in the same spectrum to be a feasible and attractive, early cooperation across regulation, business and technology domains is essential. Collaboration in the technology and innovation domain between industry and research enables validation of the enabling technologies and new concepts while ensuring economies of scale and scope in implementation. Furthermore, regulation has a key enabler role through spectrum harmonization and providing incentives for early adopter while on the other hand defines limiting factors and competition framework. The spectrum regulation has played central role in the wireless ecosystems in creating current multibillion business ecosystems, for MBB operator businesses via exclusive Quality of Service (QoS) spectrum usage rights and at the same time for unlicensed Wi-Fi ecosystem drawing from the public spurring innovations.

So far, only a subset of the spectrum sharing research has reached the regulation domain, the early studies on cognitive radio (CR) on license exempt access with intelligent user terminals and spectrum sensing as the general interference mitigation technique as one example. Furthermore, several spectrum sharing concepts widely studied, standardized and supported by national regulatory authorities (NRA) has not scaled up commercially as expected, TV White Space (TVWS) [3] and [4] being the latest example. Based on the decade of profound CR and in particular unlicensed TVWS concept studies, a couple of novel licensing based sharing models have recently emerged and are under regulatory discussion and early stage standardization, the Licensed Shared Access (LSA) [5] from Europe and the Citizens Broadband Radio Service (CBRS) 3 tier Spectrum Access System (SAS) from the US [6]. For these prominent spectrum sharing concepts currently under research, particularly the SAS, there is not much prior work available regarding their business model analysis. An initial evaluation of the general spectrum sharing concept from the business modeling point of view can be found in [7] and LSA focused analysis from [8] and [9]. That work is extended by focusing on more systemic, complex dynamic CBRS SAS sharing concept and analyzing the Mobile Network Operator (MNO) business opportunities using co-opetitive (co-operation and competition) business opportunity framework. This paper investigates:

1) How can CBRS spectrum sharing be defined for MNOs?
2) What are MNOs' business enablers and opportunities regarding CBRS?

The rest of the paper is organized as follows. First, the CBRS 3 tier sharing framework and the SAS models are presented and defined for a MNO in Section II. Theoretical background for co-opetitive business opportunity framework is introduced and elements framing business opportunities derived and evaluated in Section III. Finally, conclusions are drawn in Section IV.

 ISBN: 978-1-61208-456-5

II. CITIZENS BROADBAND RADIO SERVICE SPECTRUM SHARING FRAMEWORK

The key policy messages of the PCAST report were further strengthened in 2013 with Presidential Memorandum [10] stating that "…*we must make available even more spectrum and create new avenues for wireless innovation. One means of doing so is by allowing and encouraging shared access to spectrum that is currently allocated exclusively for Federal use. Where technically and economically feasible, sharing can and should be used to enhance efficiency among all users and expedite commercial access to additional spectrum bands, subject to adequate interference protection for Federal users, we should also seek to eliminate restrictions on commercial carriers' ability to negotiate sharing arrangements with agencies. To further these efforts, while still safeguarding protected incumbent systems that are vital to Federal interests and economic growth, this memorandum directs agencies and offices to take a number of additional actions to accelerate shared access to spectrum*."

Followed by intense discussion and consultation with the industry the Federal Communications Commission (FCC) released Report and Order and Second Further Notice of Proposed Rulemaking to establish new rules for shared use of the 3550-3650 MHz band in April 2015 [6]. The FCC sees the opening of the 3.5 GHz Band as "*a new chapter in the history of the administration of one of our nation's most precious resources—the electromagnetic radio spectrum."* The framework defines a contiguous 150 MHz block at 3550-3700 MHz for MBB that the FCC calls Citizens Broadband Radio Service. The 3550-3650 MHz spectrum is currently allocated for use by the US Department of Defense (DoD) radar systems and Fixed Satellite Services (FSS) while the 3650-3700 MHz spectrum incumbents are the FSS and the grandfathered commercial wireless broadband services. FCC prefigures CBRS as an "*innovation band*" where they can assign spectrum to commercial MBB systems like the 3GPP LTE on a shared basis with incumbent radar and FSS systems and promote a diversity of Heterogonous Network (HetNet) technologies, particularly small cells. The sharing framework consists of three tiers: Incumbent Access (IA), Priority Access (PA) and General Authorized Access (GAA), as shown in the Figure 1.

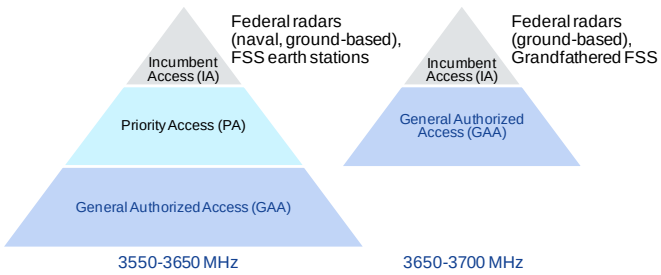

Figure 1. The US CBRS 3-tiered authorization framework with the FCC's spectrum access models for 3550-3650MHz and 3650-3700MHz spectrum segments.

The PA users will obtain a FCC PA license (PAL) to operate up to 70 MHz of the 3550-3650 MHz spectrum segment and are protected from harmful interference from the GAA operations. PA layer covers critical access users like hospitals, utilities and governmental users and non-critical users, e.g., MNOs. PA users receive short term priority authorization to operate within designated geographic areas with PALs such as 3 year 10 MHz unpaired channel in a single census track, awarded with competitive bidding. During the first application window only, an applicant may apply for up to two consecutive three-year terms for any given PAL. Licenses will be permitted to hold no more than four PALs in one census tract at one time. This will ensure availability of PAL spectrum to at least two licensed users in the geographic areas of highest demand. PALs are assigned specific frequencies within their service area, and their frequency assignment should not be dynamically controlled by the SAS database. At the end of its term, a PAL will automatically terminate and may not be renewed.

The third GAA tier will operate under a licensed-by-rule framework and will be allowed throughout the 150 MHz band without any interference protection from other CBRS users. This framework aims to facilitate the rapid deployment of compliant small cell devices while minimizing administrative costs and burdens on the public, licensees, and the FCC. GAA users may use only certified, Commission approved CBRS devices and must register with the SAS with information required by the rules, e.g., operator ID, device identification, and geo-location information.

CBRS Devices (CBSDs) which are fixed stations, or networks of such stations will be assigned spectrum dynamically by the FCC selected SAS which could be multiple. User equipments, e.g., handsets are not considered as CBSDs. SAS controls the interference environment and enforces exclusion zones to protect higher priority users as well as takes care of registration, authentication and identification of user information. As the IA users have primary spectrum rights at all times and in all areas over PA and GAA, all the CBRS users must be capable of operating across the entire 3.5 GHz band and discontinuing operation or changing frequencies at the direction of the SAS to protect IA. Automated channel assignment by a SAS will simply involve instructions to these users to use a specific channel, at a specific place and time, within 3550-3700MHz.

It will be mandatory for all the CBRS users to protect the IA users in the band. Based on nature and critical requirements of the federal incumbent the FCC adopted rules to require Environmental Sensing Capabilities (ESCs) to detect federal spectrum use in and adjacent to the 3.5 GHz the band. The federal IA user protection will be adopted in 2 phases. In the first phase, a large portion of the country outside the static exclusion zones will be available after SAS is commercially available and FCC approved, at the second phase, the rest of the country, including major coastal areas, will become available as exclusion zones will be converted to protection zones through the ESC system detecting federal incumbent use. The SAS receives input from ESCs and if needed, could order commercial tier users to vacate a

 ISBN: 978-1-61208-456-5

spectrum resource in frequency, location, or time which when in proximity to federal incumbent presents a risk of harmful interference. Prospective ESC operators must have their systems approved through the same process for SASs and SAS administrators. An ESC consists of one or more commercially operated networks of device-based or infrastructure-based sensors that would be used to detect signals from federal radar systems in the vicinity of the exclusion zones. Within 60 seconds after the ESC communication of a detected federal system signal, the SAS must either confirm suspension or relocation of operations to another unoccupied frequency.

The opportunistic GAA with no interference protection from other CBRS users is planned to provide a low-cost entry point into the CBRS band for a wide array of users and services first while PAL system operations have to wait auction process estimated to start after the US 600 MHz incentive auctions targeted for 2016. For the meanwhile, the FCC has encouraged multi-stakeholder groups to consider various issues raised by the rules. The Wireless Innovation Forum (WINNF) Spectrum Sharing Committee [11] with representatives from the MBB, Wireless broadband, Internet, Internet of Things (IoT) / machine to machine (m2m) and defense ecosystems has started initial standardization work on interfaces between a MBB system and a SAS work targeted to allow sharing of the CBRS within 2016. The US Government has initially identified an additional 2 GHz of spectrum below 6GHz owned by DoD and other users for future shared commercial use conditionally if the spectrum sharing at 3.5 GHz proves successful. This paves way to make licensed spectrum sharing a third mainstream way of licensing spectrum to commercial users complementing traditional exclusive licensing and unlicensed spectrum access. The FCC has vision to repeat WiFi success through lowering the entry barrier QoS spectrum for new entrants and verticals, e.g., enterprise, utilities, healthcare, public safety, smart cities, etc.

III. BUSINESS OPPORTUNITIES OF CBRS FOR MNOS

A. *Co-opetitive business opportunity framework*

In this section, we analyze the business opportunities of CBRS for MNOs. An entrepreneurial opportunity can be defined as the possibility to serve customers better and differently [12] framed by enablers, limiting factors as well as challenges caused by the business context. In the CBRS context, business opportunities are made to create and deliver value for the stakeholders, value that is co-created among various actors from MBB, wireless and incumbent ecosystems as a joint effort. An equally important aspect is the ability of the stakeholders to capture value, i.e., obtain profits [13], which in the context of this study can be called value co-capture. Furthermore, value co-creation can be seen as a cooperative and the parallel value co-capture as a competitive process [14]. The third term co-opetition illustrates the increased system complexity of the CBRS business environment, where companies simultaneously compete and cooperate with each other not only over spectrum but also over customers. Figure 2 below depicts the framework used in this paper to develop and frame the business opportunities for MNOs.

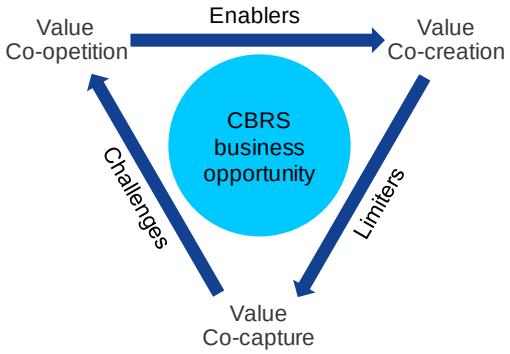

Figure 2. The Co-opetitive business opportunity framework

B. *Analysis of the business opportunities*

In the analysis for the business opportunity elements of the CBRS, five key ecosystem roles are identified: the national regulator authority, federal incumbent, MNOs, SAS administrator, infrastructure vendors and device/chip manufactures. In the systemic framework change like CBRS, all the stakeholders play a vital role in adopting of novel CBRS concept and spectrum sharing in general. In addition when developing and analyzing the opportunity frame authors argue that three domains; regulation, business, and technology, affecting spectrum sharing concept should proceed in tandem. Enabling, limiting and challenging elements framing the business opportunities for the MNO are next discussed and listed in Table 1.

Business and technology elements can be identified as enablers for value co-creation. Fast growing demand and lack of exclusive spectrum combined with the drastic changes in the consumption habits will urge the adoption of novel more flexible and efficient spectrum management concepts. Framework radically unbundles investment in spectrum, network infrastructure and services, which enables novel services and business models. Furthermore, different spectrum sharing schemes are high in regulators agenda with aims to lower the entry barrier to spectrum for new alternative types of operators which could consider entering the wireless broadband business. Utilization of the LTE ecosystem scale and harmonization will reduce risk related technology maturity and provide tools to seamlessly integrate additional capacity to MNOs HetNet, e.g., through Carrier Aggregation (CA) [15], LTE Unlicensed (LAA) [16] and Self Organizing Network (SON) [17] technologies. Big data analytics capabilities will play a major role in coping with the SAS dynamic requirements and enabling low transaction costs.

Regarding limiting factors, sound, sustainable and harmonized regulatory environment can be the limiter that needs to be addressed before MNO can co-create and co-capture value from it with ecosystem partners. The limited spectrum availability in frequency, time or location with potential restriction and uncertainties may negatively

 ISBN: 978-1-61208-456-5

influence the MNOs outlook on shared use and the spectrum valuation. A specific technology item to be considered is the degree of business (MNOs) and mission (DoD) critical information needed to share and resulting need for the ESC system. In addition to MNO opportunities, it is essential to consider reciprocal incentives for the current federal spectrum holders to further transition to CBRS.

Policy risk and uncertainty are the main elements of the co-opetitive challenges in the competitive domain. Fragmented national and global market structure deprives economies of scale and scope, raising costs and hampering innovation in the ecosystem. Furthermore, introduction of sharing models may influence the MNOs current exclusive spectrum licensing model and availability in the future. The regulatory approach and in particular the 3-tier concept could unbundle investment in spectrum, network infrastructure and services. Faster access to spectrum with lower initial investment (annuity payments for spectrum rights) enables local 'pro-competitive' deployments and further expands sharing mechanism for pooling spectrum and infra resources between operators. At the same time, the complexity of the CBRS framework and the SAS might influence the value of the spectrum and the required time of recovering the network investments. On the competence domain, MNOs need to pay attention to dynamic capabilities needed to deploy, manage and optimize multilayered HetNets under sharing conditions. Traditional MNOs support for the 3.5GHz spectrum in their networks is paramount to encourage chip and device manufacturers to support the whole 3.5GHz band introduction with competitive terminals. Attractive and dynamic spectrum market with potentially lower transaction costs may increase and change competition, e.g., through introducing new and alternative operator types locally and from other business domains.

TABLE I. ELEMENTS FRAMING BUSINESS OPPORTUNITIES

	Business opportunity framing elements
Enablers	• Lack of exclusive spectrum triggers new spectrum access approaches • Consumers MBB consumption habits are changing towards asymmetric multi-device usage • Shared spectrum allocation improves overall spectrum use efficiency • Regulators considering shared spectrum framework in the EU and the US • Unbundles investment in spectrum, network infrastructure and services • Additional lower cost capacity to cope with asymmetric traffic and improve performance • Better QoS spectrum may increase dense urban area business • Additional GAA capacity for offloading • May lower entry barriers for challenger MNOs and new alternative type of operators • Harmonized LTE technology base leverage HetNet asset optimization and offers scale • Big data and analytics capabilities with Internet domain
Limiters	• Limited spectrum availability and predictability limit MNO business opportunities • Need for global and national regulation outside of the US may slow down entry - Harmonization is a precondition to scale and enable potential benefit fully. • Real incentives for the federal incumbents unclear or missing • Federal incumbent special requirements in particular related to security and need for sensing • Regulatory framework restrictions may reduce the economic value • Degree of information sharing of business critical (MNOs) and secret information (Federal incumbent) and needed ESC system • Standardization of SAS functionalities for 3GPP ecosystem and technologies needed
Challenges	• Uncertainty and risks related to regulation in timing, term, licenses and flexibility creates exposure and risk for a MNO to proceed with the investment. • Impact on exclusive spectrum licensing model and availability in the future • Attractive and dynamic spectrum market with potentially lower transaction costs. • May increase and change competition. New operator types, and from other business domains. • Increased technical and operational complexity (SAS) with related capital and operational costs • New competencies and capabilities needed for network management and optimization • Timely availability of full band base stations and terminals and potential impact on cost and complexity

 ISBN: 978-1-61208-456-5

In summary, in order to realize the business potential of the CBRS, MNOs have occasion to simultaneously co-create and co-capture value with ecosystem players in a co-opetitive business environment where co-operation (spectrum) and competition (customers & services) exist parallel to each other. MNOs are in unique position to leverage additional multi-tiered capacity CBRS concept offers. Faster access to QoS licensed small cell optimized spectrum without mandatory coverage obligations will help them to timely cope with booming asymmetric data needs. Additional scalable and flexible spectrum resource leveraged with LTE technology enablers will enable MNOs to better retain and grow existing customer base with changing demand and consumer habits, offer differentiating services and explore new vertical segments.

IV. CONCLUSION AND FUTURE WORK

This paper discussed the transformative role of the novel Citizen Broadband Radio Service framework in the future mobile broadband networks as an endeavor to meet the growing traffic demand and changing consumption characteristics of the customers while paving the way to make licensed spectrum sharing a third mainstream way of licensing spectrum to commercial users complementing traditional exclusive licensing and unlicensed spectrum access. We utilized co-opetitive business opportunity framework for understanding mobile network operator's enablers and opportunities and how they are framed from policy, technology, and business perspectives in the future, CBRS shared spectrum networks.

We argue that policy and regulation will be on the one hand the key enabler in the path toward shared spectrum access and on the other hand will play key role in removing limiting and challenging elements critical in the first steps of that path. In particular, the sharing framework for the priority access licenses should be attractive and feasible to encourage mobile broadband industry to invest which could lower the barrier for change and furthermore create economies of scale across tiers and for the whole ecosystem.

More flexible and scalable use of the spectrum aims to increase the efficiency of spectrum use in delivering fast growing and converging mobile broadband, media and Internet content to meet changing consumer needs. The proposed opportunities enable mobile network operators to retain existing customers, acquire new customers and strengthen overall market position by offering improved personalized mobile broadband data services timely. Furthermore, through unbundling investment in spectrum, network infrastructure and services co-operative business opportunities may open with vertical segments, new alternative operator types and the internet domain.

Mobile operators are optimally positioned towards these business opportunities in parallel with their traditional business model leveraging technology enablers from mobile broadband 3GPP LTE evolution and big data analytics while waiting for the more optimized cognitive 5G solutions.

This paper serves as a starting point for analyzing the business enablers, opportunities and business environment around CBRS. We saw that the concept of co-opetition could be used to characterize the business environment regarding spectrum sharing. However, future work is needed to expand research to cover also other key stakeholders and to dwell deeper into the framework of value co-creation, co-capture and co-opetition for identifying MNOs' business models and ecosystem relations in the new CBRS concept and in the third opportunistic GAA layer in particular.

ACKNOWLEDGMENTS

This work is supported by Tekes – the Finnish Funding Agency for Technology and Innovation. The authors would like to acknowledge CORE++ project consortium: VTT, University of Oulu, Centria University of Applied Sciences, Turku University of Applied Sciences, Nokia, PehuTec, Elektrobit, Anite, Finnish Defence Forces and FICORA.

REFERENCES

[1] Cisco white paper: Cisco Visual Networking Index: Global Mobile Data Traffic Forecast Update, 2014–2019. [Online]. Available from: http://www.cisco.com/c/en/us/solutions/collateral/service-provider/visual-networking-index-vni/white_paper_c11-520862.html [retrieved: 2015.12.04]

[2] The White House: Realizing the Full Potential of Government-Held Spectrum to Spur Economic Growth. President's Council of Advisors on Science and Technology (PCAST) Report, 2012.

[3] FCC: White Spaces. [Online]. Available from: http://www.fcc.gov/topic/white-space [retrieved: 2015.12.04]

[4] Ofcom: TV White Spaces Pilot. [Online]. Available from: http://stakeholders.ofcom.org.uk/spectrum/tv-white-spaces/white-spaces-pilot/ [retrieved: 2015.12.04]

[5] ECC: Licensed Shared Access (LSA). ECC Report 205, 2014.

[6] FCC: Report and Order and second FNPRM to advance availability of 3550-3700 MHz band for wireless broadband, 2015.

[7] J. Chapin and W. Lehr, "Cognitive radios for dynamic spectrum access – The path to market success for dynamic spectrum access technology," IEEE Commun. Mag., vol. 45, no. 5, 2007, pp. 96-103.

[8] M. Matinmikko et al., "Business benefits of Licensed Shared Access (LSA) for key stakeholders," In O. Holland, H. Bogucka & A. Medeisis (eds.) Opportunistic Spectrum Sharing and White Space Access: The Practical Reality. John Wiley & Sons, 2015.

[9] P. Ahokangas, M. Matinmikko, S. Yrjölä, H. Okkonen, and T. Casey, " "Simple rules" for mobile network operators' strategic choices in future cognitive spectrum sharing networks," IEEE Wireless Communications, vol.20, no.2, 2013, pp. 20-26.

[10] The White House: Expanding America's Leadership in Wireless Innovation. Presidential Memorandum, 2013.

[11] WINNF Spectrum Sharing Committee. [Online]. Available from: http://www.wirelessinnovation.org/spectrum-sharing-committee [retrieved: 2015.12.04]

[12] D.Hansen, R. Shrader, and J. Monllor, "Defragmenting Definitions of Entrepreneurial Opportunity, Journal of Small Business Mgmnt," vol 49, Iss. 2, 2011, pp. 283-304.

[13] J. West, "Value Capture and Value Networks in open source vendor strategies," In: Proc. of the 40th Annual Hawaii International Conference on System Sciences, 2007.

 ISBN: 978-1-61208-456-5

[14] A. Brandenburger and B. Nalebuff, “Co-opetition,” New York: Doubleday, 1998.

[15] 3GPP: Technical report TR 36.808: Evolved Universal Terrestrial Radio Access (E-UTRA); Carrier Aggregation; Base Station (BS) radio transmission and reception,” 2012.

[16] 3GPP: Study on Licensed-Assisted Access using LTE. RP-141646, 2014.

[17] 3GPP: Telecommunication management; Principles and high level requirement. 3GPP TS 32.101 V12.0.0 [Rel-12], 2014.

 ISBN: 978-1-61208-456-5